MULTI-OBJECTIVE PERFORMANCE OPTIMIZATION OF MICROSTRIP PATCH ANTENNA FOR WIDE-BAND APPLICATIONS

A thesis submitted to the
University of Petroleum and Energy Studies

For the Award of
Doctor of Philosophy
in
Electronics and Communication Engineering

BY
RAJ GAURAV MISHRA

September 2020

Supervisor(s)
Dr. Piyush Kuchhal
N. Prasanthi Kumari, Ph.D.

UPES
UNIVERSITY WITH A PURPOSE

Department of Electrical and Electronics Engineering
School of Engineering
University of Petroleum and Energy Studies
Dehradun-248007: Uttarakhand

MULTI-OBJECTIVE PERFORMANCE OPTIMIZATION OF MICROSTRIP PATCH ANTENNA FOR WIDE-BAND APPLICATIONS

A thesis submitted to the
University of Petroleum and Energy Studies

For the Award of
Doctor of Philosophy
in
Electronics and Communication Engineering

BY
RAJ GAURAV MISHRA
(SAP ID: 500049145)

September 2020

Supervisor
Dr. Piyush Kuchhal
Professor, Department of Physics,
University of Petroleum and Energy Studies, Dehradun

Co-Supervisor
N. Prasanthi Kumari, Ph.D.
Associate Professor,
Department of Electrical and Electronics Engineering,
University of Petroleum and Energy Studies, Dehradun

UPES
UNIVERSITY WITH A PURPOSE

Department of Electrical and Electronics Engineering
School of Engineering
University of Petroleum and Energy Studies
Dehradun-248007: Uttarakhand

DECLARATION BY THE SCHOLAR

I here by declare that this submission is my own and that, to the best of my knowledge and belief, it contains no material previously published or written by another person nor material which has been accepted for the award of any other Degree or Diploma of the University or other Institute of Higher learning, except where due acknowledgement has been made in the text.

RAJ GAURAV MISHRA (SAP ID: 500049145)

Department of Electrical and Electronics Engineering,

School of Engineering (SOE),

University of Petroleum and Energy Studies,

Dehradun - 248007 (Uttarakhand).

THESIS COMPLETION CERTIFICATE

This is to certify that the thesis titled **MULTI-OBJECTIVE PERFORMANCE OPTIMIZATION OF MICROSTRIP PATCH ANTENNA FOR WIDE-BAND APPLICATIONS** submitted by **RAJ GAURAV MISHRA** (SAP ID: 500049145), to the University of Petroleum & Energy Studies, for the award of the degree of **DOCTOR OF PHILOSOPHY** in Electronics and Communication Engineering is a bonafide record of project work carried out by him under our supervision and guidance.

It is certified that the work has not been submitted anywhere else for the award of any other diploma or degree of this or any other University.

14/09/2020

Dr. Piyush Kuchhal
Professor,
Department of Physics

N. Prasanthi Kumari, Ph.D.
Associate Professor,
Department of Electrical and Electronics
Engineering

ABSTRACT

Microstrip or patch antenna is one of the most profound antenna technologies in modern wireless communication. Simplicity and its embedded configuration on printed circuit technology makes it an excellent choice for usage in the wireless applications. Many militaries, scientific and commercial requirements are satisfied by the usage of microstrip antennas, and these antennas have significant usage in the super high frequency (SHF) or microwave frequency range. There are some inherent disadvantages of conventional microstrip antennas such as narrow bandwidth, low gain/ directivity, low efficiency, etc. Optimized microstrip antennas have been proposed by the researchers to overcome these limitations. A large number of methods are experimented in the past to improve single-objective optimization (both manually and using optimization techniques). The use of soft-computing or optimization techniques is not new in the field of antenna design.

In this thesis work, a total of five antenna designs are proposed. These proposed antenna designs belong to three different types of structures. The objective of the antenna design was to achieve multi-objective optimized performance (this includes improvements in gain, impedance bandwidth, and reduction of return loss). All five antennas proposed in this thesis radiates at a resonating frequency between 10.5-10.9 GHz and are useful in various wireless wideband applications in the X-Band. Three different optimization techniques i.e. Genetic Algorithm, Particle Swarm Optimization, and Gray Wolf Optimization are used in the process of designing and optimization of these antennas. The step-by-step procedure of the antenna optimization is discussed along with the convergence graphs, converged antenna designs, simulated, and measurement results. Parametric analysis is also presented in this thesis for all five proposed antennas to validate the converged designs.

iii

The first proposed design is a conventional square-shaped microstrip patch antenna with complete ground plane. This design is converged using Genetic Algorithm (GA) and is constructed using RT/duroid substrate material having dielectric constant of 2.2. The dimension of the converged antenna is 38.4 mm x 38.4 mm x 1.574 mm. The proposed antenna shows the simulated bandwidth of 550 MHz (10.66-11.21 GHz) and measured bandwidth of 450 MHz (10.7-11.15 GHz). The values of return loss at the resonant frequency (of 10.9 GHz) is -32 dB (simulated) and -27 dB (measured). The simulated radiation patterns show the directional radiation characteristics. The only limitation with this design is the cost of fabrication because of the cost of substrate material RT/duroid. The proposed antenna design shows high values of simulated gain (8.35 dB), and directivity (8.35 dB) at the resonating frequency of 10.9 GHz. The comparison of the proposed design with the existing literature is also presented.

The second proposed design is a conventional rectangular-shaped microstrip patch antenna with partial ground plane. This design is converged using Genetic Algorithm (GA) and is constructed using FR4 substrate material having dielectric constant of 4.3. The dimension of the converged antenna is 41 mm x 45 mm x 1.58 mm. The proposed antenna provides sufficiently large simulated bandwidth of 850 MHz (9.95-10.8 GHz) and measured bandwidth of 670 MHz (10.04-10.71 GHz). The values of return loss at the resonant frequency (of 10.5 GHz) is -27.35 dB (simulated) and -21.51 dB (measured). The simulated radiation patterns show the omnidirectional radiation characteristics. At the resonant frequency of 10.5 GHz, the proposed antenna exhibits higher simulated values of gain and directivity. The value of simulated gain is 4.26 dB, and directivity is 7.36 dB at 10.5 GHz. The comparison of the proposed design with the existing literature is also presented.

The third proposed design is a conventional rectangular-shaped microstrip patch antenna with partial ground plane. Another optimization technique is implemented to verify whether the antenna design can be further improved. This design is converged using Particle Swarm Optimization (PSO) and is constructed using FR4 substrate material having dielectric constant of 4.3. The dimension of the converged antenna is 25.81 mm x 23.08 mm x 1.58

mm. The proposed antenna provides sufficiently large simulated bandwidth of 1.95 GHz (9.71-11.66 GHz) and measured bandwidth of 1.55 GHz (9.66-11.21 GHz). The values of return loss at the resonant frequency (of 10.5 GHz) is -28.40 dB (simulated) and -23.02 dB (measured). The simulated radiation patterns show the omnidirectional radiation characteristics. At the resonant frequency of 10.5 GHz, the proposed antenna exhibits higher simulated values of gain and directivity. The value of simulated gain is 4.07 dB, and directivity is 5.01 dB at 10.5 GHz. The comparison of the proposed design with the existing literature is also presented.

The fourth proposed design is a conventional rectangular-shaped microstrip patch antenna with partial ground plane. This design is converged using Grey Wolf Optimization (GWO) and is constructed using FR4 substrate material having dielectric constant of 4.3. The dimension of the converged antenna is 18.73 mm x 41.72 mm x 1.58 mm. The proposed antenna provides sufficiently large simulated bandwidth of 3.89 GHz (8 GHz-11.89 GHz) and measured bandwidth of 3.1 GHz (8.9-12 GHz). The values of return loss at the resonant frequency (of 10.5 GHz) is -35.51 dB (simulated) and -24.59 dB (measured). The simulated radiation patterns show the omnidirectional radiation characteristics. At the resonant frequency of 10.5 GHz, the proposed antenna exhibits simulated gain of 2.82 dB, and directivity of 3.06 dB. The comparison of the proposed design with the existing literature is also presented.

The fifth proposed design is a CPW-fed slot dipole antenna with three slots. In the existing literature, one slot dipole antennas are available, this is to explore the designs with more than one slot. This design is converged using Genetic Algorithm (GA) and is constructed using FR4 substrate material having dielectric constant of 4.3. The dimension of the converged antenna is 102 mm x 98 mm x 1.58 mm. The proposed antenna shows sufficiently large simulated bandwidth of 1.4 GHz (10.1-11.5 GHz) and measured bandwidth of 1.3 GHz (9.85-11.15 GHz). The values of return loss at the resonant frequency (of 10.6 GHz) is -25.83 dB (simulated) and -23.08 (measured). The simulated radiation patterns show the omni-directional radiation characteristics. The only limitation with this design was the antenna's size because of the use of FR4 substrate material. But, the gain and

directivity of the proposed antenna design is higher than the previous proposed designs fabricated using FR4 substrate material. This is because the CPW fed antennas have limited surface waves. The proposed antenna design shows high values of simulated gain (6 dB), and directivity (12.62 dB) at the resonating frequency of 10.6 GHz. The comparison of the proposed design with the existing literature is also presented.

ACKNOWLEDGEMENTS

First and foremost, I would like to thank Almighty God for giving me the strength, knowledge, ability and opportunity to undertake this research study and to persevere and complete it satisfactorily. Without his blessings, this achievement would not have been possible.

I would like to express my sincere gratitude to my supervisors Dr. (Prof.) Piyush Kuchhal and Dr. N. Prasanthi Kumari for their continuous support in my Ph.D related study and research, for their patience, motivation, and immense knowledge. Their guidance helped me in all the time of research and writing of this thesis. I could not have imagined having better advisors and mentors for my Ph.D work.

I would like to express my heartfelt gratitude towards the Hon`ble Chancellor and Hon`ble Vice Chancellor of UPES, who gave their kind consent to carry on this work and for providing support throughout this work.

I am thankful to Dr. Kamal Bansal, Dr. Sushabhan Choudhury, Dr. R. Gowri, Dr. Narendra B. Soni, Dr. Mukul Kumar Gupta, Dr. Rupendra Kumar Pachauri, Dr. Abhinav Sharma, Mr. Deepak Kumar, Dr. P. Vijay, Dr. Pawan Kumar Pannala, Dr. Jitendra Kumar Pandey, Dr. Syed Mohammad Tauseef for providing support and motivation in my research work.

I would be failing in my duties if I miss to thank Dr. Ranjan Mishra for his constant help and support. I am also thankful to all of my friends who lent constant motivation and support.

The greatest sense of acknowledgement would go to my family members: my parents, my grandparents, and to my wife who have been in the roots of whatever I am and have achieved in my life including this research work.

<div align="right">

RAJ GAURAV MISHRA

</div>

Contents

List of Figures

xvii

List of Tables

List of Symbols

A_e : Effective Aperture

B : Channel Bandwidth

c : Velocity of Electro-Magnetic Wave

C : Channel Capacity

D : Directivity

ΔL : Length Correction factor

E : Electric Field Component

E_t : Total Efficiency

E_r : Radiation Efficiency

ϵ_r : Permittivity or Dielectric Constant

ϵ_{eff} : Effective Permittivity or Dielectric Constant

f : Frequency of Electro-Magnetic Wave

G : Gain

h : Height of Substrate

H : Magnetic Field Component

l_e : Loss Tangent

λ : Resonant Wavelength of Electro-Magnetic wave

μ : Permeability

η : Efficiency

ϕ : Azimuth angle

Q : Quality Factor

S : Radiated Power Density

S_{11} : S-Parameter or Return Loss

σ : Thermal conductivity

τ : Reflection coefficient

θ : Elevation angle

U : Radiation Intensity

Y_{in} : Input Admittance

Z_c: Characteristic Impedance

Z_{in} : Input Impedance

Chapter 1

INTRODUCTION

In the new era, thought itself will be
transmitted by radio.

Guglielmo Marconi (1874-1937)

Radio wave's magic and mystery have captured imaginations from William Crooke's earliest speculations to the present day. The beauty of wave transmission in wireless media is a marvel in ubiquitous and instant broadcast communications. In the voices, images, data, and information are conveying vibrations quiver all around us. A radio pushes these signals out of the air and recovers the original one. A wireless radio device is made possible by an antenna. A transmitting antenna takes the signal from a source, converts it into electromagnetic waves, and transmits it in the open space. The reverse link collects electromagnetic waves and transforms back to the form of the input signals.

James Clarke Maxwell first laid out his remarkable equations describing the electrical and magnetic fields' behavior in 1865. The Maxwell equation's journey to understand electromagnetic radiation and radio waves took a long 20 years and many debates. The existence of electromagnetism resolved in 1884 with the Henrich Hertz experiment and its demonstration. Hertz led the way as the first to generate radio waves and to subject them to scientific scrutiny. Many innovators such as Nikola Tesla, Carl Barun, Alexander Popov, and Reginald Fessenden contributed key elements to radio technology. The

other leading pioneers are Oliver Lodge, Jagdish Chandra Bose, and Guglielmo Marconi. Lodge introduced the concept of transmitting and receiving using a specific frequency and tuned circuit. Bose performed pioneering work in millimeter-wave systems and invented horn antenna. But it was Marconi's remarkable work that opened the path of radio communication. Marconi first marketed radio as a means of long-range communication. The fundamental works of these great ones open the antenna technology gateway. And it requires decades of technical development to fully realize the vision of Crookes.

The boundaries of radio science are rising past high-frequency range beyond speech, and a new generation of antenna design is emerging to tackle the difficulty of broadband creation. As frequencies used in radio spectrum tens to increase, it leads to a growth in the broadband antenna. Nevertheless, not only are frequencies going high, but bandwidths also became wide. Edwin Howard Armstrong's discovery of Frequency Modulation in 1933 demands twenty times more bandwidth than Amplitude Modulation's first radio broadcast. The advent and rise of television also led to spur popularity for antennas, which can support a larger bandwidth of 7 MHz. The demand for wideband antennas led to the rediscovery of the biconic antenna by Philip Carter and the coaxial horn element by Nils Lindenbald in the late 1940s. Improvement in radio electronics led to higher and higher frequencies and fuelled demand for broadband antennas, super high-frequency antennas, and ultra-wideband antennas [1]-[5].

1.1   Types of Antennas

In several ways, an antenna can be classified [1]-[5]. A wire antenna is the simplest antenna structure. It is also one of the oldest, cheapest, multipurpose, and widely used antenna for many applications. There are three further classifications in a wire antenna.

1. **Dipole Antenna** – is also known as a linear wire antenna because it is in the form of a straight wire. This structure is the base of the radiation property of all types of antenna.

2. **Loop antenna** – it is made from a wire also, but the wire is taken the shape of a loop and hence the terminology. The loop can be of any size and geometrical shape, but circular shaped and square shape loop are most commonly used.

2

3. A **helical antenna** is made using a large section of wire in the form of helical, and the shape of the antenna defines its name. This antenna structure is also commonly referred to as the helix antenna.

Other than the wire, the solid conductor having a two-dimensional surface, of finite dimension, is used to design the antenna. The structure formed is called an aperture antenna. The different types of the antenna under aperture antenna classification are given as [1]-[5]:

1. **Horn antenna** – An antenna constructed by flaring the aperture of the waveguide is the horn antenna. The waveguide's cross-section determines horn antenna's shape, a hollow metallic tube of rectangular or circular shaped used to carry the radio waves in a closed structure. When the cross-section of one end of the waveguide is confined, it behaves like an antenna.

2. **Parabolic disc antenna** – An antenna of large aperture, mostly used for long-distance or space communication, whose surface is parabolic in shape. This antenna is also referred to as disc antenna or reflector antenna since they collect the waves by taking the property of reflection.

3. **Microstrip antenna** – A three-dimensional antenna structure is consisting of three layers. These layers are radiating patch, finite substrate, and ground plane from top to bottom. This structure is utilized in designing the desired antenna of this thesis work.

In several ways, an antenna can be further classified. Fig. 1.1 shows a classification of antennas based on their physical structures.
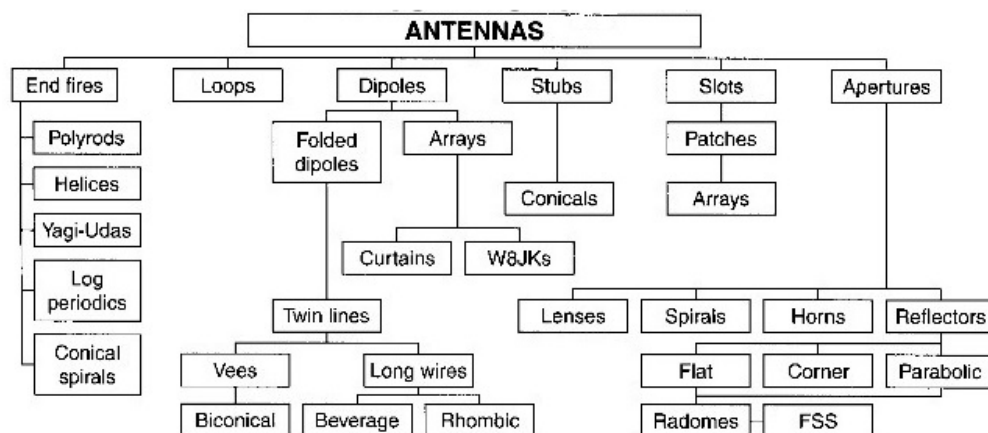
Figure 1.1: Classification of antennas based on their physical structures [2]

3

1.2 Performance Parameters of Antenna

Antennas are the backbone of wireless Antennas that validate a reciprocity property, which means that it maintains the same features as transmitting and receiving.

1.2.1 Radiation Pattern

When a signal is fed into an antenna, the antenna will emit radiation distributed in space in a certain way. A graphical representation of the relative distribution of the radiated power in space is called a radiation pattern [1]-[3] .

The radiation or antenna pattern describes the relative strength of the radiated field in various directions from the antenna, at a constant distance. The radiation pattern is a reception pattern as well since it also describes the receiving properties of the antenna. The radiation pattern is three-dimensional, but usually, the measured radiation patterns are a two-dimensional slice of the three-dimensional pattern in the horizontal or vertical planes. These pattern measurements are presented in either a rectangular or a polar format.

There are two kinds of radiation patterns: absolute and relative. Absolute radiation patterns are presented in absolute units of field strength or power. Relative radiation patterns are referenced in relative units of field strength or power. Most radiation pattern measurements are relative to the isotropic antenna, and then the gain transfer method is then used to establish the antenna's absolute gain.

The radiation pattern in the region close to the antenna is not the same as the pattern at large distances. The term near-field refers to the field pattern that exists close to the antenna, while the term far-field refers to the field pattern at large distances. The far-field is also called the radiation field and is what is most commonly of interest. Ordinarily, it is the radiated power that is of interest, and so antenna patterns are usually measured in the far-field region. The minimum acceptable distance relates to the wavelength of the antenna

and is given as equation 1.1:

$$r_{min} = 2d^2/\lambda \tag{1.1}$$

where r_{min} is the minimum distance measured from the antenna, d is the dimension, and λ is the operating wavelength of the antenna.

1.2.2 Aperture Efficiency

Aperture is the term, which accounts for the power radiation from the antenna. Every antenna has an aperture responsible for the delivery of power. For better radiation, the losses from the surface of the antenna should be kept minimum. In defining the efficiency of aperture, the physical area of the aperture also considers because the radiation's effectiveness depends upon this physical and the aperture area [1]-[3].

Mathematically,

$$\epsilon_A = A_{eff}/A_P \tag{1.2}$$

where, ϵ_A, A_{eff}, and A_P are the aperture efficiency, effective area, and physical area of the antenna.

1.2.3 Gain

The gain of an antenna is the proportion of the intensity of the radiation provided by the antenna in a given direction to the radiation intensity that would be achieved if a similar power is dissipated the antenna isotopically.

Essentially, the gain of an antenna considers the directivity also as a measure of its execution. The intensity acknowledged by the antenna when transmitted isotopically (that implies every which way), is taken as reference. In contrast to directivity, antenna gain considers the losses during radiation and, hence, takes the magnitude of intensity [1]-[3].

Mathematically,

$$G = \eta_e * D \qquad (1.3)$$

where, G, η_e, and D are the gain, efficiency, and directivity of the antenna.

Gain is measured in dB, and a gain of 5 dB equated to an isotropic antenna is referred to as 5 dBi. The radiation from the isotropic is in all directions with an equal magnitude of power. In practice, the real isotropic antenna has found no existence, but it provides an insight comparison with the practical antenna radiation property. The gain is measured by equating the test antenna with a standard calibrated antenna. An antenna doesn't generate power, so the total power radiated of any antenna is equal to that of an isotropic antenna, but the distribution in directions are not uniform.

1.2.4 Directivity

The ability to focus the radiation energy in a particular direction is termed as the directivity of the antenna. For a receiving antenna, this term defines the ability of the antenna to collect the energy from a particularly more than the other direction. So, the directivity helps in radiating or collecting the energy in a specified direction [1]-[3].

As per the definition, "The ratio of maximum radiation intensity of the subject antenna to the radiation intensity of an isotropic or reference antenna, radiating the same total power is called the directivity." The direction in which an antenna radiates it a matter of interest and the radiated power depends on the position (in angle) and the distance (in radian) from the antenna. Therefore, it is expressed in terms of and (the two-axis) both.

$$\text{Directivity} = \frac{\text{Maximum radiation intensity of subject antenna}}{\text{radiation intensity of an isotropic antenna}} \qquad (1.4)$$

During the antenna (as a transmitter or receiver), if the radiation intensity is concentrated in a given direction, then the antenna has more directivity in that given direction. If a given direction is not specified, then that direction where the antenna operates with maximum intensity defines the directivity of that antenna.

6

1.2.5   Voltage Standing Wave Ratio (VSWR)

Voltage Standing Wave Ratio (VSWR) is a measure of how efficiently the energy from a source is transmitted through an antenna for the radiation. The source and antenna are interfaced with the feedline. For an efficient transfer, and subsequently, radiation, of energy, the impedance of the source, feedline, and the antenna must be perfectly matched or balanced. Transceivers and feed lines are operated for 50 Ω impedance, so if the impedance of the antenna deviates from 50 Ω, then there is a mismatch, and it accounts for the loss of energy [1]-[3].

An ideal system made to radiate 100% of the incoming energy fed to an antenna. For this to happen, there would be an exact impedance matching between source, feedline (transmission line), and the antenna. In real systems, any mismatch in the impedance, at the interface, could lease the reflection of some energy back to the source. This results in a standing voltage over the line, and this reflection causes destructive interference that leading to the up and down of the voltage overtime at the various path along the line. VSWR is a measure of the variation of this voltage. It is the ratio of the high to low voltage along the transmission path. VSWR is very much related to the S_{11} parameter.

1.2.6   Return Loss / S-Parameters

The return loss is an additional way of conveying the impedance mismatch between the interfaces at source, line, and the antenna. The bandwidth of the antenna is easily calculated using the plot of this parameter. Another popular term for expressing this parameter is the reflection coefficient. Return loss compares the power reflected by the antenna to the power fed to the antenna, and measured usually as a logarithmic ratio in dB [1]-[3]. The mathematical relationship between a return loss (S parameter) and VSWR is expressed in equation 1.5

$$\text{Return Loss} = 20 log_{10} \frac{VSWR}{VSWR-1} \tag{1.5}$$

1.2.7 Impedance Bandwidth

The impedance bandwidth of an antenna is the operating range of frequencies (lower frequency to higher frequency) over which the antenna radiates correctly [1]-[3]. This is also the ranges of frequencies, in which the antenna exhibits a reflection coefficient of less than -10 dB or a VSWR of less than 2. All the different classes of antennas have different operating bandwidth, and also they have a limitation of operating bandwidth. The unit of bandwidth is Hz. The bandwidth of a wideband antenna in the microwave zone is usually around 500 MHz or 0.5 GHz.

1.3 Microstrip Antennas

Microstrip or patch antenna is one of the most profound antenna technologies in modern wireless communication. Simplicity and its embedded configuration on printed circuit technology make it a good choice as wide usage in the wireless applications. Deschamps, in 1953, first proposed the perception of microstrip antenna in 1953. Gutton and Baissinot, in 1955, proposed a patent on this type of microstrip antenna. Specialized devices developed in laboratories were early microstrip lines and radiators. Till 1970 no practical antenna exists due to a lack of commercially available printed circuit technology and controlled dielectric material. Robert E. Munson, in the 1970s, first worked and developed a microstrip antenna. Other researchers have accelerated development during this decade by the availability of different substrate materials.

Further development includes the availability of attractive substrate, having a better thermal and mechanical property, improvising photolithographic techniques, and better theoretical analysis. Credit for the first practical microstrip antenna goes to Munson and Howell. From 1990 onwards, extensive research work on planer and arrays of microstrip antennas took place, which ultimately led to a diversified wireless application. The characteristics features of a microstrip antenna attributes to the geometry of metallic layers (radiating and ground), and characteristics of the substrate that is engaged by the two metallic layers.

Microstrip or printed patch antennas find its wide usage to find its major contribution in modern wireless systems. The prime application of the microstrip antenna is in the microwave range or Super high-frequency range [1]-[5].

1.3.1 Characteristics of Microstrip Antennas

Microstrip antenna has demonstrated an outstanding choice in most applications compared to its conventional microwave antenna. This is because of its numerous advantages, and this finds its usage in many applications ranging from around 100 MHz to 100 GHz over the broad frequency range. Some of the advantages of MPA are as follows [1]-[5]:

- Light in weight.

- Occupy low volume.

- Configured to be low profile planer.

- Adapted to planar and non-planar surfaces.

- Ease of mass production leads to low manufacturing costs.

- Easy to implement and integrate on the device.

- Act as an effective radiator.

- Have a low cross-section of scattering.

- Mechanically robust and prone to shock and vibrations.

- Ease in manufacturing the feed line on the substrate.

However, the microstrip antenna possesses some disadvantages concerning its counterpart, conventional antenna. Some of the disadvantages are listed below [1]-[5]:

- Possess low bandwidth.

- Low gain and low directivity.

- Low efficiency.

- Low isolation between the feedline and the radiating layer.

- Require complicated feed structure in arrays.

- Meant to handle low power.

- Have large resistance loss in the feed structure of arrays.

- Produces unnecessary radiation from the junctions interface.

- Produces excitation of surface waves, which account for radiation loss.

Narrow bandwidth is the main disadvantage of the microstrip antenna as it hinders its application in broadband wireless systems. The one method to increase the bandwidth includes increasing the height of the substrate, but it leads to increases in surface wave and radiation efficiency decreases. Another way is the use of suitable feeding techniques and the impedance matching structure on it, as feeding is the interface between source and antenna. From the radiating layer, the various means of increasing the bandwidth includes carving of planer structure in the form of slot, slit, and notch on the top layer. All these ways provide a better matching that leads to wide impedance bandwidth of microstrip antennas. The length, width, and shape of these elements are the adjustable parameters [1]-[5].

Another drawback is its low gain and low directivity. The two way to increase the gain is cavity backing method and lens covering method. The first way is to remove the bidirectional radiation, and in the second way combination of microstrip radiator elements and the dielectric lens is treated as a composite structure. The gain and directivity of the microstrip antenna can be further increased by using an antenna array configuration. Usually, there is a trade-off between gain and bandwidth of an antenna because of the gain-bandwidth constant.

1.3.2   Applications of Microstrip Antennas

Many militaries, scientific and commercial requirements are satisfied by the usage of microstrip antennas, and these antennas have major usage in the Super High Frequency (SHF) or Microwave frequency. Microstrip antenna has been found in many geometrical shapes, and rectangular-shaped is the most widely found amongst them. These antennas satisfy many requirements for mobile, the military and commercial communication system in SHF or microwave frequency, and this lead to development and research of many

forms of this antenna structure. Aircraft, cellular towers, mobile phones, local networking, missiles, and business profiles are other dominant applications. These antennas are very suitable due to small size, low weight, and flexibility of installation. The requirement of these antennas is also found in other applications, in the category of the unlicensed spectrum of wireless communication.

Some of the specific applications that justified the development and suitability of microstrip antennas are listed as following [1]-[5]:

- Mobile communication systems,

- Data Networking and Wireless Sensor Networking,

- RFID application,

- Local Internetworking (LAN) and Wireless Fidelity (WiFi) applications,

- Low power Personal Area Network (LoPAN),

- Industrial, Scientific, and Medical (ISM) application,

- Missile and military applications,

- Radio altimeter,

- Biomedical applications.

The frequency ranges of 8.0–12.0 GHz are specified by the Institute of Electrical and Electronics Engineers (IEEE) as X-band. The X band is used for radar, satellite, and wireless communication and computer networks. In this thesis, applications in the X-Band of SHF is proposed. Some specific applications of microstrip antennas in the X-band are as follows [1]-[5]:

- X band is used in radar applications for weather monitoring, maritime vessel traffic control, air traffic control, vehicle speed detection, and defense tracking, etc.

- The X band's shorter wavelengths allow higher resolution imagery for target identification and discrimination (in high-resolution imaging radars).

- X band (10.15 to 10.7 GHz) segment is used for terrestrial broadband in many countries.

- International Telecommunications Union (ITU) has assigned a part of the X band exclusively for deep space telecommunications. A primary user of this allocation is the US Deep Space Network (DSN) of NASA.

- The International Telecommunication Union (ITU) has allowed amateur radio operations in the X-band (10.000 to 10.500 GHz).

- Motion detectors often use X-band (10.525 GHz). 10.4 GHz of X-band is proposed for traffic light crossing detectors. Ireland has officially allocated 10.450 GHz for Traffic Sensors.

- X-band RF sources are used to power particle accelerators. The European X-band frequency is used for powering the Compact Linear Collider.

1.3.3   Structure of Microstrip Antenna

The fundamental structure of a microstrip antenna comprises three layers [1]-[5]. The upper layer is the metallic layer whose function is radiating the energy to space and collecting it from space. The lower layer is the metallic layer referred to as the ground plane. The third layer is the substrate of finite height, having a dielectric constant and loss tangent value. The metallic layer is etched over the substrate during the process of fabrication of the microstrip antenna. The preferred choice of operating frequencies for this type of antenna is 1 − 100 GHz. The radiating layer and the ground plane layer are very thin and made of high conducting material usually gold and copper. Fig. 1.2 shows the structure of the microstrip patch antenna. The radiating layer offers low resistivity, high conductivity, resistance to rusting, and ease in soldering. These layers are of any shape, but the most common shape is rectangular. Other desired shapes, as per the performance requirements are circular, square, or regular geometrical shapes. The radiation characteristics of the microstrip antenna do not deviate, regardless of the geometrical shape, because in any case, these antennas act as a dipole. The height (thickness) of the substrate is not kept high, since a bulky substrate adds more surface waves and decreases the radiation power. The radiation from the microstrip antenna occurs because of the fringing fields, which are generated between the edges of two metallic layers (upper radiating and lower ground). These days, to achieve the compact design, researchers are designing the antenna at a higher frequency range. There is again a trade-off between size, gain, and bandwidth of a microstrip patch antenna. The threshold is to be dictated by the application based requirement.
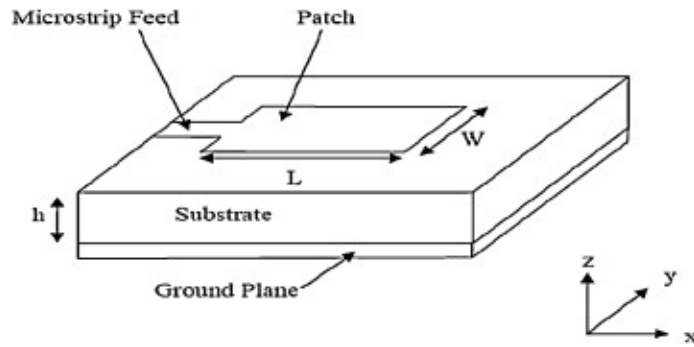
Figure 1.2: Structure of the microstrip patch antenna [1]-[5]

1.3.4 Feeding Methods for Microstrip Antenna

The feed is the interface between the source and the antenna, and it guides the energy to the antenna. The energy crossed the edges of the antenna dimension and radiated into space. The energy from the source is fed to the antenna by a variety of feeding methods. The construction and utility of all these are different from each other and they bear some advantages and disadvantages.

The feeding methods are categorized into two classes, one is contacting and another is non-contacting. Generally speaking, the contacting method is termed as the direct method, whereas the non-contacting method is termed as an indirect method. In the first-mentioned method, energy from the source is supplied directly to the radiating layer of the antenna and this is done by using a connecting element. The connecting elements may be a microstrip line or coaxial feeding or others. In the second-mentioned method, the power is transfer to the antenna by using an electromagnetic field coupling in between the source and the antenna through a microstrip line element. Coplanar waveguide feed, aperture coupling feed, and proximity coupled feed are the methods that fall under this category of feeding methods.

All these above-mentioned feeding methods affect differently on the performance parameter of the antenna. The parameters, having a profound effect on the choice of these methods, are gain, directivity, bandwidth, and radiation. For the perfect impedance matching and delivery of the maximum power from the source to the antenna, the impedance of the two should be matched perfectly and the impedance value should be 50 Ω. A brief

summary of different types of feeding methods is given herewith [1]-[5].

1.3.4.1 Microstrip Line Feed

In this method of feeding, a conducting strip connects the source and the antenna directly. The width of the strip, known as microstrip feedline, is always smaller than the width of the radiating surface, commonly termed as a patch, of the antenna. The advantage of this type of feeding method is that besides the planer structure it provides ease in fabrication, as the feedline can be printed over the substrate at the same time as the radiating layer. This advantage leads to the design of large arrays by using edge-fed radiating elements. Radiation from the feedline, as leakage of power, is the disadvantage provided by this method. In addition, as the frequency goes higher than 30 GHz, the size of the feedline is compatible with the radiating layer and leading to an excess of undesired radiation. Some design structure uses an inset cut on the radiating layer at the interface of feedline with it, and this arrangement is done to improve the impedance matching without any additional matching element. This feeding method is widely used, especially in microstrip antenna, as it provides ease of fabrication, good impedance matching, and as well as simplicity in the analysis of the antenna [1]-[5]. The microstrip feedline is shown in Fig. 1.2.

1.3.4.2 Coaxial Feed

The coaxial feed, also termed as probe feed, is the most usual feeding method, which has the flexibility of providing feed at any given location on the radiating layer. Therefore matching the impedance is easily achievable with this patch to achieve impedance matching, and it makes it a popular choice of feeding. The structure of this feed consists of a coaxial cable, consisting of two conductors sharing the same axis and separated by plastic jack along with surrounded too. The inner connector is pierced through the substrate to the radiating layer, and soldering is done, whereas its outer conductor is connected to the ground plane. These feeding method's advantages lie in the low radiation loss and placement of the feed at any desired location on the radiating layer. Besides these, it is

also easy in fabrication with less spurious radiation. However, the main drawback lies in providing less bandwidth, since the structure is not planer. The feeding is also not suitable for low dimension antenna, at higher frequencies in the microwave zone, since the coaxial feed structure is fixed. A hole is drilled in the substrate to fit the cable and it makes the asymmetrical configuration of the whole antenna structure. The coaxial feeding technique [1]-[5] is shown in Fig. 1.3.
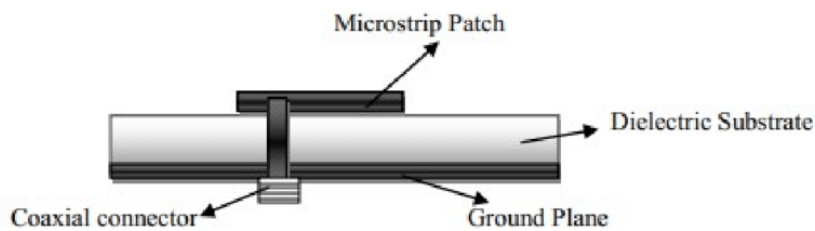
Figure 1.3: Coaxial Feedline [1]-[5]

1.3.4.3 Aperture Coupled Feed

This feeding method is used where there are two substrates in the antenna structure. The feedline is at the bottom substrate and the radiating layer is placed at the top substrate. A slot is positioned between the two substrates, and the feed is provided by coupling the feedline to the radiating layer through the slot. The slot is also referred to as an electrically small structure cut on the ground plane. The coupling is centered under the patch, and the dimension, location, and shape of aperture determine the amount of coupling. The aperture of slot behaves either as resonant or as non-resonant. The former provides another resonance, and it is in addition to existing coupling resonance to the radiating layer, thereby results in an increase in the bandwidth, which is the advantage of this feeding method. However, this structure leads to high back radiation, and this leads to the option of non-resonant aperture in normal use. The alignment of the different layers, of conducting element and substrate element, generates a relatively small error. The material for the two substrates element can be of different dielectric, as this gives an optimum antenna performance. The aperture coupled feeding technique [1]-[5] is shown in Fig. 1.4.

15
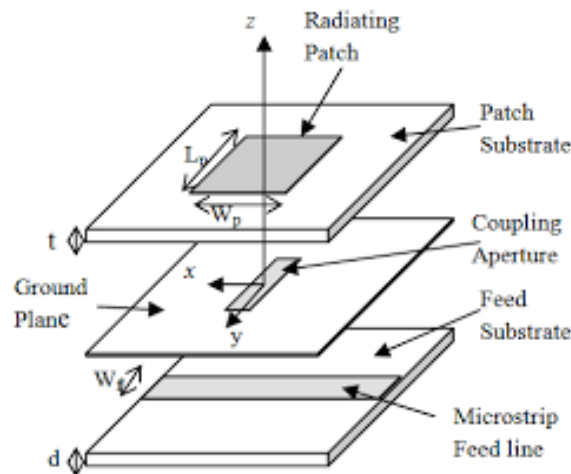
Figure 1.4: Aperture Coupled Feedline [1]-[5]

1.3.4.4 Proximity Coupled Feed

The structure of this feeding method also uses a two-layer of substrate elements. The microstrip feedline resides on the lower substrate layer, and the radiating layer is positioned on the upper substrate. Therefore, this feeding method consists of two dielectric substrates with a ground plane on the backside of the structure, and the common ground plane acts as a separator for the two substrate layers. A slotted aperture, of any shape and size, is used in the ground plane to couple the feedline and the radiating layer electromagnetically. The slot parameters are altered to match the impedance in getting an improved bandwidth. The ground plane also acts as a shield between the open end of the feed line and the radiating layer, so that radiation of the feedline is not going to influence and disturb the radiation pattern of the radiating layer. The notable advantage of this feeding method is wider bandwidth, and flexibility of the choice of two substrates with different dielectric values. The disadvantage lies in difficulty in the fabrication process, as multiple layers need to be properly aligned to get the optimum performance of the antenna. The proximity coupled feeding technique [1]-[5] is shown in Fig. 1.5.

1.3.4.5 Co-Planar Waveguide Feed (CPW)

The coplanar waveguide feed method is another coupling based method to transfer power from the source to the microstrip antenna. Here, the coplanar waveguide is printed

16
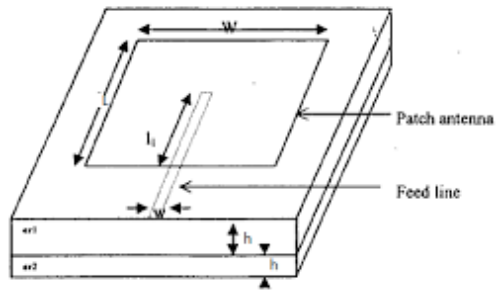
Figure 1.5: Proximity Coupled Feed Line [1]-[5]

along the same axis as the radiating layer of the antenna. This feeding method has finds its wide use in the communication system owing to some salient features possessed by it that include simple structure, ease in fabrication, compatible with printed circuit element. One of the advantages of this method is high bandwidth. The drawbacks of this method include the high radiation from the feedline element, which accounts for the poor front to back ratio, but reducing the dimension of the feedline and some modifications in the shape reduces this effect. The coplanar waveguide feeding technique [1]-[5] is shown in Fig. 1.6. From the Fig. 1.6, it can be observed that the feedline and the ground plane is separated by an air gap (s).
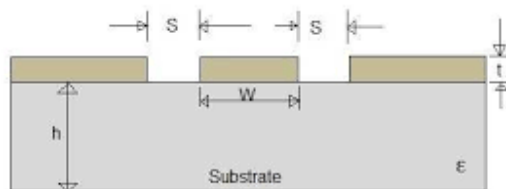
Figure 1.6: CPW Feedline [1]-[5]

Fig. 1.7 shows the comparison between various feeding techniques [1]-[5], their advantages, and their disadvantages.

Types of Feeding Techniques				
Microstrip feed line	**Co-axial feed**	**Aperture coupled feed**	**Proximity coupled feed**	**CPW feed**
High spurious feed radiation, Better reliability, Easy in fabrication, Easy in impedance matching, 2-3% BW achievable.	High spurious feed radiation, Poor reliability, Difficult in fabrication, Easy in impedance matching, 2-3% BW achievable.	Less spurious feed radiation, Good reliability, Difficult in fabrication, Easy in impedance matching, 3-5% BW achievable.	Minimum spurious feed radiation, Good reliability, Difficult in fabrication, Easy in impedance matching, 15% BW achievable.	Less spurious feed radiation, Good reliability, Easy in fabrication, Easy in impedance matching, 3% BW achievable.

Figure 1.7: Comparison of various types of feeding techniques [1]-[5]

1.3.5 Methods for Analysis of Microstrip Antenna

The microstrip antenna contains a dielectric substrate, and this is in between the lower ground plane and an upper radiating plane. The said structure is treated as a 2-D planer structure for analyzing the microstrip antenna, and the method of analysis [1]-[5] is further categorized into two categories.

The first category deals with the analysis on the basis of equivalent current distribution, which occurs on the periphery of the edges, and this analysis is more focused on the physical insight rather than accuracy. The transmission line model and the cavity model are two widely used analytical techniques here. The second category uses the electrical current distribution between the two metallic layers of the microstrip antenna. Here the analysis is more rigorous with better accuracy in the results. Numerical methods deal with this analysis are the Finite Element Method (FEM), and the Method of Moments (MoM).

1.3.5.1 Transmission Line (TL) Model

TL model [1]-[5] is simple in analysis, and grants a good physical insight. It is helpful in understanding the basic performance of the microstrip antenna. In this model, the radiating patch element is viewed as a transmission line resonator without any transverse field variations. The variation of the field is taken along the length. The radiating patch is represented by two slots separated by the length of the resonator. Fringing fields at the

open-circuited ends are the main source of the radiation. Originally this model was proposed for rectangular patches but later on, it has been extended for all generalized shape of the patch. It is also most suitable for rectangular microstrip antenna. The drawback of this model is its accuracy. It is less accurate. Although it is easy to use, in this case, all types of configurations can't be analyzed as it does not take care of field variation in the orthogonal direction of propagation.

1.3.5.2 Cavity Model

The cavity model [1]-[5] gives more precise results. It also provides good physical insight into the behavior of the field on the radiating patch. Here the portion in between the radiating patch and the ground plane is treated as a cavity. The cavity is surrounded by magnetic walls around the periphery and from the top and bottom side it is enclosed with the electric walls. The field inside the cavity is uniform since the thickness of the substrate is small. The field underneath the radiating patch is expressed as a sum of the various resonant modes. The fringing fields and the and the radiated power are found around the edges of the cavity, as they are not enclosed inside the cavity. The total radiation responsible is the combined accounts of the radiation loss, the conductor loss, skywave loss, and loss tangent of the substrate.

1.3.5.3 Method of Moments

In MoM model [1]-[5], the surface currents account in the modeling and analysis of the microstrip antenna. The fields in arose the substrate accounts for the analysis by taking care of the polarization currents in the substrate and the fringing fields are created outside the physical area of the radiating layer. The effect of currents on the radiating layer of the microstrip antenna and the feed lines, together with its images on the ground plane, accounts for the formulation of an integral and equivalent algebraic equation in this method of analysis, which provides a better and exact solution. IE3D and ADS software employs this method for their computational analysis.

1.3.5.4 Finite Element Method

This FEM method [1]-[5] is more suitable for volumetric configurations. Here the plane or volumetric structure region is distributed amongst many finite surfaces. elements. These discretized units or finite elements are of well-defined geometrical shapes. Here the computation is performed over the integration of basic functions over the entire top radiating layer of the microstrip antenna. The solution of the wave equations uses to tackle in-homogeneous boundary conditions, involves two classes of boundary value problems. One involves inhomogeneous boundary conditions with Laplace's equation and the second one is homogeneous boundary condition with an inhomogeneous wave equation. HFSS software uses this method for their computational analysis.

1.4 Optimization Techniques

Mathematical optimization, spelled alternatively as optimization, is the technique of selecting the best element, with regard to some criterion, from some set of available alternatives, and has found its wide usage in operational research and computer science. The best use of optimization techniques is to avoid hit and trial approaches to get the best performance of an antenna. An optimization problem, in the simplest case, comprises of maximizing or minimizing a real function by selecting input values systematically within an allowed set and calculating the value of the function. Optimization comprises of finding the best available values of some objective function as given a defined domain that includes a variety of different types of objective functions and domains. A large section of applied mathematics treats with the generalization of optimization techniques to other formulations.

In the last two decades, meta-heuristic optimization techniques have become very popular. A metaheuristic is an algorithmic system inspired by nature, structured to provide a near-optimal solution to an objective function.

Meta-heuristic optimization approaches give many advantages:

- Meta-heuristics is pretty basic. Mostly, they were influenced by very basic principles. Usually, the inspirations are linked to physical events, actions of animals, or evolutionary principles.

20
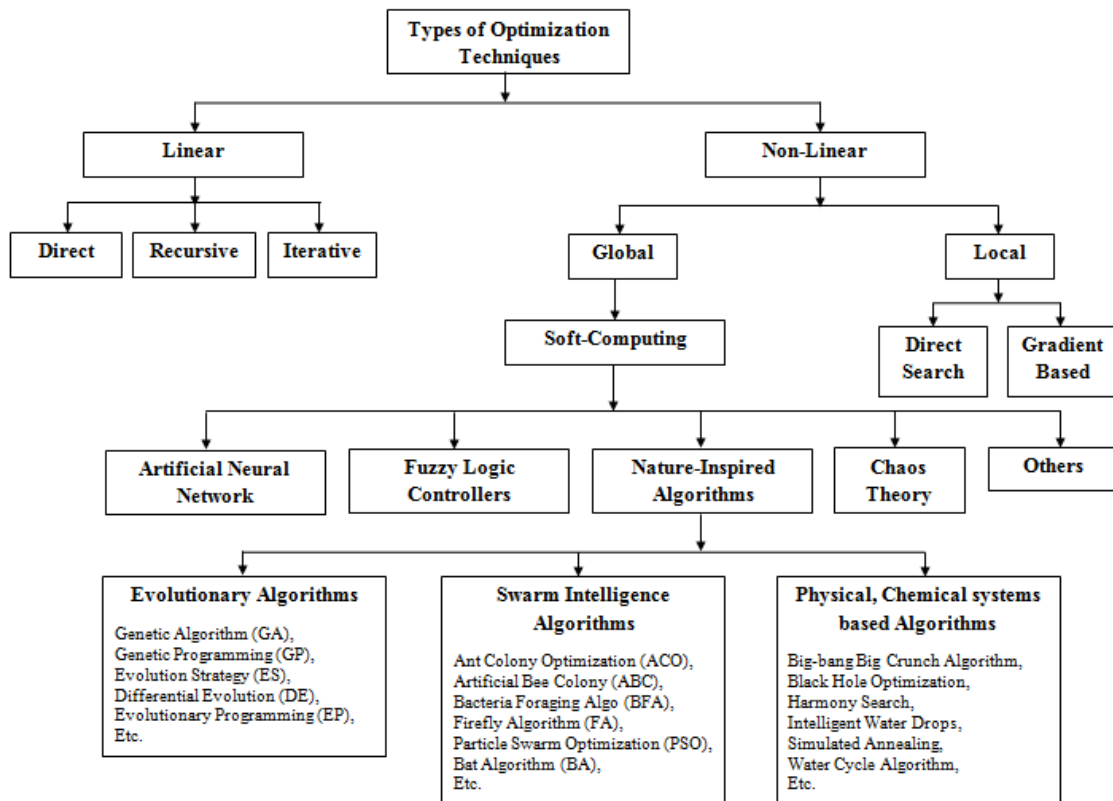
Figure 1.8: Classification of various optimization techniques [6],[7]

- Capabilities refer to the usefulness of meta-heuristics to different issues, without any specific algorithm structural changes.

- Most meta-heuristics have mechanisms free from derivation.

- Compared with traditional optimization methods, meta-heuristics have a higher contribution to avoiding local optima.

1.4.1   Genetic Algorithm (GA)

Genetic algorithms (GA) belong to a class of stochastic evolutionary techniques that have made them exceptionally important among researchers with robustness and the global quest for solutions space. The GA definition, first defined by Holland [8] and expanded to De Jong's functional optimization [9], includes the use of search strategies for optimization based on the Darwinian notion of evolutionary processes [10, 11].

A GA has considerable advantages over conventional methods of optimization as follows [12, 16, 19]:

- It is applicable to any challenge.

- In spaces of solutions, it performs a universal study.

- This does not necessitate a prior understanding of the question of optimization.

- This does not depend on the search's initial conditions.

- It optimizes parameters whether continuous or discrete.

- The cost function doesn't need derivative details.

- A large number of variables also operates effectively.

- It can run along with several computers in parallel.

- This lists the best criteria and not just a single solution.

- Parameters can be encoded.

- It can be used for numerical data, experimental data, or analytical functions.

While genetic algorithms have proven to be a fast and powerful problem-solving mechanism, it incorporates some limitations as well [20]. Listed below are some of its limitations:

- The most important, the concern is determining the representation of the problem when developing a genetic algorithm technique. The terminology used to describe objective function must be robust; i.e., random changes must be accepted in such a way that fatal errors do not occur.

22

- One big challenge to genetic algorithms is the coding of the objective (evaluation) function in order to achieve higher fitness and to provide better solutions to the challenges in hand. Failure to choose the fitness function can lead to significant issues such as being unable to search the solution to a problem, and sometimes even worse, attempting to return a wrong solution.

- Early convergence is another major issue which GA researchers need to address while generating Generic Algorithm solutions.

GAs have been a very prominent optimization method for these reasons. Their computational modeling is applied in a wide variety of disciplines on different issues, such as aerospace, operational analysis, social science, and quantum physics, etc. [8]-[21]. They have been applied in the field of electromagnetism, in the design and optimization of the geometric characteristics of antennas and arrays, in EMC problems, in array optimization problems, etc. [21]-[38].

1.4.1.1 Computation based on Genetic Algorithm (GA)

A genetic algorithm is a heuristic application, inspired by the theory of natural evolution by Charles Darwin. This algorithm illustrates the natural selection process where suitable individuals are chosen for reproduction in order to produce next-generation offspring [17].

Five phases of a Genetic Algorithm (GA) [17]:

1. **Initial population**: Implementing a GA requires an initial population generation. The cycle starts with a group of individuals that is called a Population. Every member of this population represents a binary string, called the chromosome, of length L. A set of parameters (variables) known as Genes characterizes one chromosome entity. Within a genetic algorithm, an individual's set of genes is represented using a list. Binary values (a string of 1s and 0s) are typically used. The population size is fixed. When new generations are created, those with the least fitness die, giving new offspring space. The initial population typically takes random values. Every single string is evaluated after creating an initial population, and its fitness value is then calculated. Fig. 1.9 represents the concept of the initial population [10-11].

2. **Fitness/Cost function**: The function of fitness or cost function decides just how strong an individual is. Fitness is an individual's ability to compete with other indi-

Genetic Algorithms
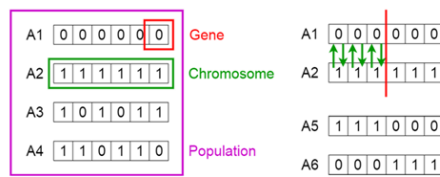
Figure 1.9: Concept of Population, Chromosome, and Gene in Genetic Algorithm [17]

viduals. It gives every single individual a fitness score. The likelihood of selecting an individual for reproduction is dependent on its fitness score. In other words, it specifies the criteria for rating possible hypotheses and for selecting them probabilistically for inclusion in the next-generation population [17, 18].

3. **Selection**: The concept of the selection process is to pick the most eligible individuals and let them transfer on their genetics to the next generation. It selects two pairs of individuals (parents) based on their fitness ratings. High-fitness individuals have a greater chance of being chosen for reproduction. The best strings out of a collection are picked based on performance. This is ensured by collection, that only the most suitable strings endure. In a wider sense, a natural selection should pick new-generation strings closer to the desired final results. Mathematically this implies that the population convergence is given [17, 18].

4. **Crossover**: Crossover describes the fragment switching between two binary strings at a crossover point chosen at random. In other words, from two parents it produces two new offspring. Two new strings are created after recombination, and these are introduced into the next population. Within a genetic algorithm, a crossover is the most significant process. A crossover point from within the genes is chosen at random for each pair of parents to be mated. For example, consider the crossover point to be 3 as shown in Fig. 1.10 [10-11]. **The crossover point**: Offspring is produced by exchanging the parents' genes among themselves before reaching the crossover point. Added new offspring to the population after the crossover operation.

5. **Mutation**: The operator is not a vital operation for the Genetic Algorithm. Mutation in a given string randomly produces a new bit or a new bit set, usually by flipping the bit or bits in the set. The mutation prevents early convergence because it causes population heterogeneity. In comparison, it means that the population converges to a global limit rather than a local limit. Mutation can be perceived as a way out of being stuck in local minima and is often implemented after crossover. Any of its genes may be subjected to a mutation with a low random probability in some new
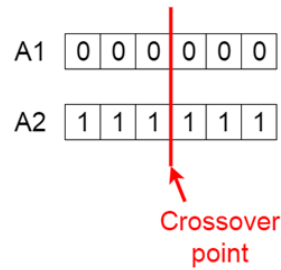
Figure 1.10: Concept of Crossover and Crossover point in Genetic Algorithm [17]
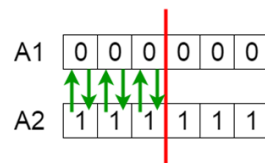
Figure 1.11: Concept of exchanging genes among parents in Genetic Algorithm [17]
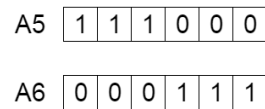
Figure 1.12: New offspring added to the population after crossover operation [17]

offspring produced. This means you can flip any of the bits in the bit series.
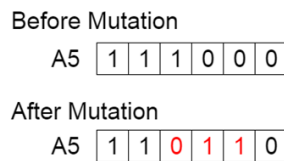
Figure 1.13: Mutation: before and after in Genetic Algorithm [17]

For each new generation, the sequence of phases is replicated to generate individuals that are better than the previous generation. If the population has converged the algorithm stops. Convergence means it does not produce offspring which vary considerably from the previous generation. The genetic algorithm is then said to have given a number of solutions to our optimization problem [17].

1.4.1.2 Developing a GA based optimizer

A code/program used for the implementation of a Genetic Algorithm (GA) based optimization process can be called as a GA based optimizer. Fig. 1.14 shows a block diagram

of a basic genetic algorithm optimizer. The parameters of each individual in the population are usually encoded as a string of bits (chromosomes) during optimization with GA. First-generation is randomly generated. Each individual's fitness is determined by its cost function. The fitter the individuals, the greater probability of reproduction is offered. Crossover and mutation are being used to allow the cost function to be explored globally. The best individual can be transferred to the next generation unchanged. This iterative cycle produces successive generations before attainment of a stop criterion [8]-[21].
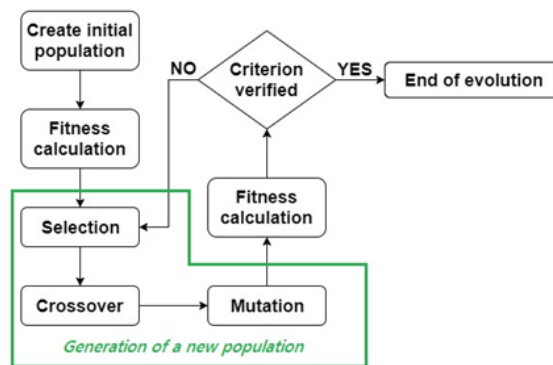
Figure 1.14: A basic genetic algorithm optimizer [21]

1.4.2 Particle Swarm Optimization (PSO)

Particle swarm optimization (PSO), which emerged from a study of the behavior of birds capturing food [39]-[46], was brought forward in the early 1990s by American scholars. During the early 1990's several studies on the social behavior of animal groups were developed. These studies have shown that individual animals belonging to a specific group, such as birds, fish, bees, and so on, are capable of exchanging knowledge within their species, and such capability confers an excellent survival advantage on these animals [39]-[46]. Inspired by these works, in 1995, Kennedy and Eberhart proposed the PSO algorithm [41, 42, 46], a metaheuristic algorithm suited to optimizing nonlinear continuous functions inspired by the idea of swarm intelligence, frequently used in animal communities, such as flocks and shoals.

A debate on the behavior of a flock is introduced to illustrate how the PSO has influenced the development of an optimization algorithm for solving complex mathematical problems. A swarm of birds flying over a location must find a point to land and, in this situation, the concept at which point the entire swarm will land is a complicated question

as it depends on many factors, that is, optimizing food supply and reducing the possibility at predator presence. In this sense, one can consider the birds' movement as a choreography; the birds walk synchronously for a period of time before the best place to land is determined, and all the flock lands at once. The question of finding the best-defined point to land features an optimization concern. For example, to optimize the survival conditions of its members, the flock must determine the best location, the latitude, and the longitude. To this end, each bird flies concurrently looking and assessing various points using multiple remaining parameters. Both of these have the benefit of understanding where the best position point is to be located before all of the swarm is identified [39]-[46].

PSO has considerable advantages over traditional techniques of optimization as follows [46]:

- The implementation of this algorithm is simple.

- Able to run computations in parallel.

- Just a few adjustable parameters.

- See a higher probability and efficiency of discovering the global optima.

- Robust methodology for optimization.

- Neither overlap nor mutate.

- Making convergence faster.

- Can be effective in solving problems with engineering.

- Had a shorter duration of computation.

Although the optimization of particle swarms has proven to be a fast and powerful problem-solving approach, some limitations are embedded in it [46]. Listed below are some of its limitations:

- Defining the initial specification criteria can be difficult. This can, however, be tackled.

- It can converge prematurely and be trapped with complex problems in particular to a local minimum. This can however be tackled.

- It cannot work out scattering problems.

PSOs have become a very common optimization method for these purposes. In a wide array of engineering disciplines, their computational modeling is applied to different problems. They have been applied in the field of electromagnetism in the design and optimization of the geometric characteristics of antennas and arrays, in EMC problems, problems of optimization of arrays, and problems of optimization using computational methods [46]-[75].

1.4.2.1 Computation based on Particle Swarm Optimization (PSO)

Optimization of particle swarm was adopted early to optimize continuous space problems. Using particle swarm optimization to solve optimization problems, the states of all the particles can be determined in the entire search space through their flying directions and distances. Three vectors (xi, pi, $pbesti$) can describe a particle: xi the particle's current position; pi the particle's current velocity; $pbesti$ the best spatial location sought by the particle.

Initialize the optimization problem for a group of random particles during the process of PSO optimization; this also involves initializing a particle's location to a random number and then iterating slowly until an optimum solution is achieved. A particle changes its position and velocity across two extremes throughout the iteration: one is the optimal solution sought by the particle itself, called specific extremum $pbest$; the other is the one found by the entire group of particles, called group extremum $gbest$.

If these two ideal values are determined, the particle can slowly change its position and orientation according to the following formula:

$$p(k + 1) = p(k) + a_1 * random() \left[pbest(k) - xi(k) \right]$$
$$+a_2 * random() \left[gbest(k) - xi(k) \right] \tag{1.6}$$

$$xi(k + 1) = xi(k) + p(k + 1) \tag{1.7}$$

Where, p is the particle velocity; the xi is the particle's current position; $a1$, $a2$ is learning factors above zero constants; $random$ is a random number between [0,1]. The velocity

requires an arbitrarily defined maximum value and minimum value, and we consider the velocity of the particle to be between $[-Pmax, +Pmax]$. There is incremental updating of their velocity during the cycle of particles:

$$
\begin{aligned}
&\text{if } p_{id} < -p_{max}, \ p_{id} = -p_{max} \\
&\text{if } p_{id} > +p_{max}, \ p_{id} = +p_{max}
\end{aligned}
\tag{1.8}
$$

From the equations, we can see that the updating of the particle's velocity takes into account not just its historical velocity but also its specific and global best location, a fact that will approximate the particle to the optimum position [40].

1.4.2.2 Developing a PSO based optimizer

As a PSO-based optimizer, a code/program used to execute a Particle Swarm Optimization (PSO) based optimization method can be named. Fig. 1.15 presents a block diagram of a simple Particle Swarm Optimizer.
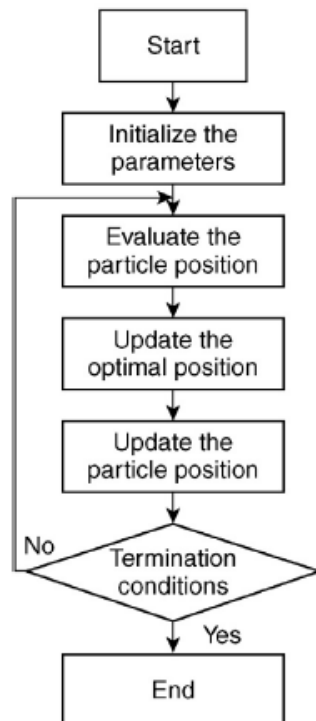
Figure 1.15: Procedure of a basic particle swarm optimizer [40]

The following is the step-wise method to understand the Particle Swarm Optimizer func-

tioning:

1. **Configure the parameters**: Initialize the particle's position and velocity in the D-dimensional search space into random numbers.

2. **Assess the particle's position**: Using a fitness function to determine the location of each particle.

3. **Make a comparison between**: (1) Compare the fitness value of step 2 with the current best value $pbest$ of the particle, and transform it into the newest $pbest$.

4. **Compare the particle's fitness** value with the global highest value $gbest$ and get the highest one.

5. **Update the particle**: Update the velocity and position of the particle according to the equations 1.6, 1.7, and 1.8.

6. **Iteration termination conditions**: Repeat to step 2 before the termination conditions are met, usually when the fitness value is optimum, or until the cumulative iterations have achieved.

1.4.3   Grey Wolf Optimization (GWO)

Grey wolf optimization (GWO) is a swarm intelligent strategy that mimics the wolves' leadership hierarchy is well known for group hunting [76]-[80]. Grey wolf is a member of the family Canidae and prefers to live in a pack. They have a rigid hierarchy of social dominance; the king is a male or female, called Alpha (α). Mostly the Alpha is responsible for making the decisions. The pack would follow the commands of the alpha wolf. The Betas (β) are subordinate wolves who support the Alpha in making decisions. The beta is an alpha counselor and packs discipline. The Grey wolf in the lower classification is Omega (ω), who must send the other superior wolves. If a wolf is not an alpha, a beta, or an omega, it is called a delta. Delta (δ) wolves rule the omega and reports to beta and alpha. Another interesting social behavior of grey wolves is group hunting. The main phases of hunting for the grey wolf are [78]:

1. Tracking, chasing, and getting closer to the prey.

2. The prey is hunted, encircled, and threatened until it ceases moving.

3. Attack to the prey.
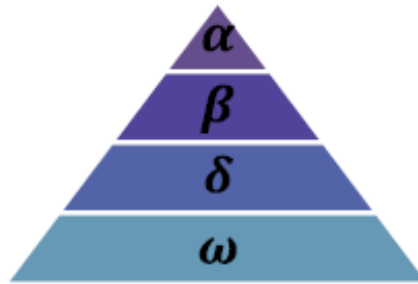
Figure 1.16: Natural social hierarchy of grey wolves [76]-[78]

The hunting techniques and the wolves' social hierarchy are modeled mathematically to develop GWO and optimize. The GWO algorithm is evaluated using standard test functions, which means that it has superior exploration and exploitation characteristics than other swarm intelligence techniques. The GWO has already been widely applied to solve numerous issues related to computer optimization [76]-[80].
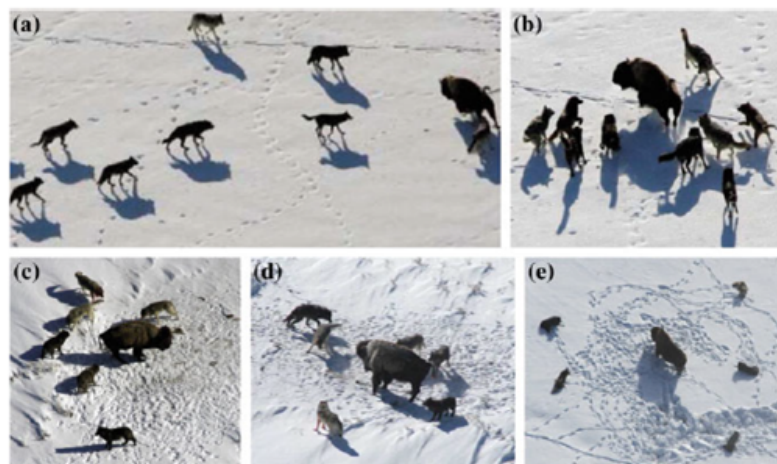
Figure 1.17: Squad behavior of Grey wolf hunting [77, 80]

1.4.3.1 Computation based on Grey Wolf Optimization (GWO)

Mathematical analysis of these social structures and hunting activities found in Grey Wolf Group and the Grey Wolf Optimization (GWO) methodology is discussed here [76]-[80]. As suggested by GWO, Al Wolves is the best solution for possible solutions, while Bt and Dl, respectively, are the second and third best solutions. The remaining potential alternatives are called Om. Al alpha wolf leads the hunting cycle. The hunting target gets

31

surrounded by Al, Bt, and Dl as the first step of hunting. From the following equations, this process is represented:

$$G(i + 1) = G_t(i) - X * W \qquad (1.9)$$

$$W = |Y * G_t(i) - G(i)| \qquad (1.10)$$

$$X = 2 * b * (a_1 - b) \qquad (1.11)$$

$$Y = 2 * a_2 \qquad (1.12)$$

Here, the Grey wolf position is G, the number of iterations is i, the target position is G_t, and the distance vector is W, the coefficient vectors are X and Y. Where b is reduced from 2 to 0 linearly by the number of iterations and $a1$, $a2$ are two random vectors between [0,1] which allow the wolves to reach any point between the current location and the target. The value of the vector b is modified to iteration i and the cumulative number of iterations T_{iter}.

$$b = 2 - i(2/T_{iter}) \qquad (1.13)$$

Al, Bt, and Dl, are known to have a clearer understanding of where the target is. G_1, G_2 and G_3 represents the three best solutions at iteration i, representing the wolves Al, Bt, and Dl. These are calculated as follows:

$$G_1 = |G_A - X_1 * W_A| \qquad (1.14)$$

$$G_2 = |G_B - X_2 * W_B| \qquad (1.15)$$

$$G_3 = |G_D - X_3 * W_D| \qquad (1.16)$$

The values of X_1, X_2, and X_3 are determined according to the equation 1.11. Following equations give the values of the distance vectors W_A, W_B and W_D:

$$W_A = |Y_1 * G_A - G| \qquad (1.17)$$

$$W_B = |Y_2 * G_B - G| \qquad (1.18)$$

$$W_D = |Y_3 * G_D - G| \qquad (1.19)$$

The Omega wolves change their positions according to Al, Bt, and Dl wolves' positions. The following equation gives the revised wolf positions:

$$G(i + 1) = (G_1 + G_2 + G_3)/3 \qquad (1.20)$$

1.4.4 HFSS® integration with MATLAB®

MATLAB is a powerful tool that offers numerous already implemented optimization algorithms and the ability to run a given user optimization algorithm. Genetic algorithms toolbox for applying GA based optimizer is picked from the numerous optimization algorithms available in MATLAB. A custom MATLAB code/program for Particle Swarm Optimization (PSO) and Grey Wolf Optimization (GWO) implementation is being developed. Then the ANSYS HFSS program is interfaced with MATLAB using the HFSS-MATLAB-APIs [82] to get the most out of all applications while allowing the user to have absolute power. Besides, the overall proposed loop has proven to be a successful tool in advanced electromagnetic engineering analysis, because the user can modify the optimization parameters as well as the antenna geometry. The main advantage of combining ANSYS HFSS and MATLAB is that the proposed methodology is completely automatic. This ensures that the optimization script produced will not allow user input until the solution is identified or thresholds are met to avoid.

HFSS-MATLAB-API [82] is a library toolbox for managing MATLAB ANSYS HFSS using the HFSS Scripting Protocol. This API provides a set of MATLAB functions by generating the required HFSS Scripts to create 3D objects in HFSS. Essentially, this feature library can do everything that can be achieved in the HFSS user interface and the 3D Modeler. When a script is created in this manner, creating the 3D model, solving it, and exporting it can be run in HFSS. In MATLAB, you can build the whole template, and simply use ANSYS HFSS to solve it.

1.5 Motivation and Objectives of this Research

There are some inherent disadvantages of conventional microstrip antennas such as its low gain, low directivity, low bandwidth, and low efficiency. Optimized microstrip antennas have been proposed by the researchers to overcome these limitations. A large number of methods are experimented in the past to improve single-objective optimization (both manually and using optimization techniques) and are discussed here. The motivation for this work came from the initial literature review, as presented below.

In 2004, Jacob Robinson et al. [83] has investigated the importance of particle swarm optimization (PSO) in Electromagnetics. Here, authors have discussed the robust stochastic evolutionary computation technique known as PSO and how it can be used for electromagnetic optimizations. Also, a study of boundary conditions is presented, and a representative example of the optimization of a profiled corrugated horn antenna is discussed.

In 2006, Neela Chattoraj et al. [24] have applied the Genetic Algorithm (GA) to the microstrip antennas for the optimization of gain by varying values of the substrate's dielectric constant and height. The optimized design was fabricated using PTFE substrate and Glass Epoxy substrate and fed using SMA connectors of 50 positions, and Cavity model analysis was done.

In 2007, L. Lizzi et al. [84] has carried out the design of a spline-shaped antenna optimized for UWB applications using particle swarm optimizer (PSO). The bandwidth achieved is about 5.5 GHz from 3.7 to 9.2 GHz frequency range.

In 2007, J. Anguera et al. [85] has designed a dual-band patch antenna with a frequency separation of the value of 1.37. The bandwidth is improved by using a stacked parasitic technique, achieving bandwidths of 12% and 5%, respectively. The stacked structure has a gain of 8.6 dB and 8.5 dB in both the frequency bands.

In 2009, Matthias John et al. [86] has investigated a printed monopole UWB antenna op-

timized using ParEGO multi-objective evolutionary algorithm. The radiating element and the ground plane are simultaneously optimized by the algorithm to achieve UWB characteristics.

In 2010, Siyang Sun et al. [31] has utilized a Genetic algorithm (GA) to design a microstrip patch antenna on Rogers RO4003 substrate material to achieve broad bandwidth. The optimized antenna design exhibited a bandwidth of approx—17.5%. Optimization improved the bandwidth to approximately three times from the base design.

In 2013, Anthony A. Minasian et al. [63] has applied particle swarm optimization (PSO) to improve the bandwidth of the rectangular patch antenna covering the full 5–6 GHz range. The design incorporated passive parasitically coupled sub patches resulting in an improved bandwidth of 19%.

In 2013, Jeevani Jayasinghe et al. [37] had developed a rectangular microstrip patch antenna and optimized the design for high-directivity using a Genetic algorithm (GA). The patch dimensions are optimized for a broadside pattern of 12 dBi directivity and fractional impedance bandwidth of 4 %.

In 2013, Anahita Ghaznavi Jahromi et al. [87] miniaturized a rectangular MPA using the metamaterial structure. The antenna is created using Rogers RT/duroid 5880 with a thickness of (h) 0.7874 mm and dielectric constant (ϵ_r) 2.2. Using the metamaterial composed of two nested split octagons in the antenna structure, the dimension of the proposed antenna is reduced.

In 2013, J. M. Jeevani W. Jayasinghe [88] applied the genetic algorithm optimization (GAO) method in designing the shape of the patch, position of the feed line, thickness of the substrate, and the selection of the substrate material. All these are done simultaneously to optimize antenna parameters like bandwidth and gain. The achieved fractional bandwidth is approx. 60% and gain is 6.5 dB.

In 2014, M. R. Ahsan et al. [89] has created an inset-fed rectangular MPA with double-P slots fabricated on a ceramic-PTFE composite material substrate having high dielectric constant. The antenna is designed for GPS and C-band applications. The fabricated antenna achieved a attained a gain of 3.52 dBi and 5,72 dBi with 81% and 87% of radiation efficiency, respectively, in the operating frequencies of 1.5GHz and 4GHz.

In 2014, M. T. Islam et al. [90] has designed two antennas for C/X band applications. The triangular- and diamond-slotted antennas are fabricated on polytetrafluoroethylene glass microfiber reinforced material substrate. The wide matching bandwidth is enabled by the microstrip feed line and antenna structure comprising a slotted radiating patch and the elliptical-slotted ground plane. The designed antenna offers fractional bandwidths of 13.69% (7.78–8.91 GHz) and 10.35% (9.16–10.19 GHz) at center frequencies of 8.25GHz and 9.95 GHz, respectively.

In 2014, Arindam Deb et al. [91] has evaluated the performance of evolutionary optimization techniques on circularly polarized microstrip antennas. Differential evolution, particle swarm optimization, genetic algorithm, and other similar variants are utilized along with three conventional feeding techniques for impedance matching over a frequency band.

In 2014, Ali Y.E.M et al. [92] has designed a two-layered microstrip patch antenna using FR4 material for GPS application. In this research, authors have demonstrated the improvements in return loss and gain by adding slots of different shapes and sizes.

In 2014, Maryam Rahimi et al. [93] has investigated periodic structures in antenna design for wireless applications and have been compared with CRLH miniaturization methods. Three antennas were created, and all antennas are tri-band, dual-polarized, and have displayed directional patterns.

In 2015, Qianying Pi et al. [94] has surveyed the applications of particle swarm optimization (PSO) in the field of Antenna design. In this work, the author has defined the basic PSO algorithm and provided insights to improve the base algorithm. Finally, major

applications of PSO in solving Antenna circuits are summarized.

In 2015, J. M. Jeevani W. Jayasinghe [95] designed a planar inverted F antenna (PIFA) optimized using a Genetic algorithm (GA) for 2.5 GHz and 5 GHz. GA is used to optimize the patch geometry, feed position, and shorting pin positions simultaneously. The converged antenna displayed fractional impedance bandwidths of 4% and 21%, respectively.

In 2016, E. J. B. Rodrigues et al. [96] has carried out the synthesis and design of particle swarm optimization (PSO) and artificial bee colony (ABC) based reconfigurable annular ring monopole antenna for UWB applications such as cognitive radio. In this design, two RF pin diodes used to connect antenna feeding lines to two microstrip stubs have used to change the frequency response of the antenna from narrowband to ultra-wideband operation.

1.5.1 Objectives of the Thesis

With taking the inputs from the above mentioned initial literature review, research gaps are identified, leading to the formulation of these three objectives for this thesis work:

1. To design and simulate the microstrip antenna (10.5-10.9 GHz of X-Band) for its multi-objective optimized performance.

2. To fabricate and characterize the optimized microstrip antenna.

3. Validation of simulated results with the measured ones.

1.6   Organization of the Thesis

This research work has been presented in six chapters. A chapter-wise summary is as follows:

Chapter 1: The first chapter explains the need and types of antennas, advantages, limitations, and applications of Microstrip Patch Antennas, their performance parameters, brief description of their excitation techniques, methods of analysis, etc. After this, a summary of existing optimization techniques is discussed. The basics of the Genetic Algorithm (GA), Particle Swarm Optimization (PSO), and Grey Wolf Optimization (GWO) are presented with their computational logic. This chapter also comprises the motivation, objectives, and a brief description of the thesis content. The formulation of the thesis objectives is primarily based on the initial literature review discussed in this chapter.

Chapter 2: The second chapter presents an elaborative literature review on soft-computing methods used for optimization of microstrip antennas. Various optimization schemes are used in the past particularly for the single-objective enhancement of impedance bandwidth, miniaturization of antenna dimensions, and improvements of the gain and radiation pattern, etc. A literature review is presented in this chapter on the use of Genetic Algorithm (GA), Particle Swarm Optimization (PSO), Differential Evolution (DE), Ant Colony Optimization (ACO), Artificial Bee Colony (ABC), and Gravity Search Algorithm (GSA) in the optimization of the antennas for various applications.

Chapter 3: This chapter presents the design, optimization, fabrication, and measurement of a conventional square-shaped microstrip patch antenna with a complete ground plane. The genetic algorithm is used in the process of design and optimization of this antenna. The step-by-step procedure of the antenna optimization is discussed along with the convergence graph, converged antenna design, simulated, and measurement results. A computerized photolithography process does the fabrication of antenna. Vector Network Analyzer (VNA) is used for the validation of the simulated results. Parametric analysis is also conducted and presented in this chapter to validate the converged design. This chapter

is concluded with the comparison of the proposed work with existing literature.

Chapter 4: This chapter presents the design, optimization, fabrication, and measurement of conventional rectangular shaped microstrip patch antenna with a partial ground plane. Three different optimization techniques - Genetic Algorithm, Particle Swarm Optimization, and Grey Wolf Optimization is used in the process of design and optimization of three different antennas. The step-by-step procedure of the antenna optimization is discussed along with the convergence graphs, converged antenna designs, simulated, and measurement results. Parametric analysis is conducted on all three designs and presented here to further support the research outcomes. This chapter is concluded with the comparison of the proposed work with existing literature.

Chapter 5: This chapter presents the design, optimization, fabrication, and measurement of a CPW-fed slot dipole antenna. The genetic algorithm is used in the process of design and optimization of this antenna. The step-by-step procedure of the antenna optimization is discussed along with the convergence graph, converged antenna design, simulated, and measurement results. A computerized mechanical etching process does the fabrication of antenna. Vector Network Analyzer (VNA) is used for the validation of the simulated results. Parametric analysis is also conducted and presented in this chapter to validate the converged design. This chapter is concluded with the comparison of the proposed work with existing literature.

Chapter 6: The conclusions drawn from the extensive results of the five converged designs are summarized in this chapter. Few suggestions on carrying out future scope related to the work are also discussed.

1.7 Chapter Summary

This chapter explains the need and types of antennas, advantages, limitations, and applications of microstrip patch antennas, their performance parameters, a brief description of their excitation techniques, methods of analysis, etc. After this, a brief review of exist-

ing optimization techniques is discussed. Out of the existing optimization techniques, the basics of the Genetic Algorithm (GA), Particle Swarm Optimization (PSO), and Grey Wolf Optimization (GWO) are presented in detail with their computational logic. This chapter also comprises the motivation, objectives, and a brief description of the thesis content. The formulation of the thesis objectives are primarily based on the initial literature review discussed in this chapter.

Chapter 2

LITERATURE REVIEW

2.1 Genetic Algorithm (GA) in Antenna Design and Optimization

In 1997, Daniel S. Weile et al. [22] has presented the concept of using Genetic algorithms as modeling methods and solution-oriented in electromagnetics because of their simplicity and their ability to optimize in complex multimodal search spaces. They defined the basic genetic algorithm and their history is recounted in the literature on electromagnetics. The implementation of sophisticated genetic operators in the field of electromagnetics is also defined, and design findings for a variety of specific applications are presented.

In 2002, H. Choo et al. [23] has presented a Genetic Algorithm (GA) based patch prototype for multiband microstrip antennas. The configured patch demonstrates a random frequency range varying from 1:1.1 to 1:2 accomplished for dual-band application. They have also created tri-band and quad-band microstrip shapes and the resulting designs display good operations at the defined frequencies. All results were confirmed using laboratory FR-4 substrate measurements.

In 2006, Neela Chattoraj et al. [24] has presented the implementation of the Genetic Algorithm (GA) is stated for maximizing the gain of microstrip antennas with and without

dielectric superstrate. In both scenarios, the cost functions are designed using the cavity method for microstrip antenna analysis. The results are verified by laboratory measurements.

In 2006, Robert K. Shaw et al. [25] has presented a Genetic Algorithm (GA) technique for the development of stacked antenna arrays for broadband or multi-band operations. In an infinite array setting, the structural and electrical properties of a single component are optimized. To optimize microstrip patch antenna components having complex geometries including non-uniform dielectric materials in the array setting, a full-wave Periodic Finite Element-Boundary Integral (PFE-BI) process is used in combination with a Genetic Algorithm (GA) in parallel. An example is also discussed which achieved a bandwidth of 35%.

In 2006, M. John et al. [26] has investigated a Genetic Algorithm optimized patch monopole antennas. During the architecture, overlapping sub-patches were used to enhance electrical interaction at the corners of such sub-patches. The findings were compared with the configuration of a rectangular monopole antenna. The bandwidth is improved by 63 % over the rectangular patch in comparison with the GA optimization technique.

In 2007, M. John et al. [27] has presented It presents a method for designing and optimizing wideband planar antennas utilizing the Genetic Algorithm (GA). GA involves sub-patches overlapping in such patterns where two sub-patches connects at the corner, thereby minimizing losses. This technique is utilized to design a higher-cellular, WLAN, and UWB wideband monopole antenna with the application. The optimal solution was fabricated to perform experimental measurements.

In 2008, P. Mythili et al. [28] has presented Compact genetic microstrip antennas design problems for mobile applications. The antennas that have been optimized using GA have a non-conventional shape and occupy less volume in comparison to the conventionally available antennas for a similar frequency band. An attempt was made to advance the performance of the genetic microstrip antenna by adjusting the ground plane to have a fishbone structure. The GA optimized antenna performs higher than the conventional an-

tenna.

In 2009, S. Y. Sun et al. [29] has utilized A Genetic Algorithm (GA) for optimizing the complicated structure of the microstrip antenna. A wireless microstrip patch antenna is proposed. An E-form patch and capacitor compensated technique are combined to increase the antenna bandwidth. To optimize the antenna structure, the Genetic Algorithm (GA) combined with Finite Element software is applied. The accuracy and output of this system are demonstrated when the optimized antenna is compared with the un-optimized antenna. The bandwidth improved from 6 % to 16 %.

In 2009, Si-Yang Sun et al. [30] has utilized the Genetic Algorithm (GA) in conjunction with the Finite Element technique to design a broadband patch antenna. By withdrawing some parts of the common patch antenna, the broadband characteristic is realized. Comparing the optimized proposed in this work with an un-optimized antenna design proves the effectiveness and stability of this technique. As a result of optimization, the bandwidth increased from 6 % to 17.8 %.

In 2010, Siyang Sun et al. [31] has implemented a Genetic algorithm (GA) for designing the patching microstrip antenna for wide bandwidth. A fair agreement between simulated results and GA-optimized design measurement values are achieved. The optimized patch configuration shows an increase in bandwidth compared to a typical microstrip antenna, demonstrating the validity of the concept.

In 2010, Siyang Sun et al. [32, 33] has presented a wide bandwidth broadband microstrip antenna. An optimization project is created to promote the antenna design based on the combination of a Genetic Algorithm (GA) with HFSS.

In 2011, Naveen K. Saxena et al. [34] has presented the Usage of the Genetic Algorithm (GA) to optimize the essential parameters of magnetically biased microstrip antenna developed on ferrite substrates. The cost functions for the GA program were developed using the cavity method for microstrip antenna evaluation. The impact of external magnetic bi-

asing has also been integrated as an essential propagation constant in the formulation of the cost function. Simulated results obtained from the optimization are in good agreement with the measured results.

In 2011, J. M. J. W. Jayasinghe et al. [35] have designed a Bluetooth and HIPERLAN lightweight dual-band patch antenna. A dielectric constant 3.2 and height 3.175 mm substrate is used for the construction. The patch element of the lower frequency band is identical to the traditional rectangular patch. Optimization through genetic algorithms is then used to optimize the feed position and the patch geometry. Simulations are conducted with the HFSS. The developed antenna offers bandwidths in Bluetooth and HIPERLAN2 frequencies of 4.1 % and 9.6 %.

In 2012, Simranjit Kaur Josan et al. [36] have applied Genetic algorithms (GA) for the measurement of Elliptical Microstrip antenna performance characteristics. The inputs to the issue include substrate thickness, dielectric constant, eccentricity, and also mode frequency. The results are the optimized semi-high axis length 'a', which is used to measure other parameters, such as semi-low axis length and odd mode frequency. GA optimization's outcomes are compared with measured results to validate the research.

In 2013, Jeevani Jayasinghe et al. [37] has proposed a single microstrip patch (MPA) high-directive antenna with a rectangular profile. It is built with the benefit of not requiring a feed network using Genetic Algorithms (GA). The patch is in a range of 2.54 x 0.25, with a wide directivity of 12 dBi and a bandwidth fractional impedance of 4 %. The antenna is developed and the measurements are compared with the simulated outcomes to validate the research.

In 2015, Mohammed H. Miry et al. [38] have presented the Designing and improving a physically low-cost print antenna for UWB radio applications. A Genetic Algorithm (GA) is used to achieve a full-band UWB specification. The antenna is made of a slot cut radiator mounted to the floor of a trapezoid-shaped ground plane, with dimensions of the antenna as 21.6 mm x 18.8 mm x 1.6 mm. The prototyped antenna's result is compatible with the

FCC regulations, with a 10 dB bandwidth or better around the frequency range 2.1 GHz - 13.2 GHz and a reasonable omnidirectional radiation pattern.

In 2016, Mohammed Lamsalli et al. [21] has presented a GA based design of rectangular patch antenna parameters for miniaturization. Performance analysis was conducted using the CST tool. The surface current path has meandered in the built antenna, which increases the electric antenna range. This means that the total surface of an antenna of the same resonance frequency is significantly reduced. It reduces the patch size to 82 % with a radiation pattern characteristic of the designed microstrip patch antenna compared to a regular patch that resonates at the same frequency.

2.2 Particle Swarm Optimization (PSO) in Antenna Design and Optimization

In 2005, Nanbo Jin et al. [47] has implemented the optimization using Particle Swarm (PSO) technique for the creation of an E-shaped patch antenna. Different cost functions are used to determine individual antenna performance, and the FDTD analyzer assesses different cost functions. The optimization is carried out on parallel clusters in order to reduce the calculation time. Characterization of the produced optimized antennas shows adequate dual-band and wideband properties.

In 2008, R. N. Biswas et al. [48] has proposed A dual-slot path microstrip antenna optimized for operation at approximately 2 GHz frequencies using APSO techniques. The APSO-IE3D combined system offers a new solution to correctly implement a low-profile dual-slot patch antenna configuration fed using a probe. The simulation results demonstrate that the antenna has a bandwidth of 28.7 MHz within the 1.95-2.0 GHz frequency range. he antenna was manufactured on a substrate having a dielectric constant of 2.4 and 1,5875 mm of thickness. The calculated values of the antenna parameters (e.g. gain, VSWR, directivity, and return-loss) were found to correlate well to the simulated results within the permissible limit. The basic theory of APSO-IE3D development and the simu-

lated vs. experimental results for a dual-slot patch is provided in this study for comparison.

In 2008, V. S. Chintakindi et al. [49] has explored PSO's ability to be used in the precise determination of an equilateral triangular micro-stream (ETMP) antenna's resonant frequency. The findings were correlated with the GA optimized design and experimental values. The findings are well established and encourage the use of Particle Swarm Optimization in the design of the antenna.

In 2009, M. T. Islam et al. [50] has implemented the optimization of particle swarm (PSO) with microstrip patch antenna using curve fitting. An IMT-2000 band patch antenna of inverted E-shape is optimized using the PSO optimization technique. The curve fitting data were collected from IE3D utilizing several geometric antenna parameters. The data generated equations that describe the relationship between different parameters of a microstrip patch antenna. To build the curve, Graphmatica curve fitting program has been used. The PSO software was planned and implemented in MATLAB and then in IE3D, the customized antenna was simulated. The distinction between a traditional antenna and an optimized PSO antenna was improved considerably over bandwidth. The bandwidth of the inverted E-shaped patch antenna increased by 15 %.

In 2009, F. A. Ali et al. [51] have implemented A hybrid PSO approach that combines the Genetic Algorithm (GA) with the PSO method. In this study, a review of the application of PSO and its variants to optimize microstrip patch antenna feeding-points was carried out. An approach to the hybrid PSO using binary operator (hPSO-B) is implemented for the optimization of the antenna. There have also presented descriptions and comparisons of the various PSO types.

In 2009, Y. Choukiker et al. [52] presented a Particle swarm optimization (PSO) system based on the IE3DTM patch antenna architecture. The benefits it provides in optimizing geometric parameters efficiently for antenna performance. The reported return loss is of -43.95 dB at 2.4 GHz and -27.4 dB at 3.08 GHz. The reported bandwidth is having ranges from 2.38 - 2.41 GHz (i.e. 33.54 MHz).

In 2009, M. Gangopadhyaya et al. [53] has utilized Particle Swarm Optimization (PSO) for the precise determination of the rectangular aperture coupled patch antenna's resonant frequency. The work is carried out in various microwave frequency ranges and extends to the Ku band. The process is repeated for a specific antenna and feed substrate dielectric constants. The optimization problem consists of three variables: stub length, aperture width, and length. The findings are reliable and promote the use of PSO.

In 2010, Y. K. Choukiker et al. [54] have developed an E-Shape Microstrip Patch Antenna for the ISM band. The patch antenna is simulated with the IE3DEM simulator and optimized using a stochastic optimizer for the evolution. Professional PSO. Optimized tests show that the antenna operates in the ISM frequency band. Such bands include the Bluetooth, IEEE 802.15.2, 802.11, and 802.11b frequency bands. The antenna has decent radiation characteristics and a reasonable gain in the operating band.

In 2010, M. Gangopadhyaya et al. [55] has utilized PSO for microstrip antenna optimization. PSO is used for optimizing the resonant frequency of the rectangular microstrip antenna fed by the coaxial cable. Research is performed at various microwave frequencies, from 3 - 18 GHz. The challenge with optimization consists of three variables i.e. feed position, patch length, and width. The findings are reliable and promote the use of PSO.

In 2010, M. Capek et al. [56] has presented the use of IFS (Iterated Function System) fractals used as a patch antenna for planar microstrips. A versatile tool named IFS Maker has been developed to generate the IFS fractals. An effective patch design is shown. Forward to fractal preliminary design, one can start by using the PSO algorithm to optimize the IFS collage. The PSOptimizer tool manages that procedure. In general, the optimization loop works with any number of conditions for optimization. This feature comes with the tool IFS Limiter. Resonant frequencies (eigenvalue problems) are calculated in the Comsol Multiphysics environment with the cavity model.

In 2010, S. Chamaani et al. [57] has developed an ultrawideband (UWB) antenna ar-

rays, a method is presented for obtaining optimum tradeoffs between side-lobe level and beam-width in the time domain. Multi-objective particle swarm optimization is utilized to address the goals. Mutual coupling effects are not taken into consideration in the optimization process. Each element in the array is a Vivaldi antenna which is antipodal. The framework for optimization is extended to three separate descriptors of time-domain patterns. In this study, the Pareto fronts obtained provides lower bandwidth and sidelobe levels as compared with the existing literature. CST Microwave Studio software was used for simulation. The 4-element simulated array shows an energy pattern gain of 13.7 to 17.2 dBi in the entire frequency spectrum from 3 to 11 GHz, and an SLL of -12 dB.

In 2011, S. K. Jain et al. [58] has presented An algorithm based on particle swarm optimization (PSO) developed to determine the patch dimensions of the dual-band square patch stacked X/Ku band antenna. The objective function for the PSO is evaluated to decrease the long and complex simulation time with the help of a neural network (NN). The findings of this PSO-based CAD model for certain standard stacked patch antennas were cross-checked with the experimental results.

In 2011, S. Kumar et al. [59] has used Particle Swarm Optimization (PSO) to improve circular microstrip patch antenna resonance frequency. Using PSO an updated formula is given for resonant frequency. The results obtained using particle swarm optimization were compared with existing literature experimental and theoretical values. The results were in good agreement with the experimental value with a 0.18 % average error.

In 2011, J. Kovitz et al. [60] has investigated Particle Swarm Optimization (PSO) to improve circular microstrip patch antenna resonance frequency. Using PSO an updated formula is given for resonant frequency. The results obtained using particle swarm optimization were compared with existing literature experimental and theoretical values.

In 2013, I. Vilović et al. [61] has presented a microstrip patch antenna design using the PSO (Particle Swarm Optimization) optimized artificial neural network algorithm. An antenna was made according to the results of neural network design. The results of the

estimated and neural network are compared with the values of measured antennas.

In 2013, R. Nagpal et al. [62] has utilized a Parallel PSO technique is applied in conjunction with the standard equation developed to calculate accurately the resonant frequency of any size and substratum thickness rectangular microstrip patch antenna. PPSO's results are better than PSO and closer to experimental values. The methodology proposed in this work appears to be a simplistic soft computing tool for calculating microstrip antenna parameters, such as resonant frequency.

In 2013, A. A. Minasian et al. [63] has demonstrated Particle Swarm Optimization (PSO) as a design tool for an array of microstrip antennas that is parasitically coupled. The antenna resulting from the application of PSO with no limitations implemented during optimization on the array shape apart from the maximum dimensions. For the IEEE 802.11a WLAN 5-6 GHz band, the structure combining passive parasitically coupled sub-patches is described to achieve a coefficient of reflection, satisfactory gain, and an omnidirectional radiation pattern.

In 2014, B. R. Behera et al. [64] has presented an assessment of selecting an appropriate patch between circular and rectangular patch for a specific operating frequency which can be extended to a frequency range. It defines all these design parameters such as area, substrate height, substrate dielectric constant, and performance parameters such as directionality, E and H-plane half-power beamwidth, coefficient of reflection, VSWR and loss of return. Using Particle Swarm Optimization (PSO), the patches are optimized, and their results are compared to determine the best patch.

In 2014, I. Vilovic et al. [65] has presented a circular microstrip antenna design and feed position determination based on PSO (Particle Swarm Optimization) algorithm is presented. PSO algorithm obtains an optimized feed position of microstrip patch antenna to attain matching input impedance. Another optimization algorithm (golden search section) compares the results obtained by the PSO algorithm, and good agreement is obtained.

In 2015, E. R. Schlosser et al. [66] has presented the use of optimization methods to synthesize linear antenna array radiation patterns. A comparison of the performance between Particle Swarm Optimization (PSO) and Genetic Algorithm (GA) for obtaining different pattern shapes is made.

In 2016, S. Dey et al. [67] has presented an optimizing microstrip patch antennas by means of a technique popularly known as Particle Swarm Optimization (PSO) to enhance the resonant frequency of rectangular gap coupled with MA. Validation is performed for frequencies in the range from 3 GHz to 18 GHz. Patch frequency, patch width, and distance width are the parameters that are taken into consideration for optimization. Results-based observation encourages the use of PSO for the most favorable outcome.

In 2016, Ç. Korkuç et al. [68] has utilized Particle swarm optimization (PSO) to make circular antenna arrays more efficient. Particle swarm optimization is chosen to curtail the side lobes of circular antenna arrays giving successful results in swarm optimization.

In 2016, A. Bhattacharya et al. [69] has presented Within the X, Ku-band of the spectrum, an ultra wide-band Monopole Antenna having Hexagonal Patch Structure is developed for many broadband applications. The patch is conceived with Ring Geometry. The design of the antenna is optimized using the technique of Particle Swarm Optimization (PSO). The antenna proposed finds its application in the frequency spectrum of microwaves from 7.5 GHz to 20 GHz.

In 2017, A. V. Miranda et al. [70] presented an effective linear antenna (USLA) array synthesis technique is proposed to reduce the peak sidelobe level (PSLL) when directing the main beam over the pre-specified scanning angles. Particle swarm optimization (PSO) algorithm is used to evaluate the optimal combination of spacing elements leading to improved design efficiency in terms of SLL reduction not only at boresight but also at various scanning angles. Throughout this analysis, the authors attempted to resolve this limitation by properly assessing the spacing of the set of elements. For optimization, a 16-element USLA array is selected and results obtained via the proposed method are tested against

uniformly spaced arrays at 300 and 450 scan angles.

In 2017, A. Lalbakhsh et al. [71] has utilized PSO in designing a near-field time-delay equalizer metasurface (TDEM) to boost the path and radiation patterns of classical band-gap electromagnetic resonator antennas. The PSO had designed three layers of conductive printed patterns on the metasurface. Predicted and measured results indicate a substantial increase in antenna efficiency, including antenna directivity enhancement of 9.6 dB, lower side lobes, and greater gain. The prototype's calculated directivity is 21 dBi and the band-width of 3 dB is 11.8 %.

In 2017, L. Pappula et al. [72] has discussed the antenna array synthesis process. It requires simultaneous optimization of conflict parameters such as peak sidelobe (PSLL) level and first null beamwidth (FNBW). For this study, the multi-objective model of the recently developed Cauchy mutated cat swarm optimization (CMCSO) is being developed and suggested for the PSLL and FNBW trade-off. Using a multi-objective (MO) type of CMCSO, conventional cat swarm optimization (CSO), and particle swarm optimization (PSO), a Pareto-optimal front with all the compromised solutions are created. Targeted compromise solutions can be selected depending on the problem in hand from the ideal Pareto line. Numerical examples indicate that MO-CMCSO produces superior performance compared to MO-CSO and MO-PSO.

In 2018, S. Narayanan et al. [73] has presented a circularly polarized (CP) microstrip patch antenna at the X-Band frequency optimized using Particle Swarm Optimization (PSO). Circular polarization is accomplished by using the pin-charged technique in the proposed design. First, to that S11 two shorting pins are inserted in the single-fed patch. Then, the placement of the inductive pins in the initial design, obtained through numerical methods, is optimized using the PSO algorithm to achieve an axial ratio in the appropriate frequency range of less than 3 dB. The converged result from the PSO algorithm fulfilled the requirements of intent and design.

2.3 Differential Evolution (DE) in Antenna Design and Optimization

In 2007, J. Li [97] has utilized Differential evolution (DE) to refine the Yagi-Uda antenna geometric parameters. For the evaluation of each antenna design produced by DE during the optimization procedure, based on thin wire molding a method of moments code. The length and spacing of many Yagi-Uda antennas and V-shaped antennas are designed to demonstrate the versatility of the process. The findings illustrate clearly that DE is a reliable and effective method for optimizing antennas to the desired target requirements.

In 2010, A. Chatterjee et al. [98] has applied the Differential Evolution (DE) algorithm to minimize the lobe rates of the concentrated ring system of isotropic antennas while retaining a fixed and variable first null beamwidth (FNBW) by optimizing ring distance and inter-element distance of each ring.

In 2011, A. M. Montaser et al. [99] has explored The effect of a defecated earth plane structure (DGS) as well as the effect of faulty radiation patch slots and the corresponding stub on the return loss (S11). The Differential Evolution (DE) technique in the UWB frequency range is considered to reduce S11 by evaluating the antenna dimensions, and the results are compared with other optimization methods such as Genetic Algorithm (GA) and Particle Swarm Optimization (PSO). The antenna is also built into a plastic case (Er = 3) to test the effect of the antenna on the radiation.

In 2011, A. Deb et al. [100] has presented It is the latest approach to applying the differential evolution (DE) algorithm to construct a T-stub mounted dual-frequency microstrip antenna. The fitness values of different DE solutions in each generation are imported from the current IE3D software process.

In 2011, A. Chatterjee et al. [101] has proposed a Method of pattern synthesis for creating a dual pattern of radiation of the sector beam pair of concentric isotropic elements with desired sidelobe rates by switching among elements sharing similar amplitude dis-

tributions between the radial phase distribution. The optimal range of radial amplitude and radial phase distributions is determined using the Differential Evolution Algorithm to produce dual radiation patterns with lower side lobe rates. The array with the highest radial amplitude and radial distributive phases produce a pencil beam, while a sector beam is produced in the vertical plane by an array with the same amplitude but optimum radial phase.

In 2011, S. K. Goudos et al. [102] has explored project methodology based on a self-adaptive SADE algorithm for real-time antenna and microwave architecture issues. Those involve a synthesis of the linear array, patch antenna, and filter configuration for the microstrip. There are 6 to 60 unknowns for design issues. The authors contrasted the DE strategy for themselves with common PSO and DE variants. They evaluated the efficiency of the algorithm with regard to convergence speed, and statistical results.

In 2011, A. Deb et al. [103] have designed Using the Differential Evolution (DE) antenna a probe-fed microstrip antenna is assembled. The DE fitness function is obtained by cavity model analysis. Results are obtained with DE correspond to those obtained by the use of a specific genetic coded algorithm (GA) and PSO.

In 2013, A. K. Behera et al. [104] has presented a cosecant squared shaped beam pattern that is produced from a linear antenna array uniformly spaced but not consistently excited, optimized with the algorithm of differential evolution (DE). The beam pattern for the angular beamwidth of 320 is synthesized by lowering the lateral lobe level (SLL) to -20,06 dB and nearly without rippling in the formed area.

In 2014, S. Das et al. [105] has applied the Differential Evolution (DE) search algorithm (BSA) to find almost optimal practical solutions for eliminating interference from linear antenna arrays. The problem of raising the lateral lobe level concerning the main beam is considered. For convenience antenna arrays, ideal elements are discussed, and thus the reciprocal coupling effect is ignored—combined quest results in this problem of intrusion suppression.

In 2015, M. Gangopadhyaya et al. [106] has implemented Differential evolution (DE) algorithm to regulate the resonant frequencies of the rectangular patch antenna fed on the inset line taking into account its geometric parameters such as patch duration, patch width, and inset position as the unknown variable. Simulation tests for the different microwave frequencies of the optimized antennas (3 to 18 GHz) were demonstrated.

In 2016, A. Mukhopadhyay et al. [107] has presented Differential Evolution (DE) and Cuckoo Search (CS) algorithms for specifying the microstrip antenna configuration parameters. In this analysis, a relationship has been defined among the geometrical parameters and bandwidth of a co-axis-fueled patch antenna using the Curve fitting model. The inquiry is performed over a certain spectrum for microwave frequencies. A comparative analysis is carried out between the results obtained by optimizing the patch frequency, the patch width, and the feed positions using DE and CS algorithms for improving bandwidth.

In 2016, A. Mukherjee et al. [108] has proposed for minimization of the maximum sidelobe (SLL) stage, non-uniformly spaced planar antenna arrays (NUSPAA) of different geometries with uniform arousal are considered. The inter-element locations of the remaining elements can be optimized using the Differential Evolution (DE) algorithm by simply turning some of the elements off of the standard rectangular array. With the simple feed network of uniformly excited antenna arrays (UEAA) the suggested approach will effectively reduce the number of antenna elements with SLL reduction. The simulated outcome of an optimized SLL with different geometries from a 17 / 17 spectrum is presented and the efficiency of the proposed solution is compared.

In 2016, H. Liu et al. [109] has proposed A differential evolution (DE) with several constraints mapping matrix for sparse rectangular, flat arrays. The numbers of elements, the minimum distance of the neighboring elements, the planar array aperture are included. The highly restricted optimization problem is transformed by implementing the new matrix mapping between the element distance and DE variables into a non-complicated problem with only lower and higher limits, and the inaccessible solutions are obviously avoided

54

during the optimization process. The results of the simulation demonstrate the high efficiency and robustness of the proposed procedure and demonstrate that our system can produce better results than current methods.

In 2018, A. Deb et al. [110] have undertaken Performance compared with many antenna and tablet prototypes with various variants and hybridized DE algorithms. These include DE, biogeography-based optimization with DE (BBODE), DE with global and local neighborhood search (DEGL), self-adaptive DE (SADE), MDE with p-best crossover strategy (MDE-pBX), modified DE (MDE), improved DE (IDE), harmonic search DE (HSDE), adaptive DE with optimization-state estimation (ADE), and DE with an individual dependent mechanism (DE-IDP-IDM).

2.4 Ant Colony Optimization (ACO) in Antenna Design and Optimization

In 2011, K. Tenglong et al. [111] has demonstrated an antenna layout optimized using ACO algorithm. The traditional ant colony optimization algorithm has the limitations of simple local capture and difficult to optimize continuous functionality. Therefore, discordant variable encoding and nearby optimization are used in the algorithm modified, resulting in enhanced search efficiency and not easy to catch local optimum. Computer simulations have shown that the algorithm can produce better performance.

In 2012, R. E. Zich et al. [112, 113] has presented the results of some optimization strategies in antenna optimization (DE, BBO, SGA). In this research, new evolutionary techniques refine an elliptical reflect antenna: Ant Colony Optimization (ACO), Biogeography Based Optimism (BBO), Differential Evolution (DE), Stud Genetic Algorithm (SGA), and Population-Based Incremental Learning (PBIL). The optimized architecture of the reflection array aims to equate its output with a complex problem of EM optimization. Results show some techniques (DE, BBO, SGA) in antenna optimization to be particularly successful.

In 2014, Y. Yang et al. [114] have implemented the Genetic-Ant hybrid colony optimization (GACO) antenna architecture algorithm. The hybrid algorithm is a hybridization of the algorithm Ant Colony Optimization (ACO) and the genetic algorithm (GA). The algorithm allows the ACO algorithm to search rapidly and the genetic algorithm (GA) to search globally. It, therefore, prevents ACO's behavior from dropping into optimal local behavior and can also be extended to the global continuous optimization problem. This work blends the GACO algorithm with HFSS applications for antenna architecture. The approach is seen in an example: the design of a rectangular antenna with a U-slot for double band antennas and a broadband antenna.

In 2017, M. Akila et al. [115] has investigated the Optimization of Particle Swarm (PSO), Genetic Algorithm (GA), and Colony Optimization (ACO) for electromagnetic optimization problems. This work is performed using ACO, PSO, and GA based PSO (GA-PSO) to optimize the feed position of a plain patch and the distance between the portion in a linear array to achieve the desired beamwidth. ACO seems to be offering solutions with less computational time for the above-mentioned problems.

In 2018, A. Reineix et al. [116] has explored The antenna's complex far-field radiation pattern and its optimization into an extended algorithm for Ant Colony Optimization (ACO). The model is meshless, i.e. it can be implemented in a full-wave system without having to adhere to the meshing that is currently used for carrier modeling. The FDTD approach is used to test the dipolar model and its integration with a carrier. Hence, one major interest of this method is to obtain a representation of the Cartesian grid antenna de-correlated. The example of this method is also given.

2.5 Artificial Bee Colony (ABC) in Antenna Design and Optimization

In 2001, R. Holtzman et al. [117] has designed an ultra-wide-band (UWB) semi-conical antenna mounted on an infinite ground plane. The specification is such that the ratio of the transmitted pulse's principal limit to its temporal sidelobes will be maximized. They made use of the Genetic Algorithm (GA), and Artificial Bee Colony (ABC) as the optimization technique for this purpose. As a mathematical model, it is coupled with the Yee variant of the FDTD process.

In 2013, J. Yang et al. [118] has presented a hybrid algorithm based on the ABC algorithm and differential evolution (DE) called ABC-DE is applied to pattern synthesis problems of various types of time-modulated arrays (TMAs). It includes small equal-ripple side-lobe (SLL) pattern syntheses, deep null level pattern, multiple-beam patterns, and satellite footprint pattern. The results of the experiment show that ABC-DE has a good output in convergence rate and capacity to explore. This is compared to other improved evolutionary algorithms, suggesting that the proposed algorithm could be an efficient solution to synthesis problems with TMAs.

In 2018, X. Zhang et al. [119] has discussed the use of an artificial bee colony (ABC) algorithm in solving electromagnetic inverse problems. The ABC algorithm, however, costs too many iterations and converges slowly in the antenna configuration. This paper proposes an adaptive ABC (AVDABC) variable differential system. This approach reduces the range of decision variables to be altered. Existing modified ABC algorithms in one iteration using the same search equation. The proposed adaptive variable approach assigns the selected decision variables in one iteration with various search equations and is more complex than current ABC algorithms. The AVDABC algorithm is demonstrated by numerical simulation of mathematical functions by the design of a sparse non-uniform antenna array and Yagi-Uda antenna that achieve promising results. It helps to overcome antenna array configuration issues with the proposed algorithm.

2.6 Gravity Search Algorithm (GSA) in Antenna Design and Optimization

In 2016, P. Swain et al. [120] has presented an application of nature motivated population-based algorithm called Gravitational Search Algorithm (GSA) for optimization of Linear Dipole Antenna Array (LDAA). The LDAA's design parameters to be optimized are the length of the dipole antenna elements and the spacing out of each of the two adjacent device classes. Using MATLAB, the self-developed GSA is used to refine the LDAA's design parameters to evaluate a set of LDAA performance parameters such as directionality and sidelobe level. The main objective of designing an antenna is to achieve high directional gain, narrow beamwidth, and low side lobe. The tailored radiation patterns show that GSA's approach to the issue of optimization is found to be successful in achieving a higher path and lower sidelobe.

2.7 Chapter Summary

This chapter presented an elaborative literature review on soft-computing methods used for optimization of microstrip antennas. Various optimization schemes are used in the past particularly for the single-objective enhancement of impedance bandwidth, miniaturization of antenna dimensions, and improvements of the gain and radiation pattern, etc. A literature review is presented in this chapter on the use of Genetic Algorithm (GA), Particle Swarm Optimization (PSO), Differential Evolution (DE), Ant Colony Optimization (ACO), Artificial Bee Colony (ABC), and Gravity Search Algorithm (GSA) in the optimization of the antennas for various applications.

Chapter 3

DESIGN OF MICROSTRIP PATCH ANTENNA WITH COMPLETE GROUND PLANE

3.1   Design and optimization using Genetic Algorithm (GA)

This chapter presents the design, optimization, fabrication, and measurement of the conventional square-shaped microstrip patch antenna with a complete ground plane. Genetic Algorithm is used in the design and optimization of this antenna. The step-by-step procedure of the antenna optimization is discussed along with the convergence graph, converged antenna design, simulated, and measurement results. A computerized photolithography process does the fabrication of antenna. Vector Network Analyzer (VNA) is used for the validation of the simulated results.

3.1.1   Design objectives, cost-function and stepwise procedure of optimization

The objective was to design and simulate the microstrip antenna for its multi-objective optimized performance, i.e.:

59

- to radiate at a resonating frequency of 10.9 GHz;

- have minimum return loss at resonating frequency;

- have limited impedance bandwidth (up to 500 MHz);

- achieve high gain.

The code for the GA algorithm is integrated with the HFSS environment using MAT-LAB. A block diagram of a GA based simple optimizer is shown in Fig. 1.14 [21].

Stepwise Genetic Algorithm procedure for antenna design is summarized as follows:

1. **Step 1 - Initializing a population**: A primary population is created by producing a random binary string. GA parameters such as a string of bits (chromosome), population size, and the total number of generations are used to optimize antenna geometry. These parameters are discussed in Table 3.1.

GA Parameters	Selected Values
Population Type	BitString
No. of decision variables (Chromosomes in Bit)	34
Total number of Generations and Population Size	200
Scaling Basis	Rank
Selection Criteria	Roulette
Reproduction Elite Count	2
Mutation	Uniform (0.01)
Crossover and its fraction	Single Point Crossover (0.8)
Penalty factor and Initial Penalty	100 and 10

Table 3.1: GA parameters used for the purpose of antenna design

2. **Step 2 - Process of pre-checking designs**: Some design checks (as shown in Fig. 3.1) are applied to validate the strings of bits (chromosomes). These design based checks helped in saving a lot of optimization time by discarding useless chromosomes from getting processed. These checks are shown in Fig. 3.1. Length of the substrate is shown as L_S, range of the patch as L_P, length of overall feedline as L_{Feed} (L_{FL} + $L_{FL-stub}$), the width of the substrate as W_S and width of the patch as W_P. After completion of design checks, these conditions are solved in HFSS, the values of S_{11} parameter and gain at resonating frequency are calculated and returned to primary function automatically (in MATLAB). These returned values are used for further calculations by fitness function (in MATLAB).

60
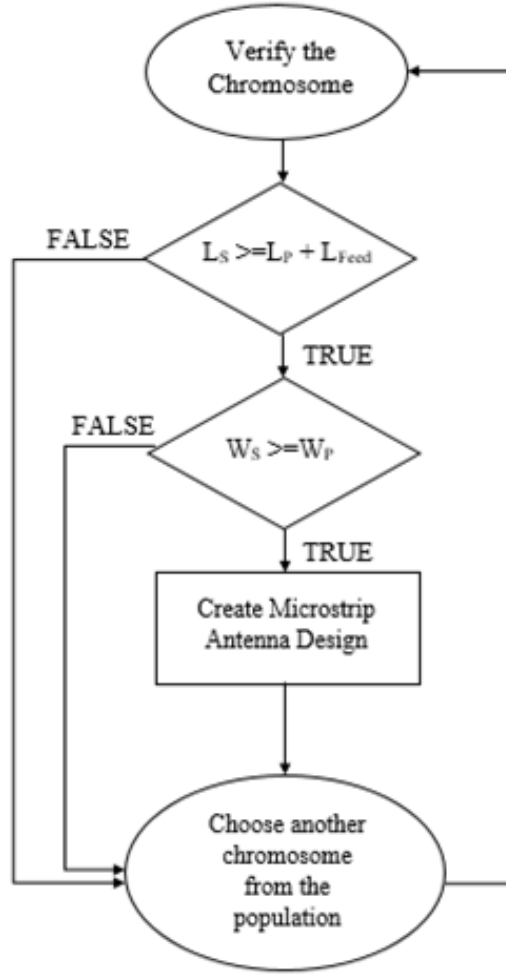
Figure 3.1: Flowchart of the design checks to validate the strings of bits (chromosomes)

3. **Step 3 - Evaluation of the fitness function**: Fitness function is defined in equation 3.1. If the stopping criterion is satisfied, stop the GA procedure; otherwise, go to Step 4. By default, the Genetic Algorithm minimizes the cost (fitness) function. The value of cost function varies from 0 to the most optimal value of -90.

$$F = [-(3 * Gain) - (60 * BW) + S_{11(Res)}] \tag{3.1}$$

$$Gain = \begin{cases} 10 \text{ dB; for Gain}_{cal} \geq 10 \text{ dB;} \\ \text{Gain}_{cal}; \text{ for Gain}_{cal} < 10 \text{ dB;} \end{cases} \tag{3.2}$$

$$BW = \begin{cases} 0.5 \text{ GHz; for BW}_{cal} \geq 0.5 \text{ GHz;} \\ \text{BW}_{cal}; \text{ for BW}_{cal} < 0.5 \text{ GHz;} \end{cases} \tag{3.3}$$

$$BW_{cal} = f_H - f_L \tag{3.4}$$

61

$$S_{11(Res)} = \begin{cases} -30 \text{ dB; for } S_{11} \leq -30 \text{ dB;} \\ S_{11}; \text{ for } S_{11} > -30 \text{ dB;} \end{cases} \tag{3.5}$$

Where BW is the impedance bandwidth of the microstrip antenna calculated using equation 3.3. It is simply the difference between the upper operating frequency, f_H, and lower frequency, f_L. The value of BW_{cal}, as used in equation 3.3, is calculated using the formulae shown in equation 3.4 (implemented in MATLAB code) utilizing the simulated values of return loss received after simulating the design in HFSS. Similarly, the values of $S_{11}(f_1;\ldots; f_n)$ (used in equation 3.4) are the simulated values of return loss at different frequencies. $S_{11(Res)}$ is the value of return loss at resonating frequency calculated using equation 3.5.

4. **Step 4 - Creation of next-generation chromosomes**: Using the operators of the Genetic Algorithm such as scaling, selection, crossover, mutation, etc. (refer Table 3.1), next-generation is created.

5. **Step 5**: Repeat the process from Step#2 onwards unless the termination conditions are met.

The initial geometry of the antenna is based on the values of bits (chromosomes), as discussed in Table 3.2. A random single-point crossover method and uniform mutation operation (with a factor of 0:01) are used. The convergence is obtained after the 35th iteration.

Square Patch (in mm)	Square Substrate and Ground Plane (in mm)	Feedline (in mm)		Feedline-stub (in mm)	
Length (L_P) and Width (W_P)	Length and Width (L_S, W_S, L_G, W_G)	Length (L_{FL})	Width (W_{FL})	Length $(L_{FL-stub})$	Width $(W_{FL-stub})$
5-10.11 Resolution of 0.01	20-45.5 Resolution of 0.1	4-6.55 Resolution of 0.01	0.5-1.9 Resolution of 0.1	6-11.11 Resolution of 0.01	1.89-7 Resolution of 0.01

Table 3.2: GA parameters (Chromosome selection) used for antenna design.

3.1.2 Optimization results, convergence graph, and converged antenna design

The objective of the antenna design was to achieve multi-objective optimized performance (this includes improvements in gain, impedance bandwidth, and reduction of return loss). The antenna proposed is in X-band of super-high frequency to radiate at a resonating frequency of 10.9 GHz. The design has a square substrate and a patch with a full ground plane. The transmission line is connected with a stub for perfect impedance matching. The configuration of the antenna optimized using the Genetic Algorithm (GA) is represented in Fig. 3.2. Fig. 3.3 displays the fabricated antenna converged using GA. In this design, commercially available substrate material RT/duroid with a height of 1.574 mm with a dielectric constant of 2.2 is utilized. The converged antenna geometry is summarized in Table 3.3. A computerized photolithography process is used for the fabrication of the antenna. The Return loss (S_{11}) of the fabricated antenna are measured using a Vector Network Analyzer (VNA). Fig. 3.4 shows the rate of convergence for GA optimization.
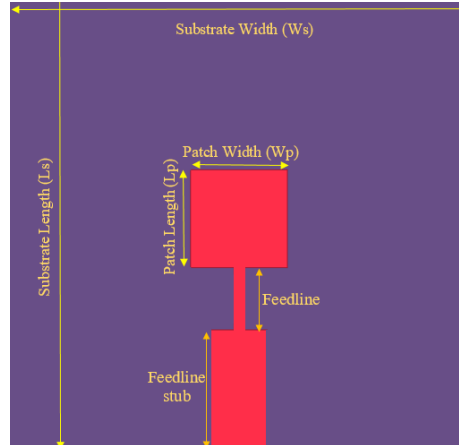
Figure 3.2: Proposed microstrip patch antenna configuration

3.1.2.1 Simulated and Measured Results

Return loss (S_{11}), Voltage Standing Wave Ratio (VSWR), Real and Imaginary Impedance (Z_{11}):
Fig. 3.5 shows the simulated and measured values of return loss (S_{11}) at 10.9 GHz in the X-Band. The return loss (S_{11}) curve with the resonant frequency at 10.9 GHz is having -32
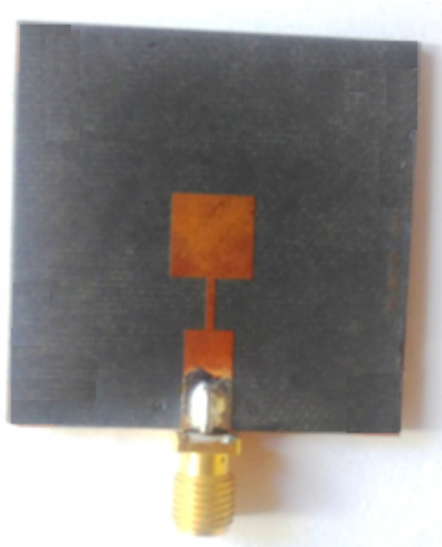
Figure 3.3: Fabricated antenna with full ground plane
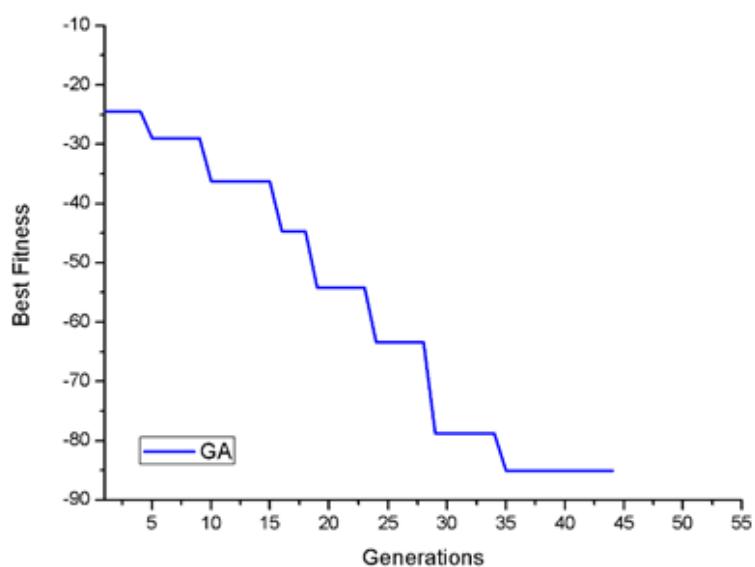
Figure 3.4: Rate of convergence for GA optimization

dB (simulated results) and -27 dB (measured results) values of return loss. The proposed antenna shows 550 MHz (simulated results) from 10.66 GHz to 11.21 GHz and 450 MHz (measured results) from 10.7 GHz to 11.15 GHz of impedance bandwidth. Fig. 3.6 shows the simulated values of Voltage Standing Wave Ratio (VSWR), the value of VSWR at 10.9 GHz is 1.288. Fig. 3.7 shows the real and imaginary impedance (Z_{11}). The values of real impedance at 10.9 GHz are 56.23 Ω, and imaginary impedance at 10.9 GHz is 11.96 Ω.

Parameters	Values (in mm)
Substrate Length (L_S)	38.4
Substrate Width (W_S)	38.4
Ground Plane Length (L_G)	38.4
Ground Plane Width (W_G)	38.4
Patch Length (L_P)	8.08
Patch Width (W_P)	8.08
Feedline Length (L_{FL})	5.18
Feedline Width (W_{FL})	0.8
Feedline-stub Length ($L_{FL-stub}$)	9.98
Feedline-stub Width ($L_{FL-stub}$)	4.79

Table 3.3: GA converged antenna geometry.
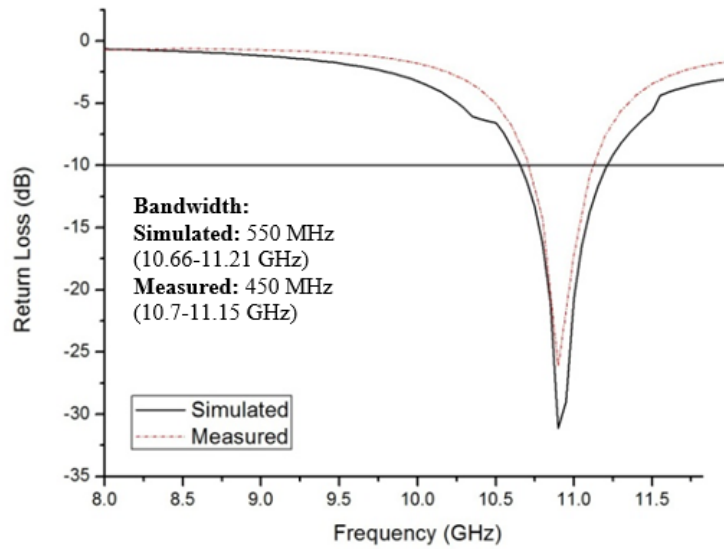
Figure 3.5: Simulated vs. measured values of return loss (S_{11})

Radiation Patterns (2D and 3D), E-Plane, H-Plane, Co and Cross Polarization:

Fig. 3.8 shows the simulated values of 3-Dimensional radiation patterns for gain and directivity at 10.9 GHz. The 2D plots of radiation patterns are shown in Fig. 3.9 for E-Plane and H-plane respectively. A 2-D plot of co-polarization and cross-polarization at 10.9 GHz is shown in Fig. 3.10. Figs. 3.8 and 3.9 show the directive behavior of the proposed antenna.
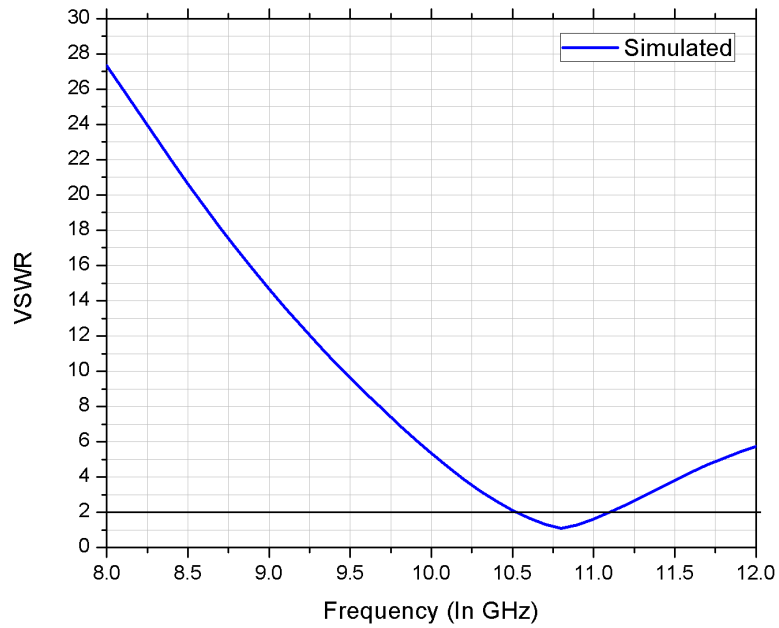
Figure 3.6: Simulated values of Voltage Standing Wave R atio (VSWR)
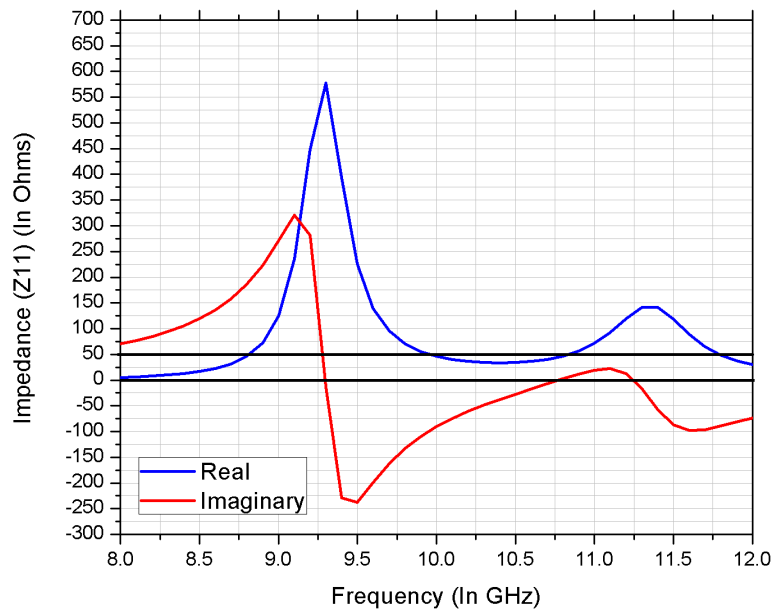
Figure 3.7: Simulated values of real and imaginary impedance (Z_{11})

Gain and Directivity:

A plot of gain and directivity of the proposed antenna over the X-band is presented in Fig. 3.11. At the resonant frequency of 10.9 GHz, the proposed antenna exhibits higher simulated values of gain and directivity (8.35 dB, respectively).
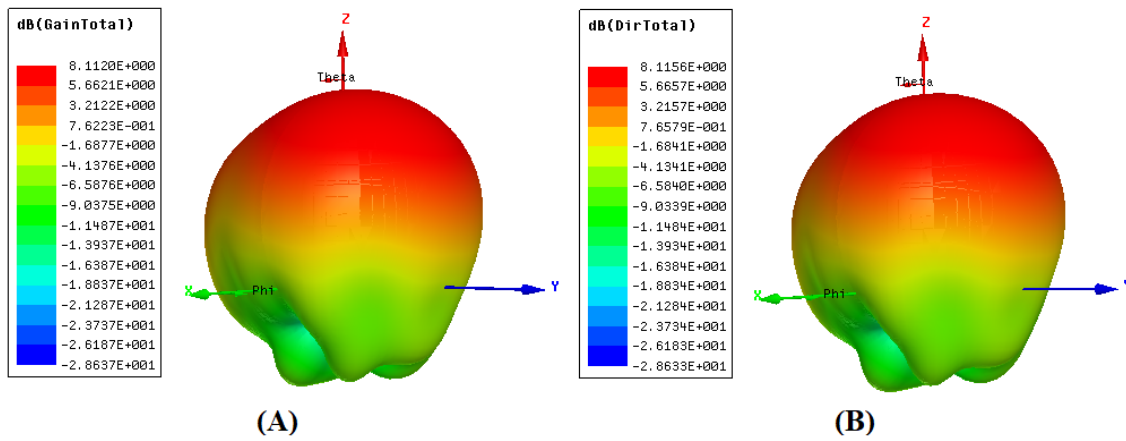
Figure 3.8: Simulated values of 3-Dimensional Radiation Patterns (A) Gain (B) Directivity
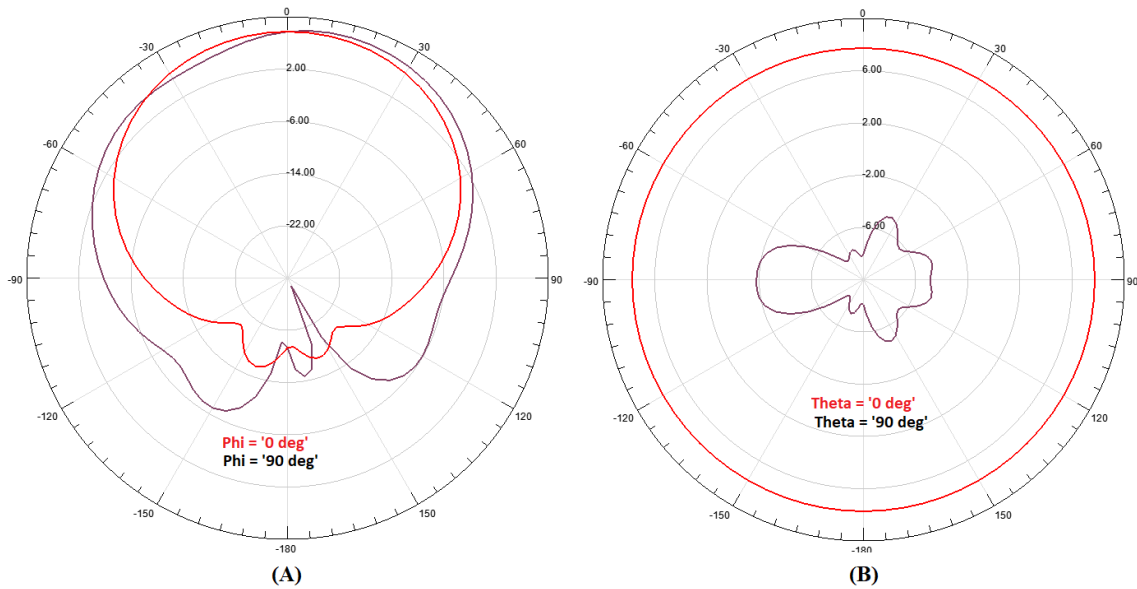
Figure 3.9: Simulated values of 2-Dimensional Radiation Patterns (A) Gain E-Plane (B) Gain H-Plane

3.1.3 Parametric Analysis of the Proposed Antenna

In the following subsection, an analysis is carried out to determine the effect of the design parameters of the microstrip patch antenna on the resonating frequency and the impedance bandwidth. Fig. 3.12-3.19 demonstrates all the analyzed parameters. The participation of a specific parameter is analyzed at a time while preserving all other parameters to their suboptimal values (as per Table 3.3 – GA converged antenna geometry). This parametric analysis shows the validity of the GA converged antenna design.
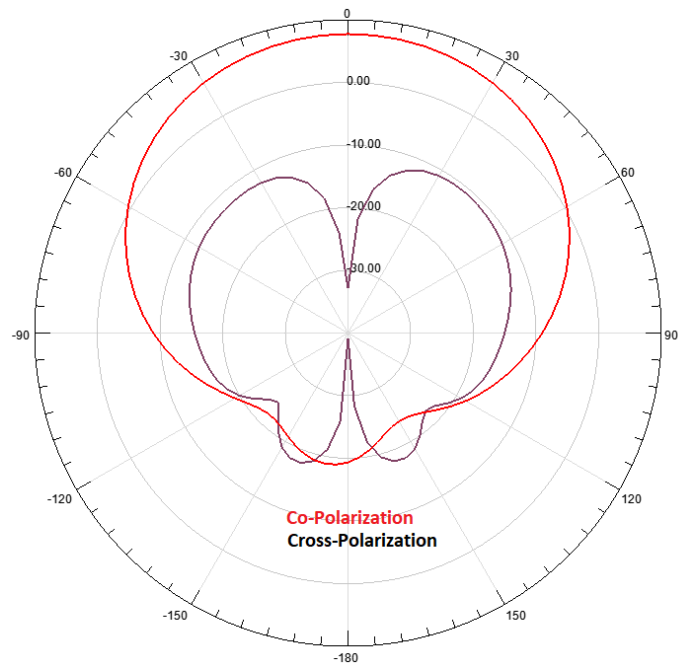
Figure 3.10: Simulated values of 2-Dimensional Radiation Patterns XZ-Plane (Co and Cross-Polarization)
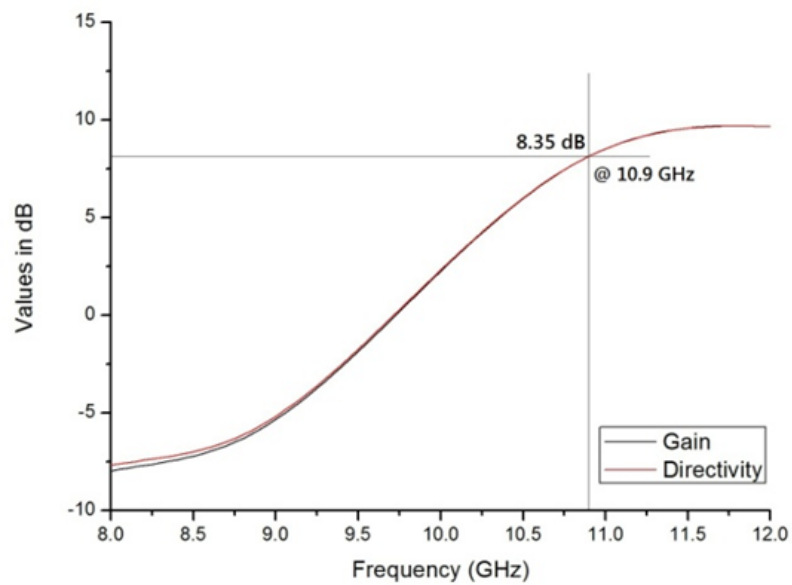
Figure 3.11: Simulated values of gain and directivity over the X-Band.

3.1.3.1 Effect of length of the substrate (L_S)

The substrate's length is considered to be vital as it impacts the overall size of the microstrip patch antenna. In this subsection, the effect of varying the length of the substrate (L_S) as illustrated in Fig. 3.12, is studied. It is observed that there is no significant shift

in the resonating frequency and the impedance bandwidth except slight variations in the values of return loss (S_{11}). The optimized value of substrate's length is 38.4 mm, achieved return loss is -32 dB, and the bandwidth is 550 MHz.
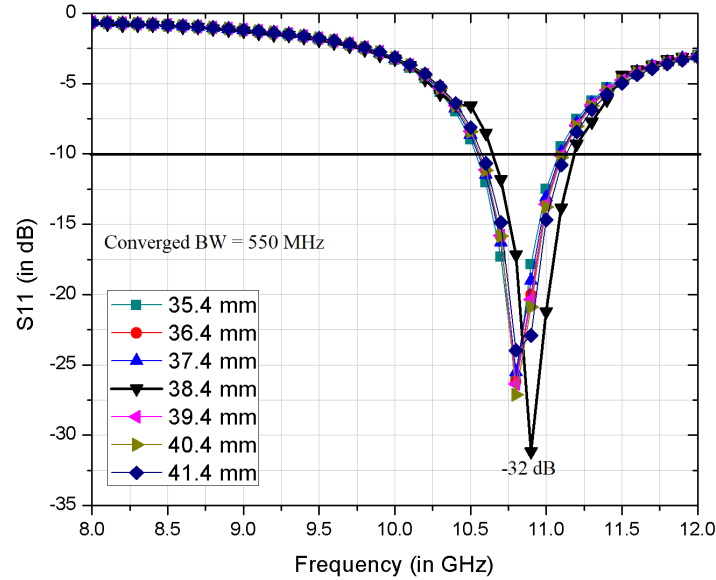
Figure 3.12: Effect of changes in the length of the substrate (keeping all other parameters constant – as per Table 3.3)

3.1.3.2 Effect of the width of the substrate (W_S)

Like the length of the substrate, its width also impacts the overall size of the microstrip patch antenna and is thus considered an important factor in design. In this subsection, the effect of varying the width of the substrate (W_S), as illustrated in Fig. 3.13, is studied. It is observed that there is no significant shift in the resonating frequency and impedance bandwidth except for slight variations in S_{11}. The optimized value of substrate's width is 38.4 mm, achieved return loss is -32 dB, and the bandwidth is 550 MHz.

3.1.3.3 Effect of the length of the patch (L_P)

In this subsection, the effect of varying the length of the patch (L_P), as illustrated in Fig. 3.14, is studied. It is observed that fine-tuning of the resonating frequency is possible by changing the L_P from 5.08 mm to the optimal value of 8.08 mm. It is also seen that

69
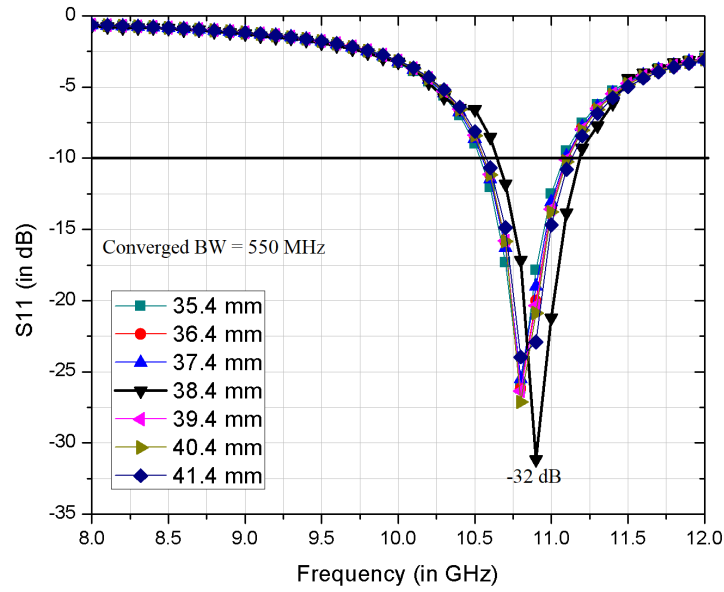
Figure 3.13: Effect of changes in the width of the substrate (keeping all other parameters
constant – as per Table 3.3)

there are no significant improvements in the impedance bandwidth and the values of return
loss (S_{11}) at resonating frequency. However, the values of return loss (S_{11}) remains below
-15 dB. The optimized value of patch's length is 8.08 mm, achieved return loss is -32 dB,
and the bandwidth is 550 MHz.
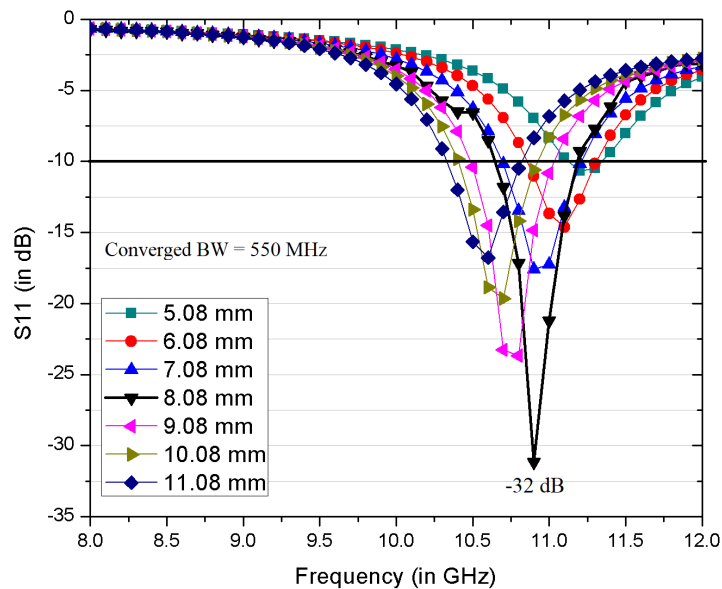
Figure 3.14: Effect of changes in the length of the patch (keeping all other parameters
constant – as per Table 3.3)

3.1.3.4 Effect of the width of the patch (W_P)

In this subsection, the effect of varying the width of the patch (W_P), as illustrated in Fig. 3.15, is studied. It is observed that a significant change in the resonating frequency can be achieved by varying the W_P from 5.08 mm to the optimal value of 8.08 mm. It is also observed that there is no significant improvement in the impedance bandwidth. It is also found that the antenna is kept on radiating ($S_{11} < $ -10 dB) throughout the studied range of W_P. The optimized value of patch's width is 8.08 mm, achieved return loss is -32 dB, and the bandwidth is 550 MHz.
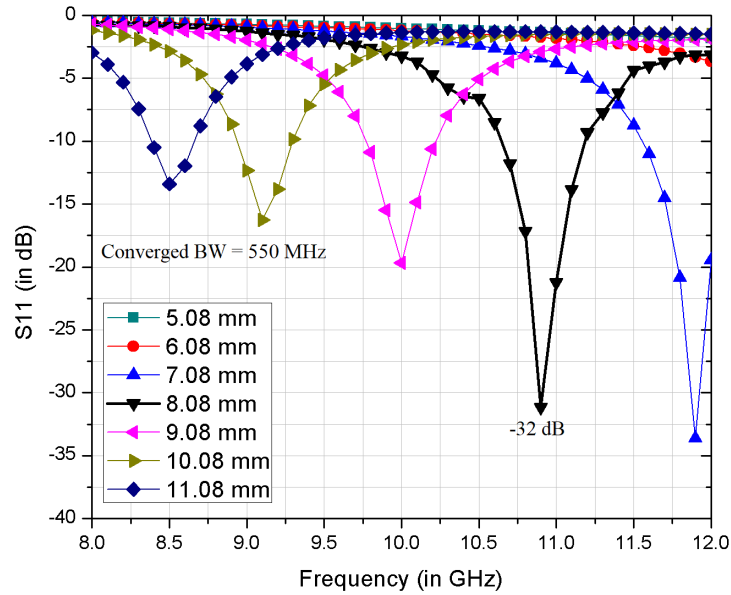
Figure 3.15: Effect of changes in the width of the patch (keeping all other parameters constant – as per Table 3.3)

3.1.3.5 Effect of length of the feedline (L_{FL} and $L_{FL-stub}$)

In this subsection, the effect of varying the length of the feedline (L_{FL} and $L_{FL-stub}$), as illustrated in Figs. 3.16 and 3.17, is studied. It is observed there is no significant shift in the resonating frequency and impedance bandwidth with the change in length of stub feedline ($L_{FL-stub}$). It is also observed that fine-tuning of the resonating frequency is possible by changing the length of feedline (L_{FL}) from 2.18 mm to the optimal value of 5.18 mm. It is also observed that there is no significant improvement in the impedance

bandwidth. The optimized value of L_{FL} is 5.18 mm, $L_{FL-stub}$ is 9.98 mm, achieved return loss is -32 dB, and the bandwidth is 550 MHz.
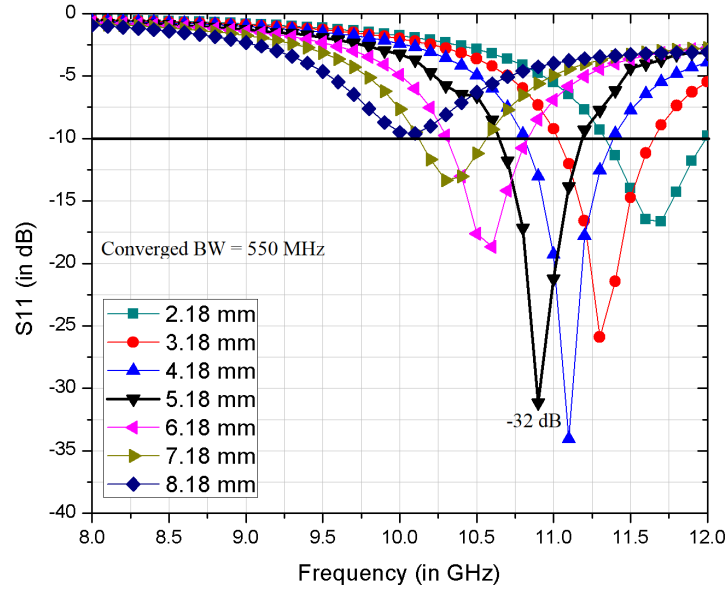
Figure 3.16: Effect of changes in the length of the feedline (keeping all other parameters constant – as per Table 3.3)
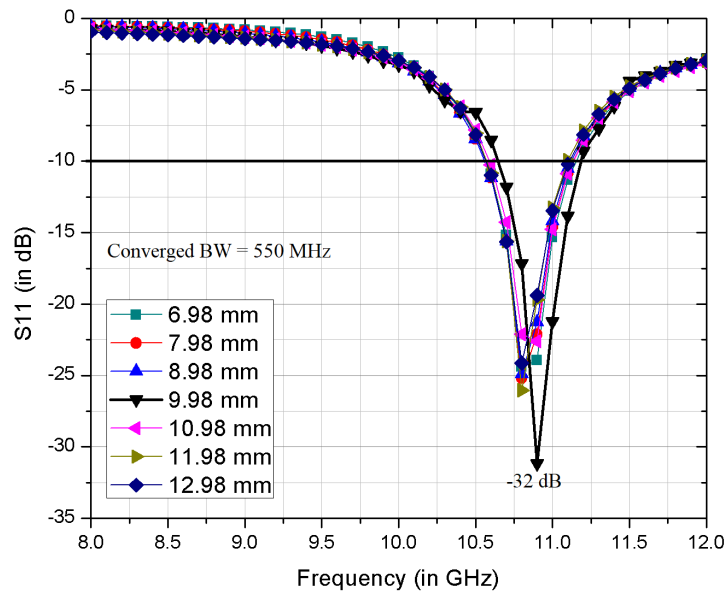
Figure 3.17: Effect of changes in the length of the feedline ($L_{FL-stub}$) (keeping all other parameters constant – as per Table 3.3)

72

3.1.3.6 Effect of width of the feedline (W_{FL} and $W_{FL-stub}$)

In this subsection, the effect of varying the width of the feedline (W_{FL} and $W_{FL-stub}$), as illustrated in Figs. 3.18 and 3.19, is studied. It is observed there is no significant shift in the resonating frequency and impedance bandwidth with the changes in both widths of stub feedline ($W_{FL-stub}$) and feedline (W_{FL}). The optimized value of W_{FL} is 0.8 mm, $W_{FL-stub}$ is 4.79 mm, achieved return loss is -32 dB, and the bandwidth is 550 MHz.
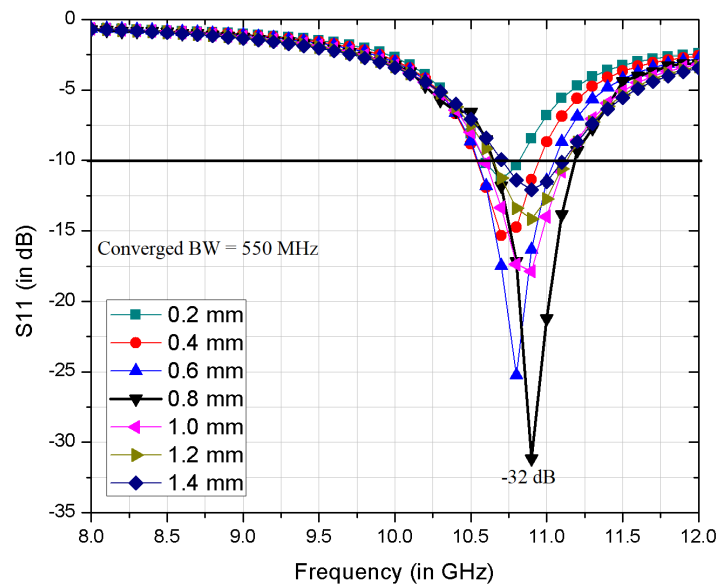
Figure 3.18: Effect of changes in the width of the feedline (keeping all other parameters constant – as per Table 3.3)

3.2 Comparison of Results

The results of proposed antenna is compared with the existing designs/literature and is summarized in Table 3.4. It is observed that the proposed design is better in terms of its achieved gain and directivity.
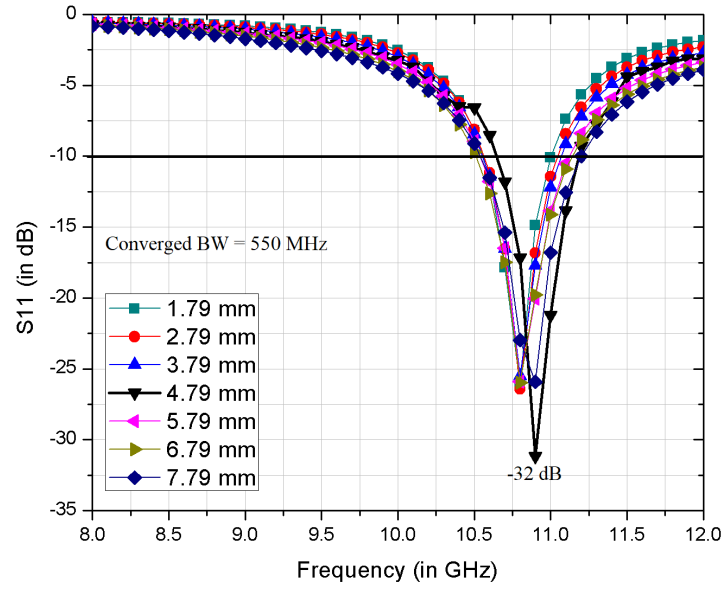
Figure 3.19: Effect of changes in the width of the feedline ($W_{FL-stub}$) (keeping all other parameters constant – as per Table 3.3)

Ref.	Operating frequency (f_o)	Impedance Bandwidth	Return Loss at f_o	Gain at f_o	Directivity at f_o	Dimensions (in mm^3)
[121]	10.5 GHz	3 GHz [M]	-20 dB [M]	5.35 dB [M]	Not available	30 x 21 x 1.5
[122]	10.5 GHz	1.7 GHz [M]	-14 dB [M]	4 dB [S]	Not available	30 x 30 x 1.58
[123]	10.04 GHz	2.95 GHz [S]	-42.57 [S]	1.06 dB [S]	1.21 dB [S]	30 x 35 x 1.58
Proposed Antenna	10.9 GHz	550 MHz [S]; 450 MHz [M]	-32 dB [S]; -27 dB [M]	8.35 dB [S]	8.35 dB [S]	38.4 x 38.4 x 1.574

Table 3.4: Comparison of the proposed antenna with existing literature. (Simulated [S] and Measured [M]).

3.3 Chapter Summary

This chapter presented the design, optimization, fabrication, and measurement of conventional square shaped microstrip patch antenna with a complete ground plane. The Genetic Algorithm is used in the process of design and optimization of the conventional square-shaped microstrip patch antennas with a complete ground plane. The objective of the antenna design was to achieve multi-objective optimized performance (this includes

74

improvements in gain, impedance bandwidth, and reduction of return loss). A step-by-step procedure of the antenna optimization using Genetic Algorithm (GA) is discussed along with the convergence graph, geometry of the converged antenna design, its simulated, and measurement results. The antenna proposed in this chapter radiates at a resonating frequency of 10.9 GHz and is useful for various wireless wideband applications in the X-Band. A number of potential applications in X-Band are discussed in chapter 1. RT/duroid with a height of 1.574 mm and a dielectric constant of 2.2 is used as a substrate material of the proposed antenna. The transmission line is connected with a stub for perfect impedance matching. The dimension of the converged antenna is 38.4 mm x 38.4 mm x 1.574 mm. The proposed antenna shows the simulated bandwidth of 550 MHz (10.66-11.21 GHz) and measured bandwidth of 450 MHz (10.7-11.15 GHz). The values of return loss at the resonant frequency (of 10.9 GHz) is -32 dB (simulated) and -27 dB (measured). The simulated radiation patterns show the directional radiation characteristics. The proposed antenna design shows high values of simulated gain (8.35 dB), and directivity (8.35 dB) at the resonating frequency of 10.9 GHz. Parametric analysis is also presented in this chapter to further validate the converged design. The comparison of results with existing designs/literature is done and it is observed that the proposed design is better in terms of its achieved gain and directivity. The only limitation with this design is the cost of fabrication because of the cost of substrate material RT/duroid. In the next chapter, three antenna designs are proposed using the FR4 substrate material to compensate the cost of the fabrication. These designs are optimized using three different optimization techniques to verify whether the antenna design can be further improved.

Chapter 4

DESIGN OF MICROSTRIP PATCH ANTENNA WITH PARTIAL GROUND PLANE

This chapter presents the design, optimization, fabrication, and measurement of conventional rectangular shaped microstrip patch antenna with a partial ground plane. Three different optimization techniques - Genetic Algorithm, Particle Swarm Optimization, and Gray Wolf Optimization- are used to design and optimize three different antennas. The step-by-step procedure of the antenna optimization is discussed along with the convergence graphs, converged antenna designs, simulated, and measurement results. Parametric analysis is conducted on all three designs and presented here to validate the research outcomes. This chapter is concluded with the comparison of the proposed antennas with existing literature.

4.1   Design and Optimization using Genetic Algorithm (GA)

This section presents the design, optimization, fabrication, and measurement of conventional rectangular shaped microstrip patch antenna with a partial ground plane. Genetic Algorithm is used in the design and optimization of this antenna. The step-by-step proce-

dure of the antenna optimization is discussed along with the convergence graph, converged antenna design, simulated, and measurement results. A computerized photolithography process is used in the fabrication of the antenna. Vector Network Analyzer (VNA) is used for the validation of the simulated results.

4.1.1 Design objectives, cost-function and stepwise procedure of optimization

The objective was to design and simulate the microstrip antenna for its multi-objective optimized performance, i.e.:

- to radiate at a resonating frequency of 10.5 GHz;

- have minimum return loss at resonating frequency;

- have high impedance bandwidth (up to 1.5 GHz);

- achieve high gain.

The code for the GA algorithm is integrated with the HFSS environment using MAT-LAB. A block diagram of a GA based simple optimizer is shown in Fig. 1.14 [21]. Step-wise Genetic Algorithm procedure for antenna design is summarized as follows:

1. **Step 1 - Initializing a population**: A primary population is created by producing a random binary string. GA parameters such as a string of bits (chromosome), population size, and the total number of generations are used to optimize antenna geometry. These parameters are discussed in Table 4.1.

GA Parameters	Selected Values
Population Type	BitString
No. of decision variables (Chromosomes in Bit)	34
Total number of Generations and Population Size	200
Scaling Basis	Rank
Selection Criteria	Roulette
Reproduction Elite Count	2
Mutation	Uniform (0.01)
Crossover and its fraction	Single Point Crossover (0.8)
Penalty factor and Initial Penalty	100 and 10

Table 4.1: GA parameters used for the purpose of antenna design

2. **Step 2 - Process of pre-checking designs**: Some design checks (as shown in Fig. 4.1) are applied to validate the strings of bits (chromosomes). These design based checks helped in saving a lot of optimization time by discarding useless chromosomes from getting processed. In Fig. 4.1, the length of the substrate is shown as L_S, length of the patch as L_P, length of feedline as L_F, length of the ground plane as L_G, the width of the substrate as W_S, and width of the patch as W_P. After completion of design checks, these conditions are solved in HFSS, the values of S_{11} parameter and gain at resonating frequency are calculated and returned to primary function automatically (in MATLAB). These returned values are used for further calculations by fitness function (in MATLAB).
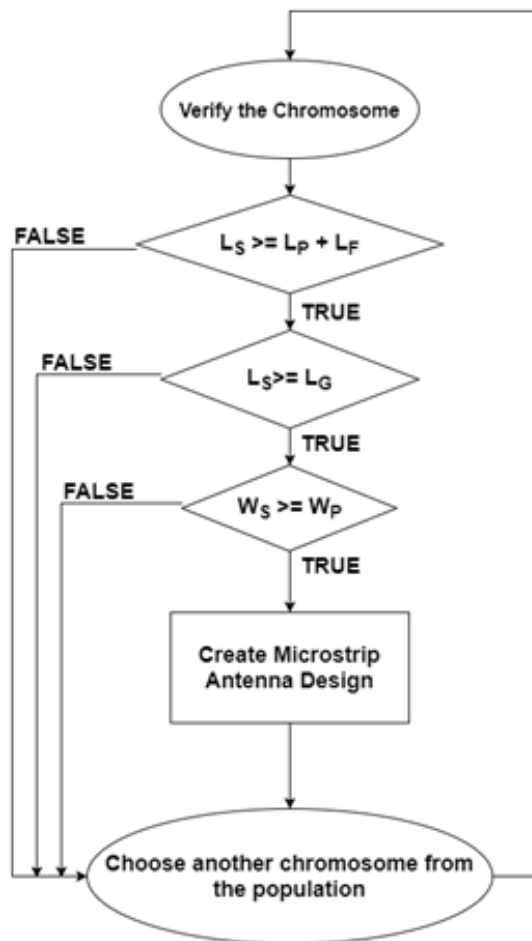
Figure 4.1: Flowchart of the design checks to validate the strings of bits (chromosomes)

3. **Step 3 - Evaluation of the fitness function**: Fitness function is defined in equation 4.1. If the stopping criterion is satisfied, then stop the GA procedure; otherwise, go to Step 4. By default, the Genetic Algorithm minimizes the cost (fitness) function.

The value of cost function varies from 0 to the most optimal value of -90.

$$F = [-(3 * Gain) - (20 * BW) + S_{11(Res)}] \tag{4.1}$$

$$Gain = \begin{cases} 10 \text{ dB; for Gain}_{cal} \geq 10 \text{ dB;} \\ \text{Gain}_{cal}; \text{ for Gain}_{cal} < 10 \text{ dB;} \end{cases} \tag{4.2}$$

$$BW = \begin{cases} 1.5 \text{ GHz; for BW}_{cal} \geq 1.5 \text{ GHz;} \\ \text{BW}_{cal}; \text{ for BW}_{cal} < 1.5 \text{ GHz;} \end{cases} \tag{4.3}$$

$$BW_{cal} = f_H - f_L \tag{4.4}$$

$$S_{11(Res)} = \begin{cases} -30 \text{ dB; for S}_{11} \leq -30 \text{ dB;} \\ \text{S}_{11}; \text{ for S}_{11} > -30 \text{ dB;} \end{cases} \tag{4.5}$$

Where BW is the impedance bandwidth of the microstrip antenna calculated using equation 4.3. It is simply the difference between the upper operating frequency, f_H, and lower frequency, f_L. The value of BW_{cal}, as used in equation 4.3, is calculated using the formulae shown in equation 4.4 (implemented in MATLAB code) utilizing the simulated values of return loss received after simulating the design using HFSS. Similarly, the values of $S_{11}(f_1; \ldots; f_n)$ (used in equation 4.4) are the simulated values of return loss at different frequencies. $S_{11(Res)}$ is the value of return loss at resonating frequency (f_o) calculated using equation 4.5.

4. **Step 4 - Creation of next-generation chromosomes**: Using the operators of the Genetic Algorithm such as scaling, selection, crossover, mutation, etc. (refer Table 4.1), next-generation is created.

5. **Step 5**: Repeat the process from Step#2 onwards unless the termination conditions are met.

The antenna's initial geometry is based on the values of bits (chromosomes), as discussed in table 4.2. A random single-point crossover method and uniform mutation operation (with a factor of 0:01) are used. The convergence is obtained after the 39th iteration.

Patch (in mm)		Substrate (in mm)		Feedline (in mm)		Ground Plane (in mm)	
Length (L_P)	Width (W_P)	Length (L_S)	Width (W_S)	Length (L_{FL})	Width (W_{FL})	Length (L_G)	Width (W_G)
5-40	5-40	18-50	18-50	4-20	1-8	5-50	$= W_S$
Resolution: 1 mm (for each parameter)							

Table 4.2: GA parameters (Chromosome selection) used for antenna design.

4.1.2 Optimization results, convergence graph, and converged antenna design

The objective of the antenna design was to achieve multi-objective optimized performance (this includes improvements in gain, impedance bandwidth, and reduction of return loss). The antenna proposed is in X-band of super-high frequency to radiate at a resonating frequency of 10.5 GHz. The antenna design has a conventional rectangular substrate and patch with a partial ground plane. The configuration of the antenna optimized using the Genetic Algorithm (GA) is represented in Fig. 4.2. Fig. 4.3 displays the fabricated antenna converged using GA. In this design, an inexpensive FR4 substrate material is utilized. The height of the FR4 substrate is 1.58 mm, having a dielectric constant of 4.3 and a loss tangent of 0.02. The converged antenna geometry is summarized in Table 4.3. A computerized photolithography process is used for the fabrication of the antenna. The return loss (S_{11}) of the fabricated antenna are measured using a Vector Network Analyzer (VNA). Fig. 4.4 shows the rate of convergence for GA optimization.
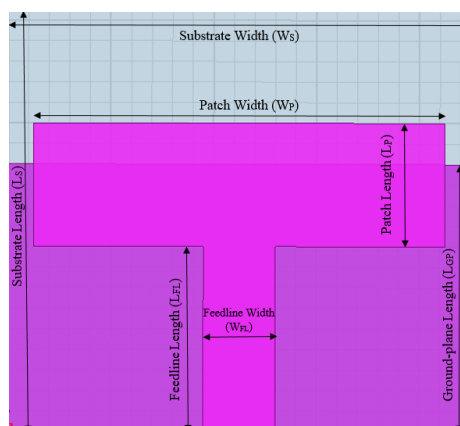
Figure 4.2: Proposed microstrip patch antenna configuration

(A)   (B)
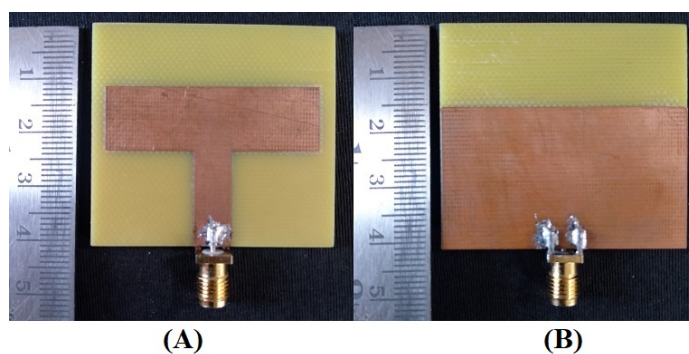
Figure 4.3: Fabricated antenna with partial ground plane (A) Front (B) Rear
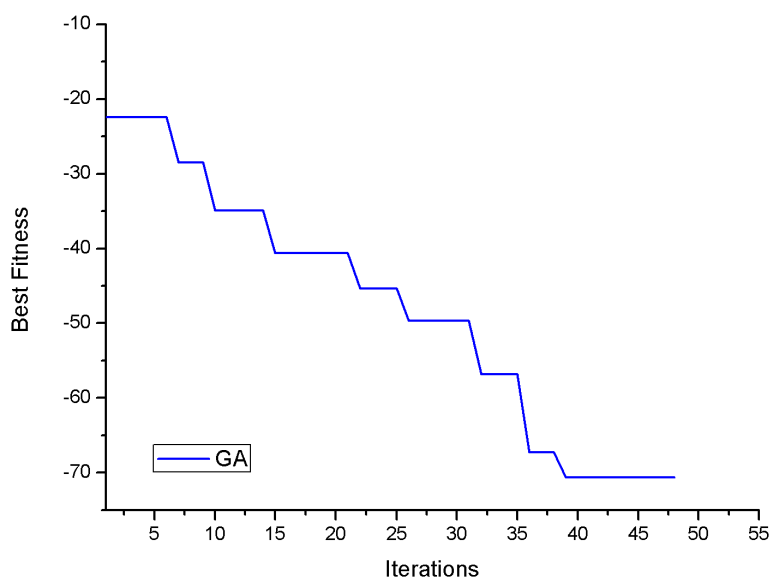
Figure 4.4: Rate of convergence for GA optimization

Parameters	Values (in mm)
Substrate Length (L_S)	41
Substrate Width (W_S)	45
Ground Plane Length (L_G)	26
Ground Plane Width (W_G)	45
Patch Length (L_P)	12
Patch Width (W_P)	40
Feedline Length (L_{FL})	18
Feedline Width (W_{FL})	7

Table 4.3: GA converged antenna geometry.

4.1.2.1 Simulated and Measured Results

Return loss (S_{11}), Voltage Standing Wave Ratio (VSWR), Real and Imaginary Impedance (Z_{11}):

81

Fig. 4.5 shows the simulated and measured values of return loss (S_{11}) at 10.5 GHz in the X-Band. The return loss (S_{11}) curve with the resonant frequency at 10.5 GHz is having -27.35 dB (simulated results) and -21.51 dB (measured results) values of return loss. The proposed antenna shows 850 MHz (simulated results) from 9.95 GHz to 10.8 GHz and 670 MHz (measured results) from 10.04 GHz to 10.71 GHz of impedance bandwidth. Fig. 4.6 shows the simulated and measured values of Voltage Standing Wave Ratio (VSWR), the value of VSWR at 10.5 GHz is 1.096 (simulated) and 1.183 (measured). Fig. 4.7 shows the real and imaginary impedance (Z_{11}). The values of real impedance at 10.5 GHz are 49.25 Ω, and imaginary impedance at 10.5 GHz is 4.29 Ω.
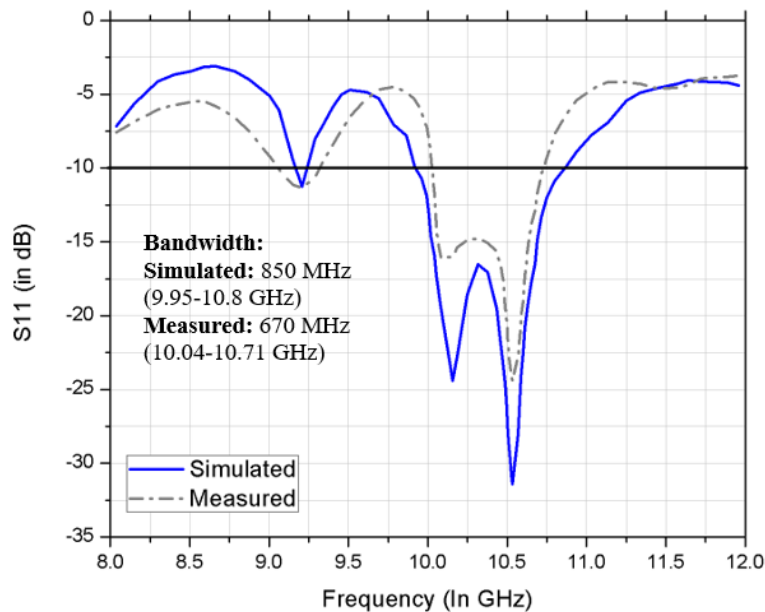
Figure 4.5: Simulated vs. measured values of return loss (S_{11})

Radiation Patterns (2D and 3D), E-Plane, H-Plane, Co and Cross Polarization:

Fig. 4.8 shows the simulated values of 3-Dimensional radiation patterns for gain and directivity at 10.5 GHz. The 2D plots of radiation patterns are shown in Fig. 4.9 for E-Plane and H-plane, respectively. A 2-D plot of co-polarization and cross-polarization at 10.5 GHz is shown in Fig. 4.10. Figs. 4.8 and 4.9 show the omnidirectional behavior of the proposed antenna.
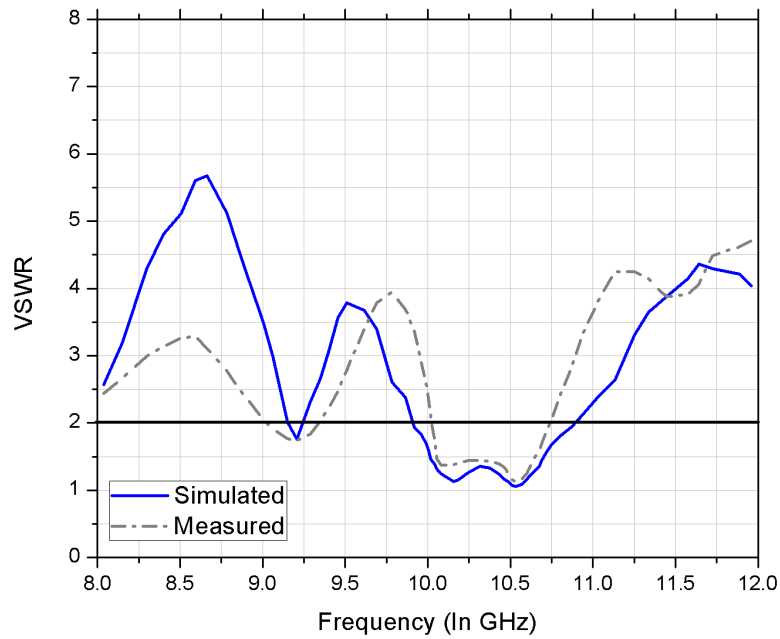
Figure 4.6: Simulated vs. measured values of Voltage Standing Wave Ratio (VSWR)
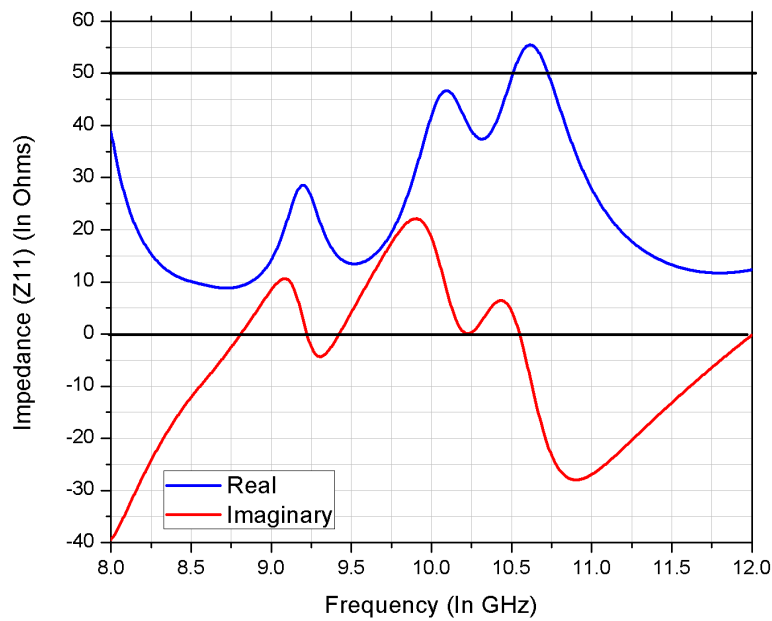
Figure 4.7: Simulated values of real and imaginary impedance (Z_{11})

Gain and Directivity:

A plot of gain and directivity over the impedance bandwidth of the proposed antenna is presented in Fig. 4.11. At the operating frequency of 10.5 GHz, the proposed antenna exhibits higher simulated values of gain and directivity. The value of simulated gain is 4.26 dB, and directivity is 7.36 dB at 10.5 GHz.
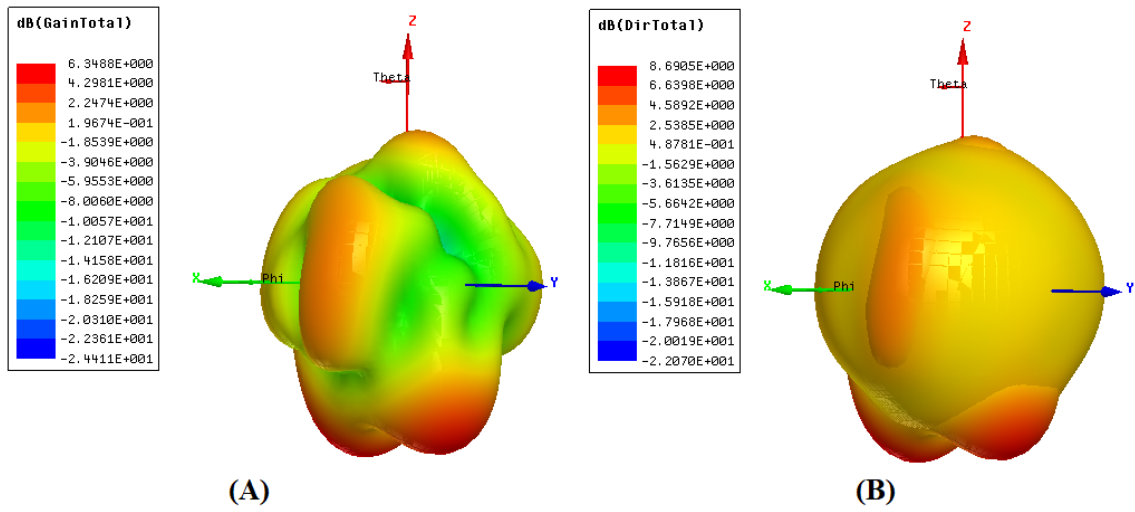
Figure 4.8: Simulated values of 3-Dimensional Radiation Patterns (A) Gain (B) Directivity
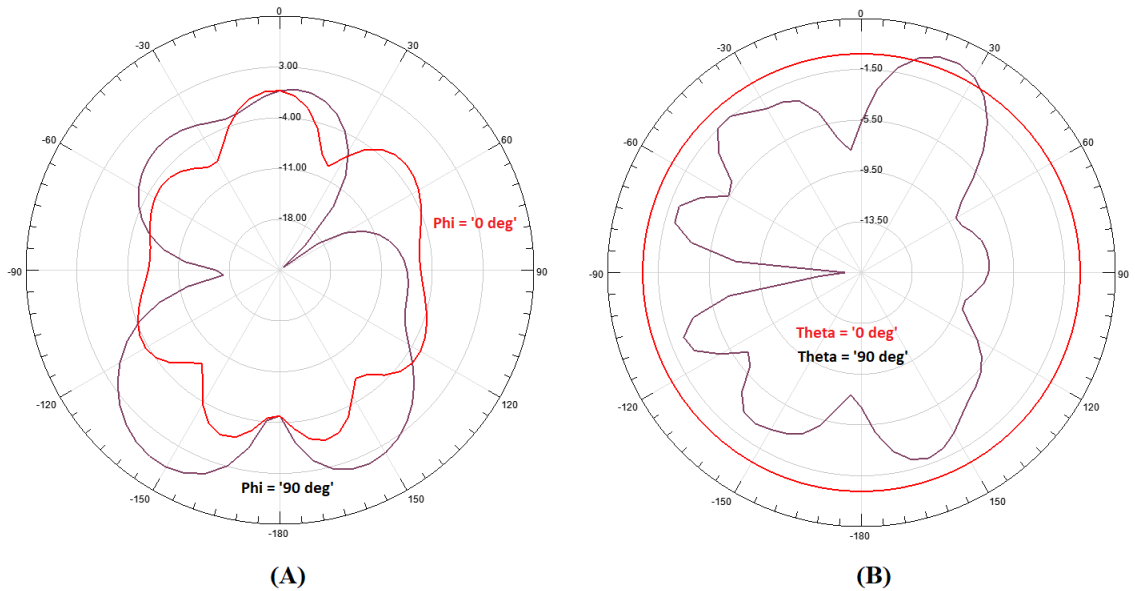
Figure 4.9: Simulated values of 2-Dimensional Radiation Patterns (A) Gain E-Plane (B) Gain H-Plane

4.1.3 Parametric Analysis of the Proposed Antenna

In the following subsection, an analysis is carried out to determine the effect of the microstrip patch antenna's design parameters on the resonating frequency and the impedance bandwidth. Fig. 4.12-4.18 demonstrates all the analyzed parameters. The participation of a specific parameter is analyzed at a time while preserving all other parameters to their suboptimal values (as per Table 4.3 – GA converged antenna geometry). This parametric analysis shows the validity of the GA converged antenna design.
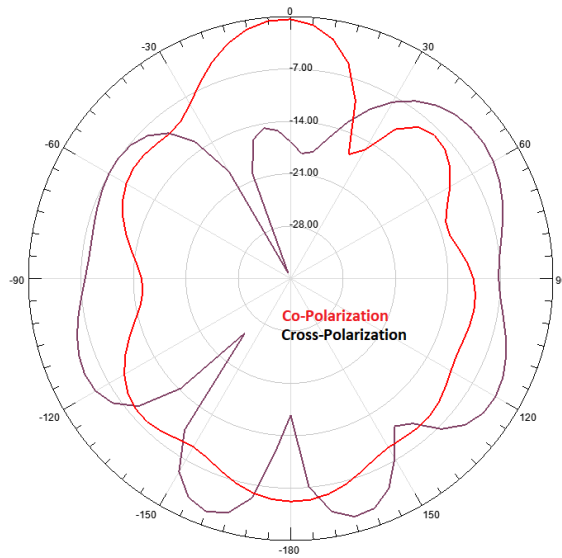
Figure 4.10: Simulated values of 2-Dimensional Radiation Patterns XZ-Plane (Co and Cross-Polarization)
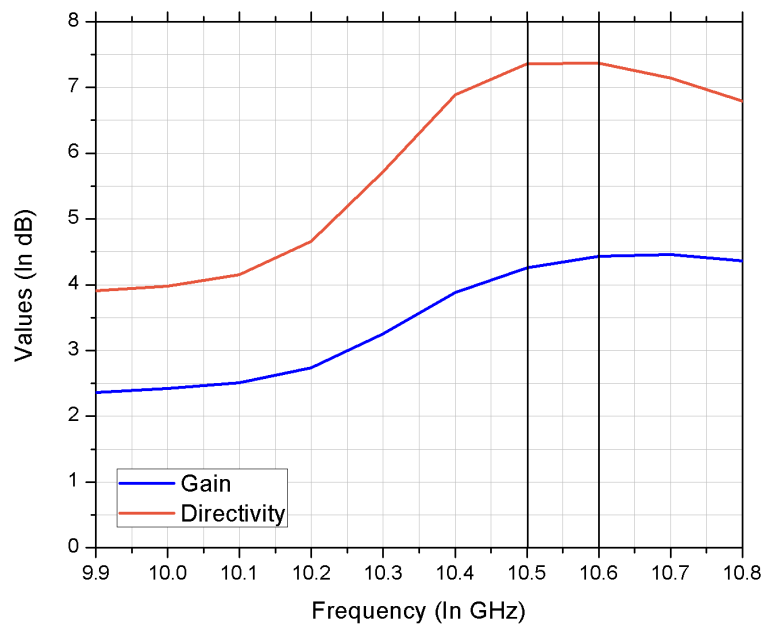
Figure 4.11: Simulated values of gain and directivity over the impedance bandwidth

4.1.3.1 Effect of length of the substrate (L_S)

The substrate's length is considered to be important as it impacts the overall size of the microstrip patch antenna. In this subsection, the effect of varying the length of the substrate (L_S), as illustrated in Fig. 4.12, is studied. It is observed that a significant change in the impedance bandwidth can be achieved by varying the L_S. It is also observed that,

a decrement in the substrate's length can shift the resonating frequency slightly to the higher frequencies of the X-band, with a decrement in the impedance bandwidth (ranging from 850 MHz to 600 MHz) as well. The optimized value of substrate's length is 41 mm, achieved return loss is -27.35 dB, and the bandwidth is 850 MHz.
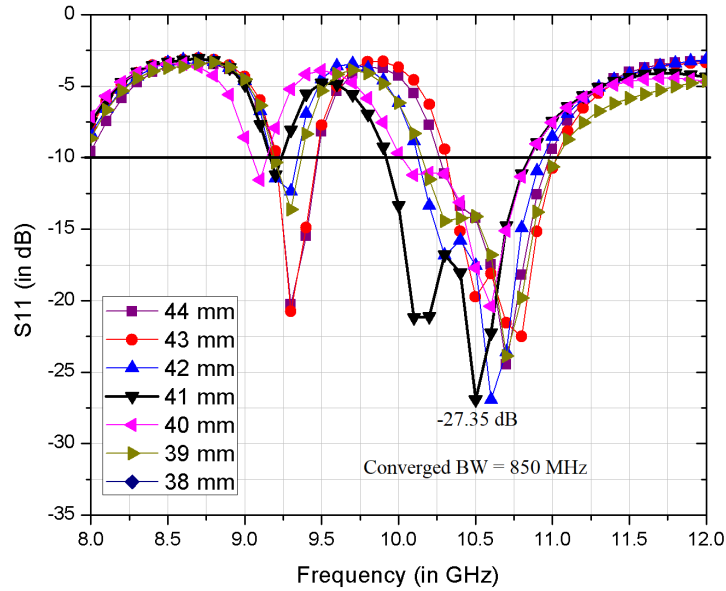
Figure 4.12: Effect of length of the substrate (L_S) (keeping all other parameters constant – as per Table 4.3)

4.1.3.2 Effect of the width of the substrate (W_S)

Like the length of the substrate, its width also impacts the overall size of the microstrip patch antenna and is thus considered an important factor in design. In this subsection, the effect of varying the width of the substrate (W_S), as illustrated in Fig. 4.13, is studied. It is observed that a significant change in the resonating frequency, as well as impedance bandwidth, can be achieved by varying the W_S. Changes in the substrate's width can shift the resonating frequency to the higher frequencies of the X-band and also shows multi-band behaviors. While changing the W_S, impedance bandwidth is also changing in the designs. The optimized value of substrate's width is 45 mm, achieved return loss is -27.35 dB, and the bandwidth is 850 MHz.
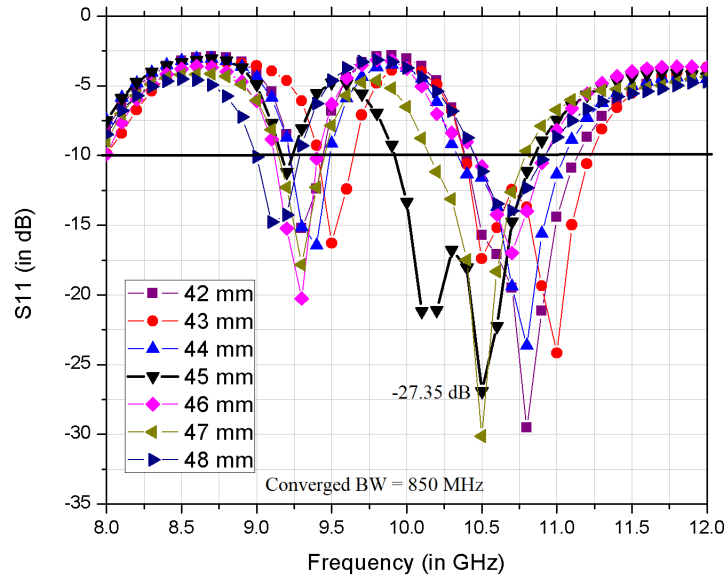
Figure 4.13: Effect of the width of the substrate (W_S) (keeping all other parameters constant – as per Table 4.3)

4.1.3.3 Effect of length of the patch (L_P)

In the following subsection, the effect of varying the length of the patch (L_P), as illustrated in Fig. 4.14, is studied. It is observed that fine-tuning of the resonating frequency is possible by changing the L_P from 9 mm to the optimal value of 12 mm. It is also observed that there are no significant improvements in the impedance bandwidth and the values of return loss (S_{11}) at resonating frequency. The optimized value of patch's length is 12 mm, achieved return loss is -27.35 dB, and the bandwidth is 850 MHz.

4.1.3.4 Effect of the width of the patch (W_P)

In this subsection, the effect of varying the width of the patch (W_P), as illustrated in Fig. 4.15, is studied. It is observed that a significant change in the resonating frequency, and impedance bandwidth, can be achieved by varying the W_P. Changes in the width of the patch can slightly shift the resonating frequency to the higher frequencies of the X-band (ranging from 9.3 to 10.8 GHz), and also shows multi-band behaviors. The optimized value of patch's width is 40 mm, achieved return loss is -27.35 dB, and the bandwidth is 850 MHz.
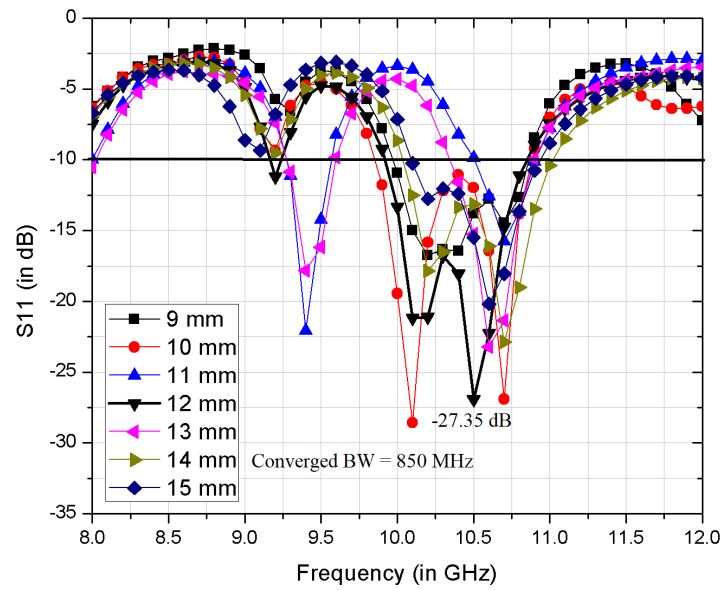
Figure 4.14: Effect of length of the patch (L_P) (keeping all other parameters constant – as per Table 4.3)
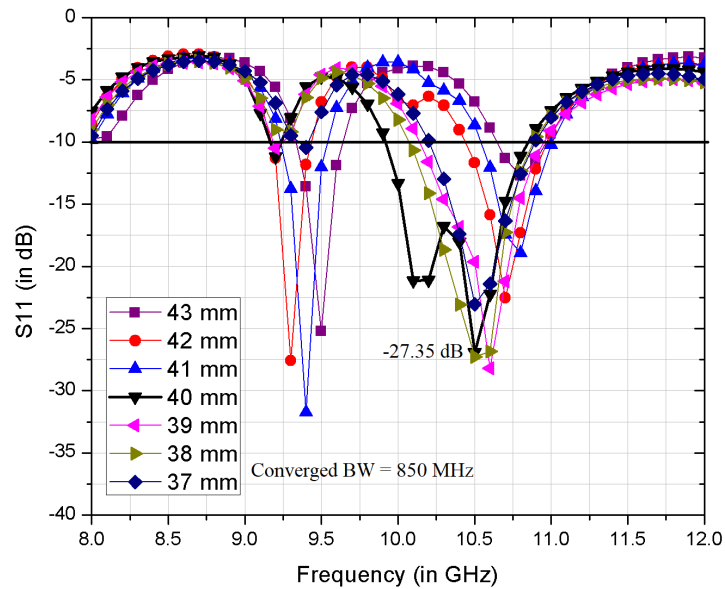
Figure 4.15: Effect of the width of the patch (W_P) (keeping all other parameters constant – as per Table 4.3)

4.1.3.5 Effect of length of the feedline (L_{FL})

In this subsection, the effect of varying the length of the feedline (L_{FL}), as illustrated in Fig. 4.16, is studied. It is observed there is no significant shift in the resonating frequency and impedance bandwidth with the change in length of feedline (L_{FL}). It is also

observed that the fine-tuning of the resonating frequency is possible by changing the length of the feedline (L_{FL}). It is also observed that there is no significant improvement in the impedance bandwidth. The optimized value of feedline's length is 18 mm, achieved return loss is -27.35 dB, and the bandwidth is 850 MHz.
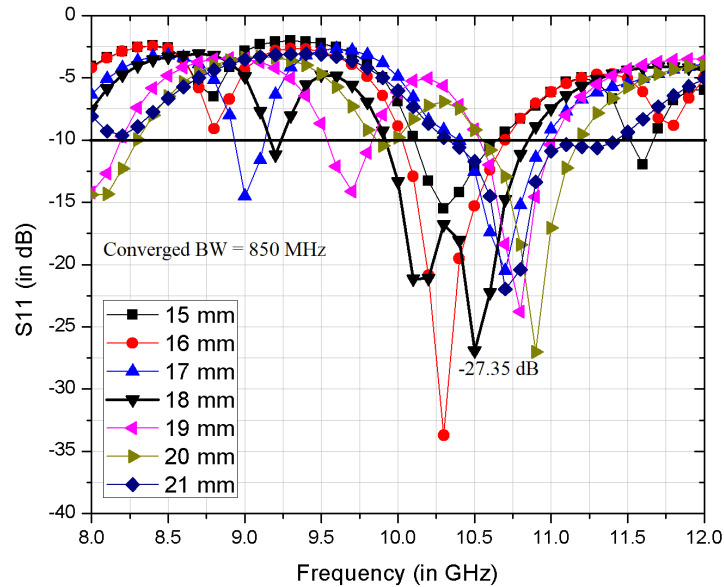
Figure 4.16: Effect of length of the feedline (L_{FL}) (keeping all other parameters constant – as per Table 4.3)

4.1.3.6   Effect of the width of the feedline (W_{FL})

In this subsection, the effect of varying the width of the feedline (W_{FL}), as illustrated in Fig. 4.17, is studied. It is observed there is no significant shift in the resonating frequency and impedance bandwidth with the change in the width of the feedline (W_{FL}). It is also observed that a fine-tuning of the resonating frequency is possible by changing the width of the feedline (W_{FL}). It is also observed that return loss at resonating frequency can be improved at a cost of impedance bandwidth. The optimized value of feedline's width is 7 mm, achieved return loss is -27.35 dB, and the bandwidth is 850 MHz.
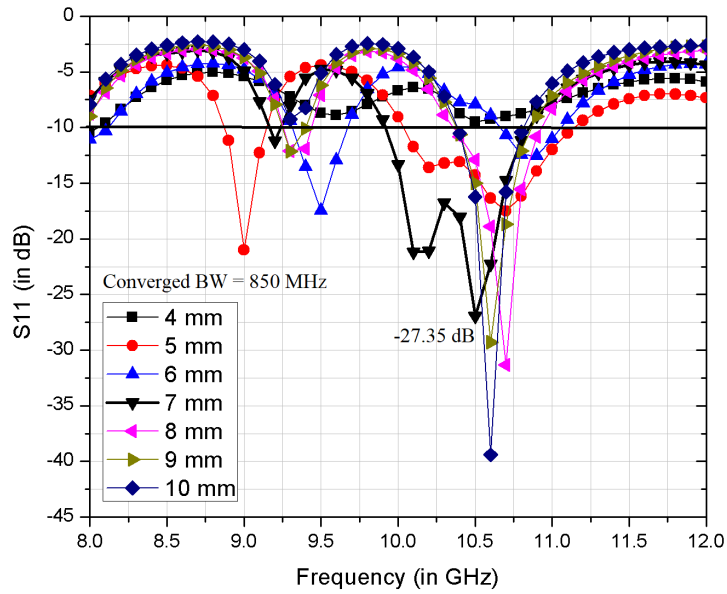
Figure 4.17: Effect of the width of the feedline (W_{FL}) (keeping all other parameters constant – as per Table 4.3)

4.1.3.7   Effect of length of the ground plane (L_G)

In this subsection, the effect of varying the length of the ground plane (L_G), as illustrated in Fig. 4.18, is studied. It is observed that, there is a significant shift in the resonating frequency (ranging from 9 to 10.7 GHz) at a cost of impedance bandwidth with the change in the length of the ground plane (L_G). It is also observed that tuning the resonating frequency is possible by changing the ground plane (L_G). It is also observed that there is no significant improvement in the impedance bandwidth with the changes in the L_G. The optimized value of ground plane's length is 26 mm, achieved return loss is -27.35 dB, and the bandwidth is 850 MHz.
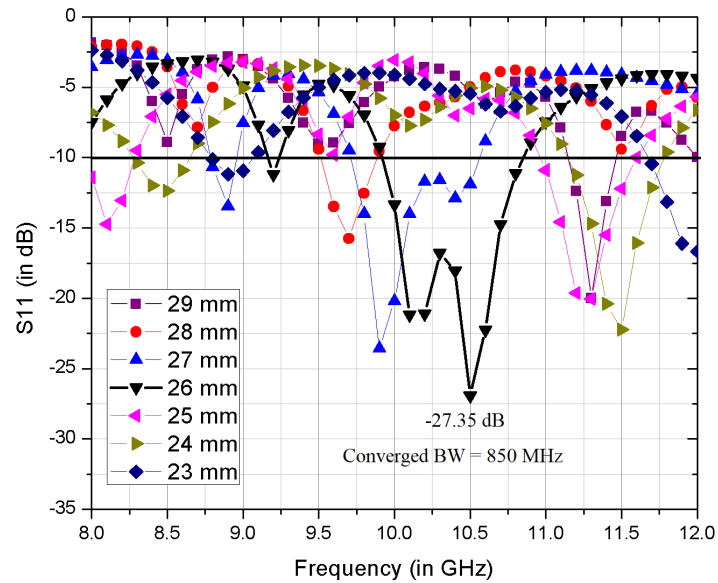
Figure 4.18: Effect of length of the ground plane (L_G) (keeping all other parameters constant – as per Table 4.3)

4.2 Design and Optimization using Particle Swarm Optimization (PSO)

This section presents the design, optimization, fabrication, and measurement of conventional rectangular shaped microstrip patch antenna with the partial ground plane. Particle Swarm Optimization (PSO) is used in the process of design and optimization of this antenna. The step-by-step procedure of the antenna optimization is discussed along with the convergence graph, converged antenna design, simulated, and measurement results. The fabrication of antenna is done by a computerized photolithography process. Vector Network Analyzer (VNA) is used for the validation of the simulated results.

4.2.1 Design objectives, cost-function and stepwise procedure of optimization

The objective was to design and simulate the microstrip antenna for its multi-objective optimized performance, i.e.:

- to radiate at a resonating frequency of 10.5 GHz;

91

- have minimum return loss at resonating frequency;

- have high impedance bandwidth (up to 1.5 GHz);

- achieve high gain.

The code for the PSO algorithm is integrated with the HFSS environment using MAT-LAB. A block diagram of a PSO based simple optimizer is shown in Fig. 1.15 [40].

Procedure used by Particle Swarm Optimization (PSO) for antenna design and optimization is summarized as follows:

1. **Step 1 - Initializing the parameters**: Parameters such as position and speed of the particle to random numbers in the D-dimensional search space. PSO parameters such as particle's position, speed of particles, etc. used for the optimization of antenna geometry are determined by the parameters discussed in Table 4.4.

PSO Parameters	Selected Values
Size of Population	200
The dimension of the problem	7
Maximum number of iterations	500
Minimum weight	0.2
Maximum weight	0.9
Acceleration factors c1, c2	2, 2
Stopping criteria on the basis of stale generations	10 stale generations

Table 4.4: PSO parameters used for the purpose of antenna design

2. **Step 2 - Evaluation of the particle's position using a fitness function**: The fitness function used for the purpose of optimization is defined in the equations 4.6. Equations 4.7-4.10 are used in the calculation of fitness function. If the stopping criterion is satisfied, stop the PSO procedure; otherwise, go to Step#4. By default, PSO minimizes the cost (fitness) function. The value of cost/fitness function varies from 0 to the most optimal value of -90.

$$F = [-(3 * Gain) - (20 * BW) + S_{11(Res)}] \tag{4.6}$$

$$Gain = \begin{cases} 10 \text{ dB; for Gain}_{cal} \geq 10 \text{ dB;} \\ \text{Gain}_{cal}; \text{ for Gain}_{cal} < 10 \text{ dB;} \end{cases} \tag{4.7}$$

$$BW = \begin{cases} 1.5 \text{ GHz; for BW}_{cal} \geq 1.5 \text{ GHz;} \\ \text{BW}_{cal}; \text{ for BW}_{cal} < 1.5 \text{ GHz;} \end{cases} \tag{4.8}$$

$$BW_{cal} = f_H - f_L \tag{4.9}$$

$$S_{11(Res)} = \begin{cases} -30 \text{ dB; for } S_{11} \leq -30 \text{ dB;} \\ S_{11}\text{; for } S_{11} > -30 \text{ dB;} \end{cases} \tag{4.10}$$

Where BW is the impedance bandwidth of the microstrip antenna calculated using equation 4.8. It is simply the difference between the upper operating frequency, f_H, and lower frequency, f_L. The value of BW_{cal}, as used in equation 4.8, is calculated using the formulae shown in equation 4.9 (implemented in MATLAB code) utilizing the simulated values of return loss received after simulating the design using HFSS. Similarly, the values of $S_{11}(f_1;\ldots; f_n)$ (used in equation 4.9) are the simulated values of return loss at different frequencies. $S_{11(Res)}$ is the value of return loss at resonating frequency (f_o) calculated using equation 4.10.

3. **Step 3: Making a comparison between** the fitness value received from step 2 with the particle's personal best value $pbest$, and updating the best value as new $pbest$; Second, by comparing the particle's fitness value with the global best value $gbest$, and updating the best value as new $gbest$.

4. **Step 4 - Updating the particle**: Update the velocity and position of the particles according to the equations 1.6, 1.7, and 1.8.

5. **Step 5 - The termination conditions of iteration**: Repeat the process from Step#2 onwards unless the termination conditions are met. Generally, when the fitness value reaches to its optimal or the optimization process reaches the maximum number of iterations, termination conditions are satisfied.

Some design checks are applied to validate the antenna design. These design based checks helped in saving a lot of optimization time by non-feasible designs from getting processed. These checks are shown in Fig. 4.19. Length of the substrate is shown as L_S, length of the patch as L_P, length of feedline as L_F, length of the ground plane as L_G, the width of the substrate as W_S, and width of the patch as W_P. The initial geometry of the antenna is based on the values discussed in Table 4.5. The convergence is obtained after the 18th iteration.
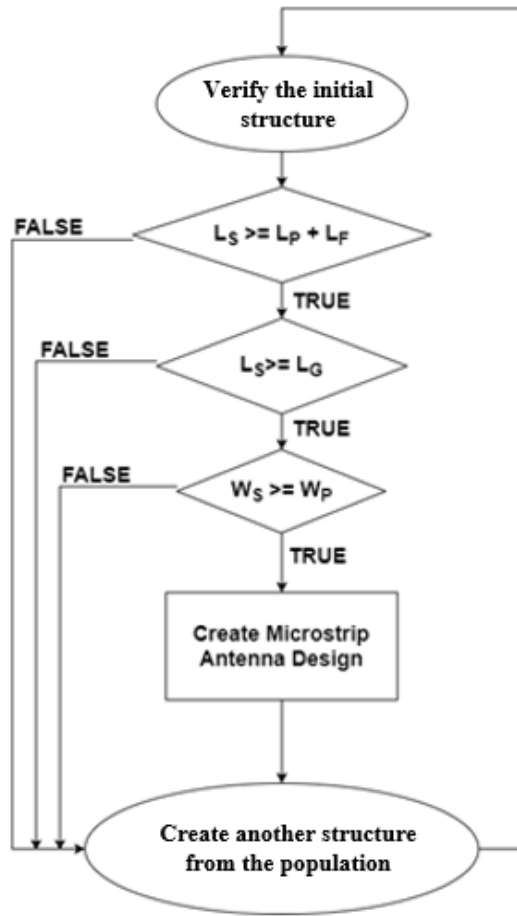
Figure 4.19: Flowchart of the design checks to validate the antenna design

Patch (in mm)		**Substrate** (in mm)		**Feedline** (in mm)		**Ground Plane** (in mm)	
Length (L_P)	Width (W_P)	Length (L_S)	Width (W_S)	Length (L_{FL})	Width (W_{FL})	Length (L_G)	Width (W_G)
5-40	5-40	18-50	18-50	4-20	1-8	5-50	$= W_S$
Resolution: 1 mm (for each parameter)							

Table 4.5: PSO parameters used for Antenna design.

4.2.2 Optimization results, convergence graph, and converged antenna design

The objective of the antenna design was to achieve multi-objective optimized performance (this includes improvements in gain, impedance bandwidth, and reduction of return loss). The antenna proposed is in X-band of super-high frequency to radiate at a resonating frequency of 10.5 GHz. The antenna design has a conventional rectangular substrate and patch with a partial ground plane. The configuration of the antenna optimized using

94

the Particle Swarm Optimization (PSO) is represented in Fig. 4.20. Fig. 4.21 displays the fabricated antenna converged using PSO. In this design, an FR4 substrate is utilized as it is inexpensive and eases in fabrication. The height of the FR4 substrate is 1.58 mm, having a dielectric constant of 4.3 and a loss tangent of 0.02. The converged antenna geometry is summarized in Table 4.6. The fabrication of antenna is done by a computerized photolithography process. The return loss (S_{11}) of the fabricated antenna is measured using a Vector Network Analyzer (VNA). Fig. 4.22 shows the rate of convergence for PSO optimization.
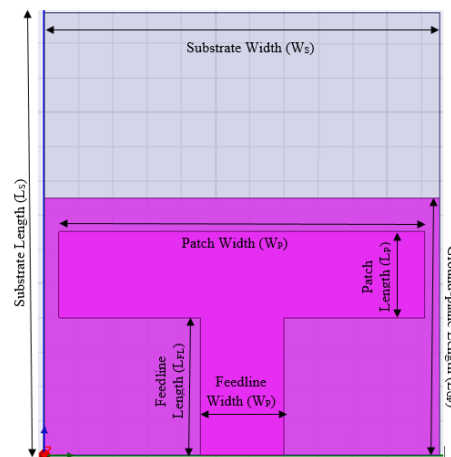
Figure 4.20: Proposed microstrip patch antenna configuration
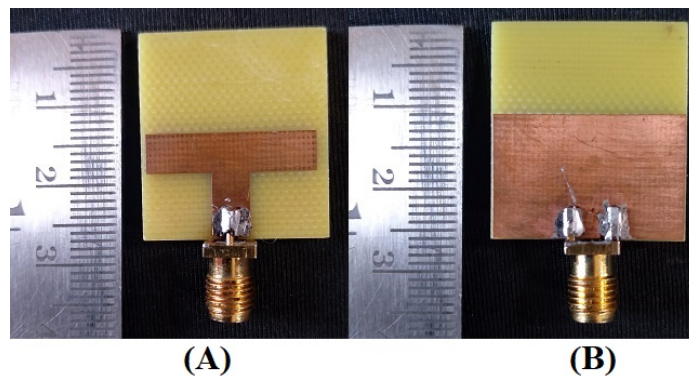
Figure 4.21: Fabricated antenna with partial ground plane (A) Front (B) Rear

4.2.2.1 Simulated and Measured Results

Return Loss (S_{11}), Voltage Standing Wave Ratio (VSWR), Real and Imaginary Impedance (Z_{11}):
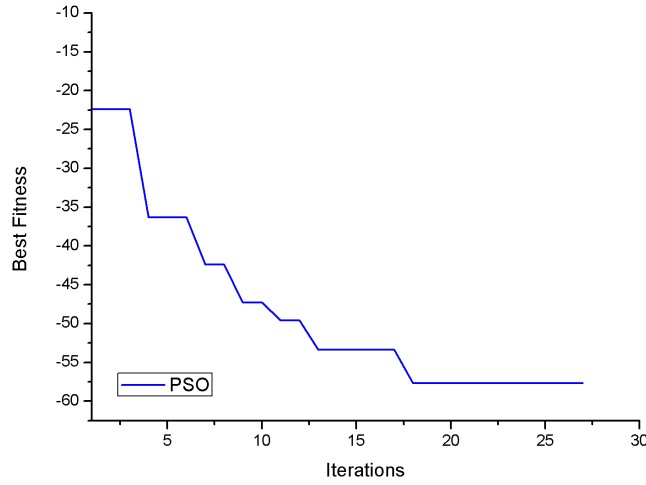
Figure 4.22: Rate of convergence for PSO optimization

Parameters	Values (in mm)
Substrate Length (L_S)	25.81
Substrate Width (W_S)	23.08
Ground Plane Length (L_G)	14.97
Ground Plane Width (W_G)	23.08
Patch Length (L_P)	5
Patch Width (W_P)	21.37
Feedline Length (L_{FL})	8.03
Feedline Width (W_{FL})	4.82

Table 4.6: PSO converged Antenna geometry.

Fig. 4.23 shows the simulated and measured values of return loss (S_{11}) at 10.5 GHz in the X-Band. The return loss (S_{11}) curve with the resonant frequency at 10.5 GHz is having -28.40 dB (simulated results) and -23.02 dB (measured results) values of return loss. The proposed antenna shows 1.95 GHz (simulated results) from 9.71 GHz to 11.66 GHz and 1.55 GHz (measured results) from 9.66 GHz to 11.21 GHz of impedance band-width. Fig. 4.24 shows the simulated and measured values of Voltage Standing Wave Ratio (VSWR). The value of VSWR at 10.5 GHz is 1.079 (simulated) and 1.152 (measured). Fig. 4.25 shows the real and imaginary impedance (Z_{11}). The values of real impedance at 10.5 GHz are 48.39 Ω, and imaginary impedance at 10.5 GHz is 3.38 Ω.

Radiation Patterns (2D and 3D), E-Plane, H-Plane, Co and Cross Polarization:

Fig. 4.26 shows the simulated values of 3-Dimensional radiation patterns for gain and
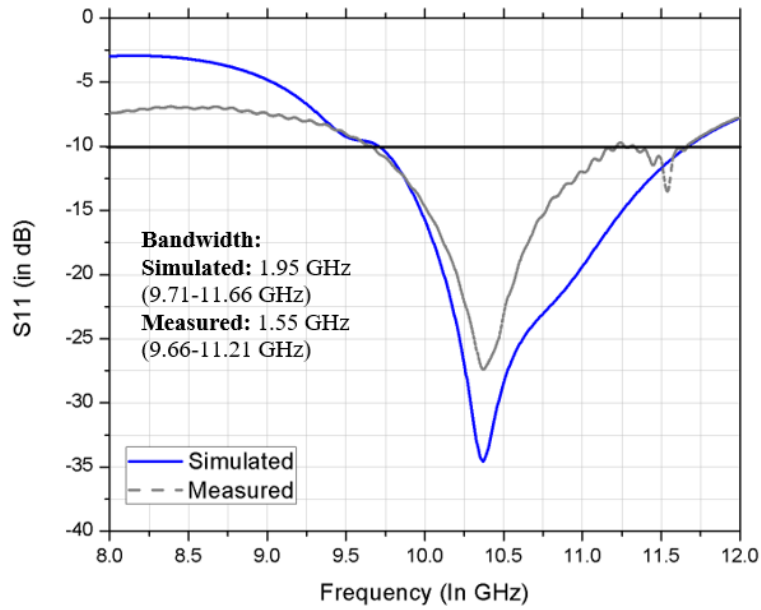
Figure 4.23: Simulated vs. measured values of return loss (S_{11})
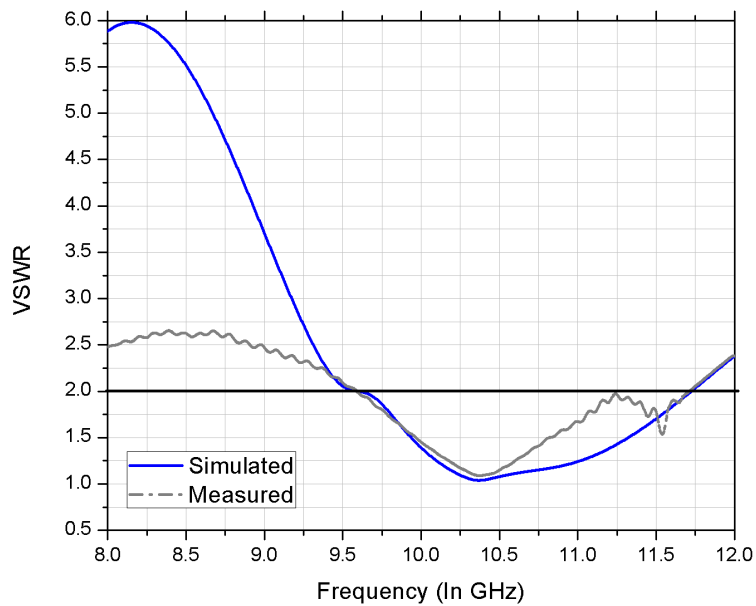
Figure 4.24: Simulated vs. measured values of Voltage Standing Wave Ratio (VSWR)

directivity at 10.5. The 2D plots of radiation patterns are shown in Fig. 4.27 for E-Plane and H-plane, respectively. A 2-D plot of co-polarization and cross-polarization at 10.5 GHz is shown in Fig. 4.28. Figs. 4.26 and 4.27 show the omnidirectional behavior of the proposed antenna.
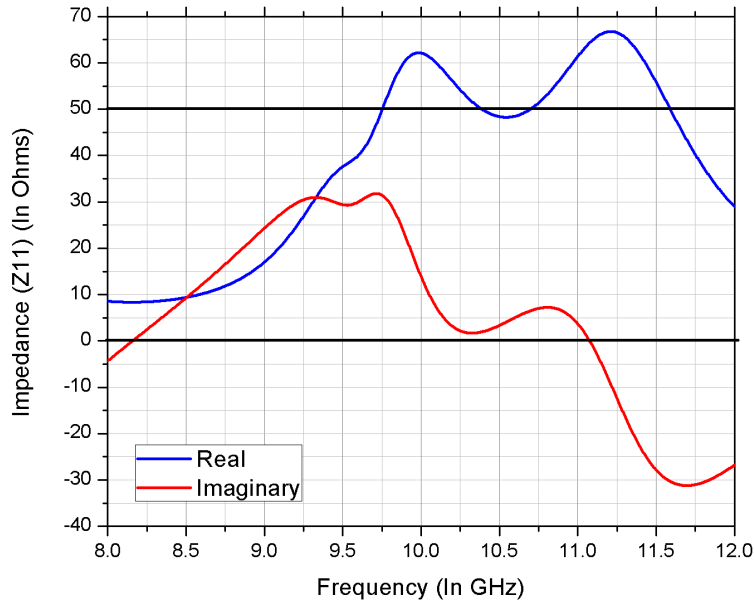
Figure 4.25: Simulated values of real and imaginary impedance (Z_{11})

(A)   **(B)**
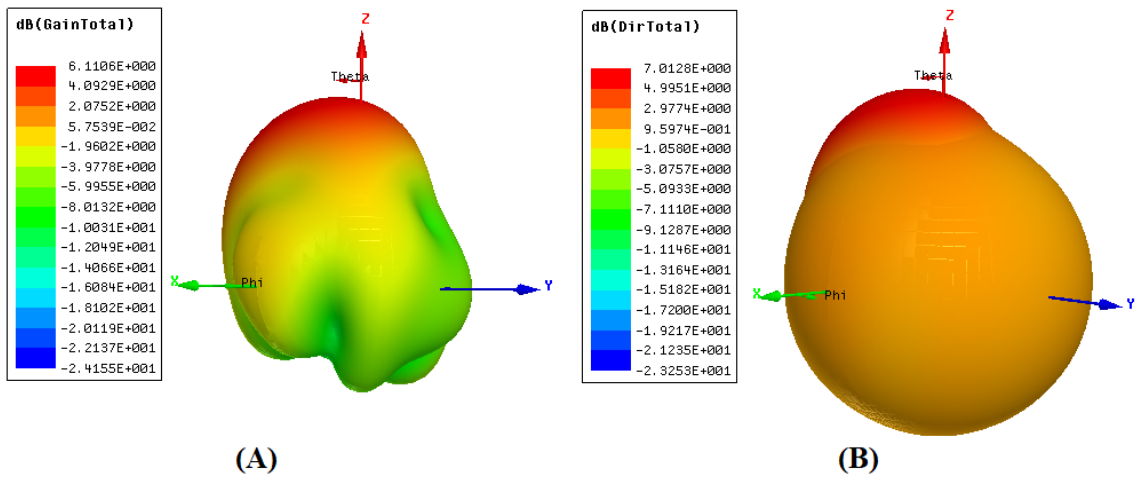
Figure 4.26: Simulated values of 3-Dimensional Radiation Patterns (A) Gain (B) Directivity

Gain and Directivity:

A plot of gain and directivity over the impedance bandwidth of the proposed antenna is presented in Fig. 4.29. At the resonant frequency of 10.5 GHz, the proposed antenna exhibits higher simulated values of gain and directivity. The value of simulated gain is 4.07 dB, and directivity is 5.01 dB at 10.5 GHz.
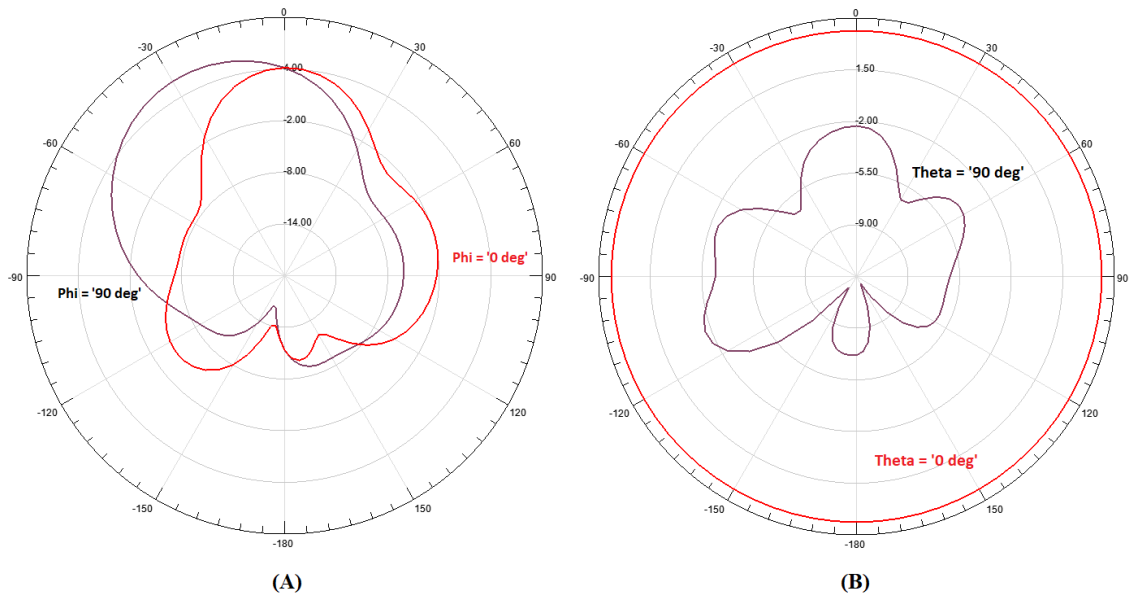
Figure 4.27: Simulated values of 2-Dimensional Radiation Patterns (A) Gain E-Plane (B) Gain H-Plane
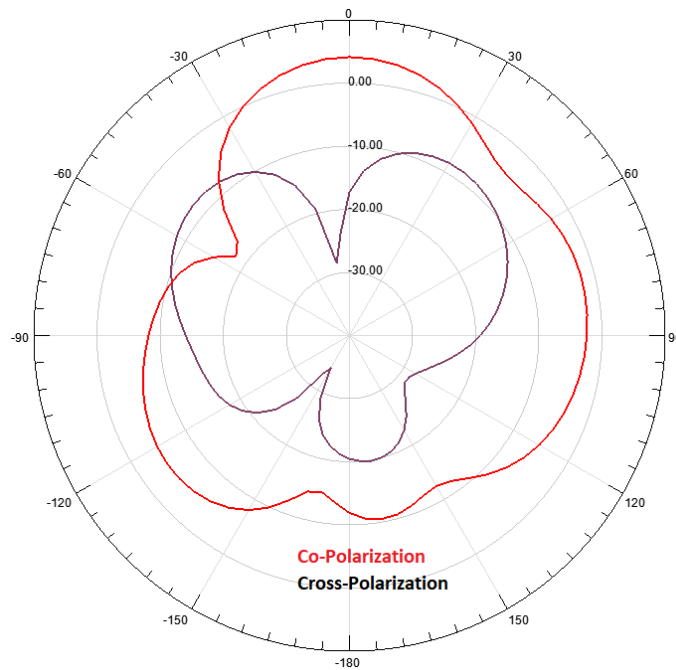
Figure 4.28: Simulated values of 2-Dimensional Radiation Patterns XZ-Plane (Co and Cross-Polarization)

4.2.3 Parametric Analysis of the Proposed Antenna

In the following subsection, an analysis is carried out to determine the effect of the microstrip patch antenna's design parameters on the resonating frequency and the impedance
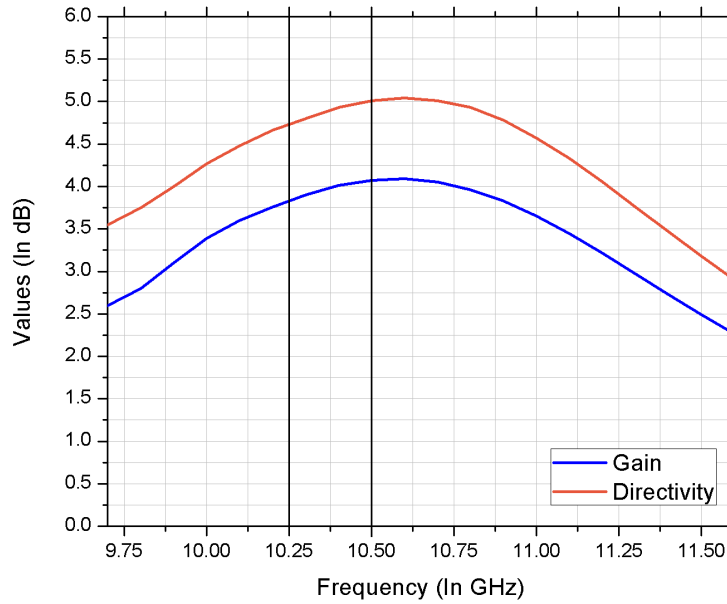
Figure 4.29: Simulated values of gain and directivity over the impedance bandwidth

bandwidth. Fig. 4.30-4.36 demonstrates all the analyzed parameters. The participation of a specific parameter is analyzed at a time while preserving all other parameters to their suboptimal values (as per Table 4.6 – PSO converged antenna geometry). This parametric analysis shows the validity of the PSO converged antenna design.

4.2.3.1 Effect of length of the substrate (L_S)

The substrate's length is considered to be important as it impacts the overall size of the microstrip patch antenna. In this subsection, the effect of varying the length of the substrate (L_S), as illustrated in Fig. 4.30, is studied. It is observed that a significant change in the impedance bandwidth can be achieved by varying the L_S. Changes in the substrate's length can shift the resonating frequency slightly to the higher as well as lower frequencies in the X-band, with changes in the impedance bandwidth. The optimized value of substrate's length is 25.81 mm, achieved return loss is -33.63 dB, and the bandwidth is 1.9 GHz.
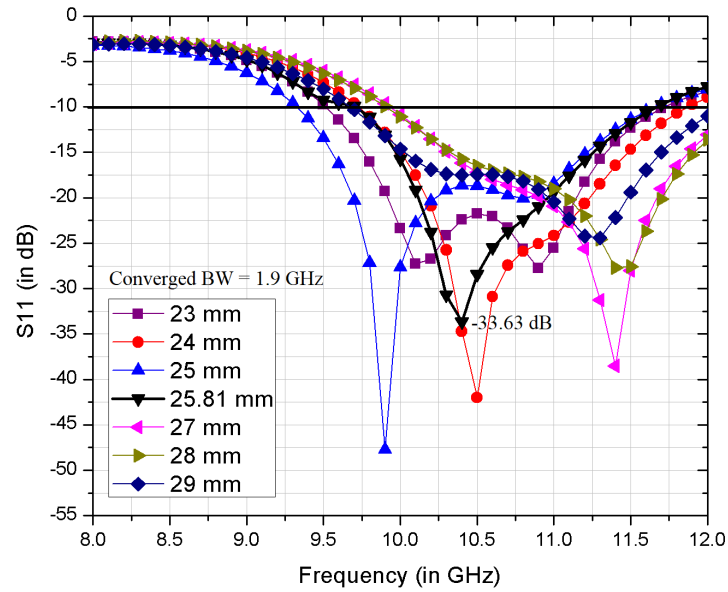
Figure 4.30: Effect of length of the substrate (L_S) (keeping all other parameters constant –
as per Table 4.6)

4.2.3.2 Effect of the width of the substrate (W_S)

Like the length of the substrate, its width also impacts the overall size of the microstrip patch antenna and is thus considered an important factor in design. In this subsection, the effect of varying the width of the substrate (W_S), as illustrated in Fig. 4.31, is studied. It is observed that a significant change in the resonating frequency, as well as impedance bandwidth, can be achieved by varying the W_S. Changes in the substrate's width can shift the resonating frequency to the higher and lower frequencies in the X-band. While changing the W_S, impedance bandwidth is also changing in the designs. This parameter can be considered as an important parameter for manual optimization. The optimized value of substrate's length is 23.08 mm, achieved return loss is -33.63 dB, and the bandwidth is 1.9 GHz.

4.2.3.3 Effect of length of the patch (L_P)

The effect of varying the length of the patch (L_P), as illustrated in Fig. 4.32, is studied. It is observed that a significant change in the resonating frequency, and impedance bandwidth, can be achieved by varying the L_P. Changes in the patch's length can shift
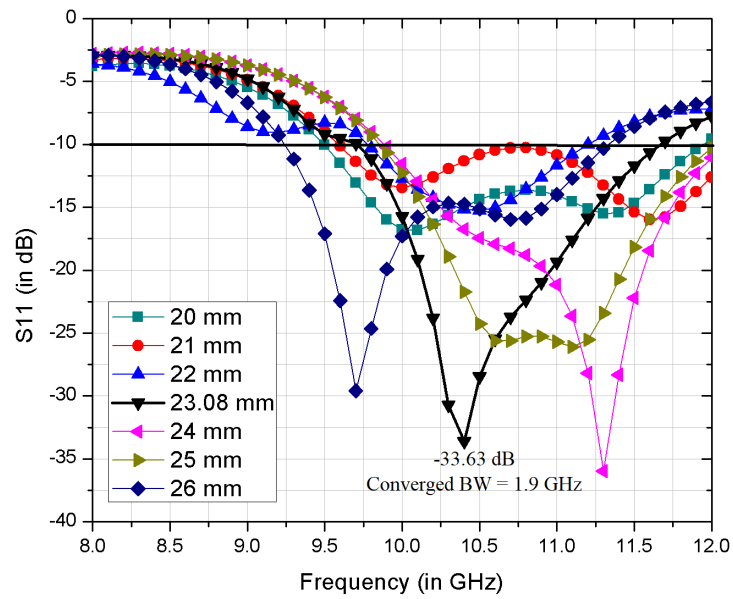
Figure 4.31: Effect of the width of the substrate (W_S) (keeping all other parameters constant – as per Table 4.6)

the resonating frequency to the lower frequencies of the X-band. While changing the L_P, impedance bandwidth is also changing in the designs. The optimized value of patch's length is 5 mm, achieved return loss is -33.63 dB, and the bandwidth is 1.9 GHz.
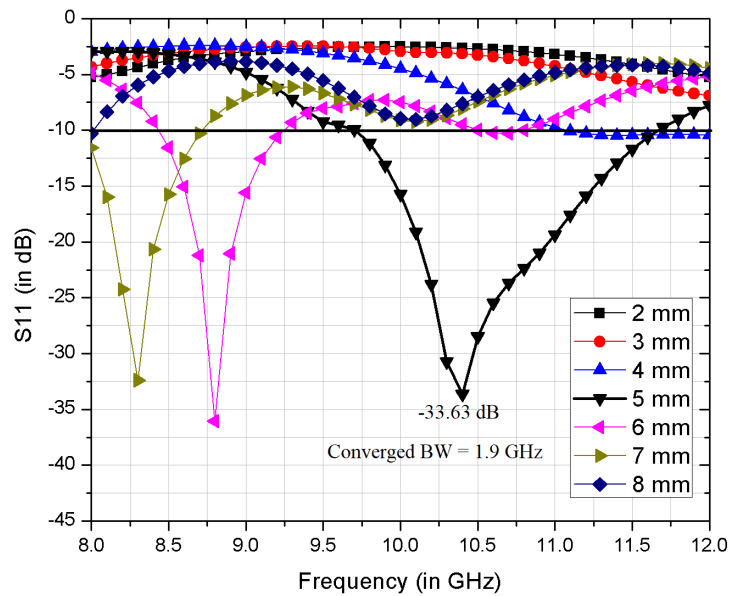
Figure 4.32: Effect of length of the patch (L_P) (keeping all other parameters constant – as per Table 4.6)

4.2.3.4 Effect of the width of the patch (W_P)

In this subsection, the effect of varying the width of the patch (W_P), as illustrated in Fig. 4.33, is studied. It is observed that a significant change in the resonating frequency and impedance bandwidth can be achieved by varying the W_P. Changes in the patch's width can slightly shift the resonating frequency to the higher frequencies of the X-band. While changing the W_P, impedance bandwidth is also changing in the designs. The optimized value of patch's width is 21.37 mm, achieved return loss is -33.63 dB, and the bandwidth is 1.9 GHz.
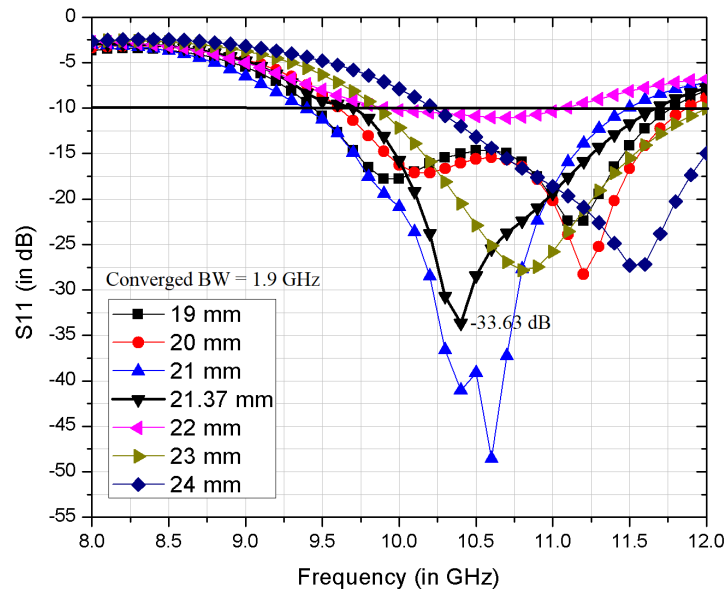
Figure 4.33: Effect of the width of the patch (W_P) (keeping all other parameters constant – as per Table 4.6)

4.2.3.5 Effect of length of the feedline (L_{FL})

In this subsection, the effect of varying the length of the feedline (L_{FL}), as illustrated in Fig. 4.34, is studied. It is observed that, there is a significant shift in the resonating frequency and impedance bandwidth with the change in length of feedline (L_{FL}). It is also observed that tuning the resonating frequency is possible by changing the feedline (L_{FL}). It is also observed that there is a significant improvement in the impedance bandwidth possible with the changes in the L_{FL}. The optimized value of feedline's length is 8.03

mm, achieved return loss is -33.63 dB, and the bandwidth is 1.9 GHz.
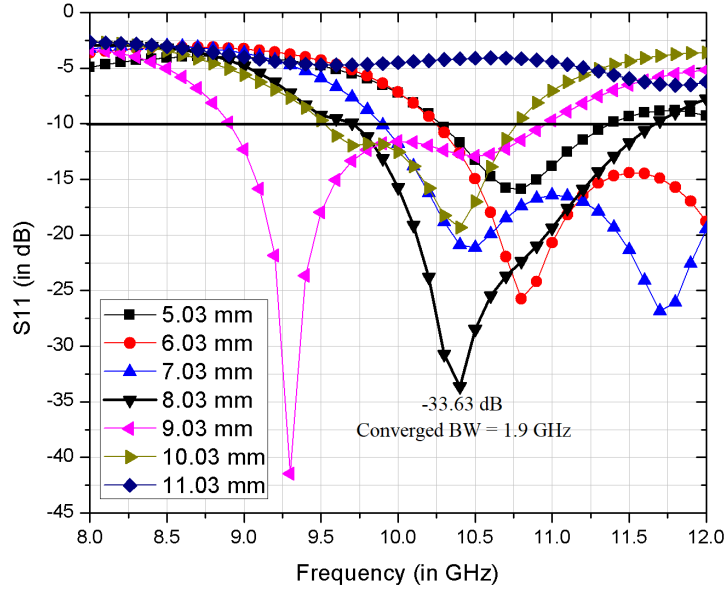
Figure 4.34: Effect of length of the feedline (L_{FL}) (keeping all other parameters constant – as per Table 4.6)

4.2.3.6 Effect of the width of the feedline (W_{FL})

In this subsection, the effect of varying the width of the feedline (W_{FL}), as illustrated in Fig. 4.35, is studied. It is observed that, there is a significant shift in the resonating frequency and impedance bandwidth with the change in the width of the feedline (W_{FL}). It is also observed that tuning the resonating frequency is possible by changing the feedline (W_{FL}). It is also observed that there is a significant improvement in the impedance bandwidth possible with the W_{FL} changes. The optimized value of feedline's width is 4.82 mm, achieved return loss is -33.63 dB, and the bandwidth is 1.9 GHz.

4.2.3.7 Effect of length of the ground plane (L_G)

In this subsection, the effect of varying the length of the ground plane (L_G), as illustrated in Fig. 4.36, is studied. It is observed that, there is a slight shift in the resonating frequency with the change in length of the ground plane (L_G). It is also observed that tuning the resonating frequency is possible by changing the ground plane (L_G). It is also
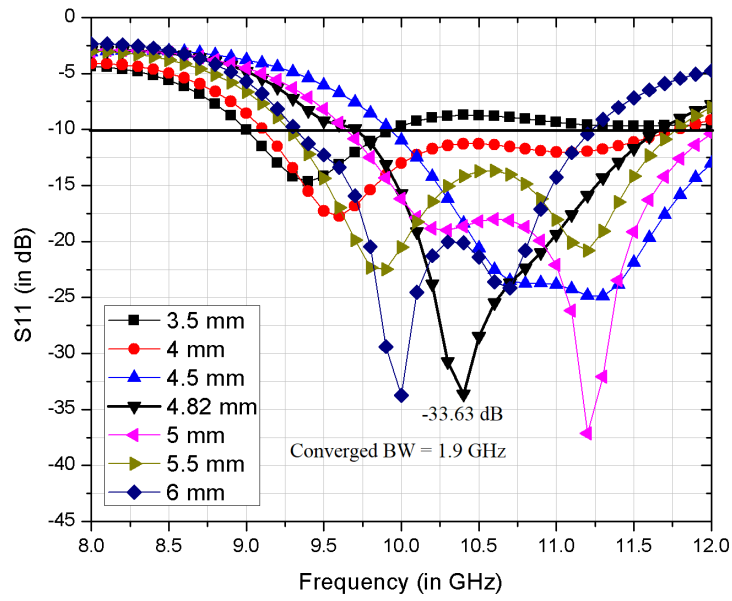
Figure 4.35: Effect of the width of the feedline (W_{FL}) (keeping all other parameters constant – as per Table 4.6)

observed that there is a significant improvement in the impedance bandwidth possible with L_G's changes. The optimized value of ground plane's width is 14.97 mm, achieved return loss is -33.63 dB, and the bandwidth is 1.9 GHz.
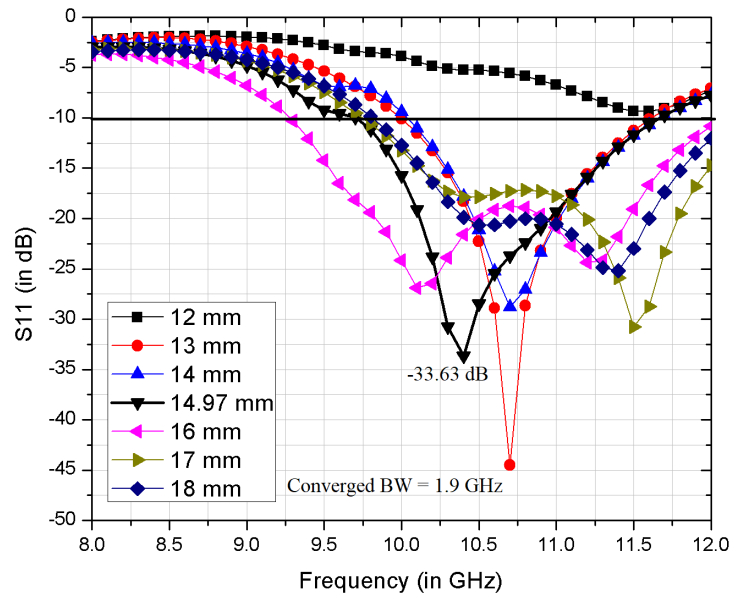
Figure 4.36: Effect of length of the ground plane (L_G) (keeping all other parameters constant – as per Table 4.6)

4.3 Design and Optimization using Grey Wolf Optimization (GWO)

This section presents the design, optimization, fabrication, and measurement of conventional rectangular shaped microstrip patch antenna with a partial ground plane. Grey Wolf Optimization (GWO) is used in the design and optimization of this antenna. The step-by-step procedure of the antenna optimization is discussed along with the convergence graph, converged antenna design, simulated, and measurement results. The fabrication of antenna is done by a computerized photolithography process. Vector Network Analyzer (VNA) is used for the validation of the simulated results.

4.3.1 Design objectives, cost-function and stepwise procedure of optimization

The objective was to design and simulate the microstrip antenna for its multi-objective optimized performance, i.e.:

- to radiate at a resonating frequency of 10.5 GHz;

- have minimum return loss at resonating frequency;

- have high impedance bandwidth (up to 1.5 GHz);

- achieve high gain.

The code for the GWO algorithm is integrated with the HFSS environment using MATLAB. Computational procedure of a GWO based optimizer [76]-[80] is discussed in chapter 1.

Grey Wolf Optimization (GWO) technique for antenna design and optimization is summarized as follows:

1. **Step 1 - Initializing the parameters**: Parameters such as number of Grey wolves, number of iterations, populations of alpha, beta, delta and omega wolves, etc. used for the optimization of antenna geometry are determined by the parameters discussed in Table 4.7.

GWO Parameters	Selected Values
Search Agents	30
The dimension of the problem	7
Maximum number of iterations	500
Stopping criteria based on stale generations	10 stale generations

Table 4.7: GWO parameters used for antenna design

2. **Step 2 - Estimate the target positions**: The target positions of alpha, beta, and delta wolves can be estimated using a fitness function. Fitness or cost function used for optimization is defined in the equation 4.11. Equations 4.12-4.15 are used in the calculation of fitness function. If the stopping criterion is satisfied, stop the GWO procedure; otherwise, go to Step 4. By default, GWO minimizes the cost (fitness) function. The value of cost/fitness function will vary from 0 to the most optimal value of -90.

$$F = [-(3 * Gain) - (20 * BW) + S_{11(Res)}] \quad (4.11)$$

$$Gain = \begin{cases} 10 \text{ dB; for Gain}_{cal} \geq 10 \text{ dB;} \\ \text{Gain}_{cal}; \text{ for Gain}_{cal} < 10 \text{ dB;} \end{cases} \quad (4.12)$$

$$BW = \begin{cases} 1.5 \text{ GHz; for BW}_{cal} \geq 1.5 \text{ GHz;} \\ \text{BW}_{cal}; \text{ for BW}_{cal} < 1.5 \text{ GHz;} \end{cases} \quad (4.13)$$

$$BW_{cal} = f_H - f_L \quad (4.14)$$

$$S_{11(Res)} = \begin{cases} -30 \text{ dB; for S}_{11} \leq -30 \text{ dB;} \\ \text{S}_{11}; \text{ for S}_{11} > -30 \text{ dB;} \end{cases} \quad (4.15)$$

Where BW is the impedance bandwidth of the microstrip antenna calculated using equation 4.13. It is simply the difference between the upper operating frequency, f_H, and lower frequency, f_L. The value of BW_{cal}, as used in equation 4.13, is calculated using the formulae shown in equation 4.14 (implemented in MATLAB code) utilizing the simulated values of return loss received after simulating the design using HFSS. Similarly, the values of $S_{11}(f_1; \ldots; f_n)$ (used in equation 4.14) are the simulated values of return loss at different frequencies. $S_{11(Res)}$ is the value of return loss at resonating frequency (f_o) calculated using equation 4.15.

3. **Step 3: Making a comparison** between the Grey wolves' positions received from step #2 with the wolves' previous best positions.

4. **Step 4: Updating the Grey wolves' positions** according to the standard GWO equations.

5. **Step 5 - The termination conditions of iteration**: Repeat the process from Step#2 onwards unless the termination conditions are met. Generally, when the fitness value reaches to its optimal or the optimization process reaches the maximum number of iterations, termination conditions are satisfied.

Some design checks are applied to validate the antenna design. These design based checks helped in saving a lot of optimization time by non-feasible designs from getting processed. These checks are shown in Fig. 4.37. Length of the substrate is shown as L_S, length of the patch as L_P, length of feedline as L_F, length of the ground plane as L_G, the width of the substrate as W_S, and width of the patch as W_P. The initial geometry of the
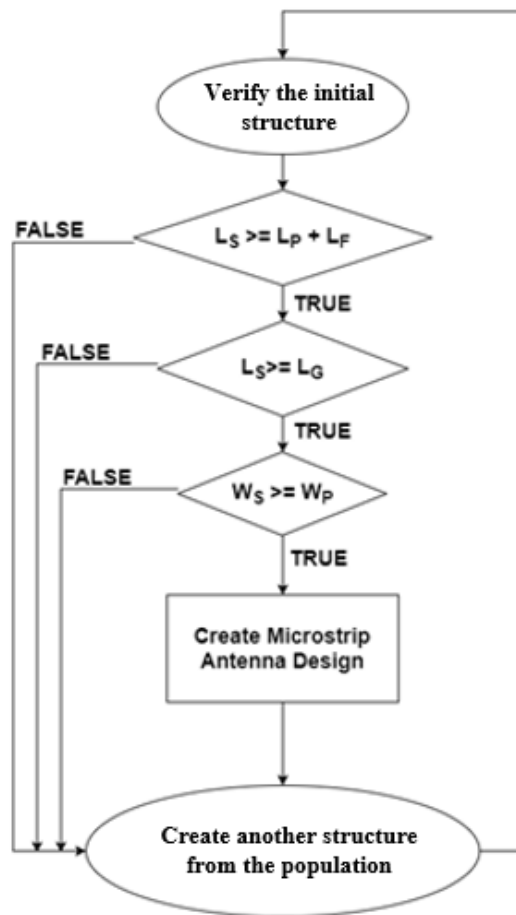
Figure 4.37: Flowchart of the design checks to validate the antenna design

antenna is based on the values discussed in Table 4.8. The convergence is obtained after the 27th iteration.

Patch		Substrate		Feedline		Ground Plane	
Length (L_P)	Width (W_P)	Length (L_S)	Width (W_S)	Length (L_{FL})	Width (W_{FL})	Length (L_G)	Width (W_G)
5-40	5-40	18-50	18-50	4-20	1-8	5-50	$= W_S$
All dimensions in mm. Resolution: 1 mm (for each parameter)							

Table 4.8: GWO parameters used for antenna design.

4.3.2 Optimization results, convergence graph, and converged antenna design

The objective of the antenna design was to achieve multi-objective optimized performance (this includes improvements in gain, impedance bandwidth, and reduction of return loss). The antenna proposed is in X-band of super-high frequency to radiate at a resonating frequency of 10.5 GHz. The antenna design has a conventional rectangular substrate and patch with a partial ground plane. The configuration of the antenna optimized using the Grey Wolf Optimization (GWO) is represented in Fig. 4.38. Fig. 4.39 displays the fabricated antenna converged using GWO. In this design, an FR4 substrate is utilized as it is inexpensive and eases in fabrication. The height of the FR4 substrate is 1.58 mm, having a dielectric constant of 4.3 and a loss tangent of 0.02. The converged antenna geometry is summarized in Table 4.9. A computerized photolithography process is used in the fabrication of the proposed antenna. The Return loss (S_{11}) of the fabricated antenna are measured using a Vector Network Analyzer (VNA). Fig. 4.40 shows the rate of convergence for GWO optimization.
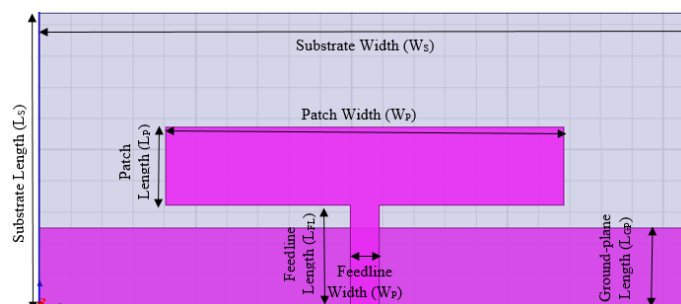
Figure 4.38: Proposed microstrip patch antenna configuration

(A)   (B)
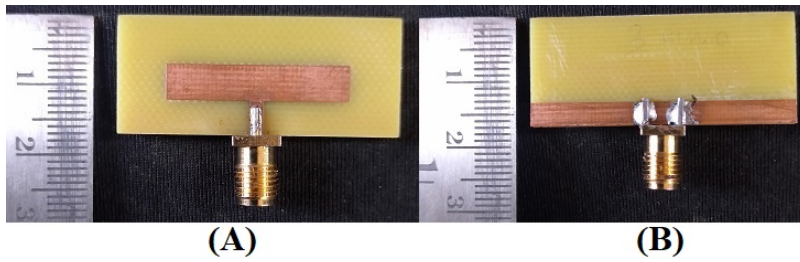
Figure 4.39: Fabricated antenna with partial ground plane (A) Front (B) Rear
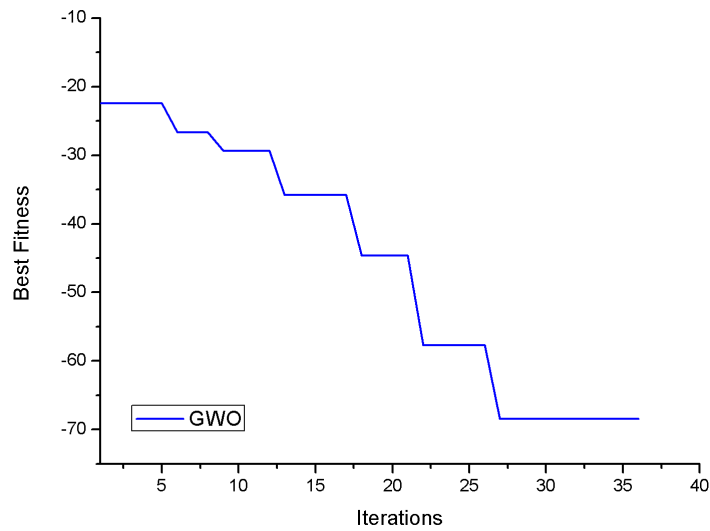
Figure 4.40: Rate of convergence for GWO optimization

Parameters	Values (in mm)
Substrate Length (L_S)	18.73
Substrate Width (W_S)	41.72
Ground Plane Length (L_G)	5
Ground Plane Width (W_G)	41.72
Patch Length (L_P)	5
Patch Width (W_P)	25.52
Feedline Length (L_{FL})	6.44
Feedline Width (W_{FL})	1.82

Table 4.9: GWO converged antenna geometry.

4.3.2.1   Simulated and Measured Results

Return Loss (S_{11}), Voltage Standing Wave Ratio (VSWR), Real and Imaginary Impedance (Z_{11}):

Fig. 4.41 shows the simulated and measured values of return loss (S_{11}) at 10.5 GHz in the X-Band. The return loss (S_{11}) curve with the resonant frequency at 10.5 GHz is having

-35.51 dB (simulated results) and -24.59 dB (measured results) values of return loss. The proposed antenna shows 3.89 GHz (simulated results) from 8 GHz to 11.89 GHz and 3.1 GHz (measured results) from 8.9 GHz to 12 GHz of impedance bandwidth. Fig. 4.42 shows the simulated and measured values of Voltage Standing Wave Ratio (VSWR). The value of VSWR at 10.5 GHz is 1.034 (simulated) and 1.125 (measured). Fig. 4.43 shows the real and imaginary impedance (Z_{11}). The values of real impedance at 10.5 GHz are 50.33 Ω, and imaginary impedance at 10.5 GHz is 1.64 Ω.
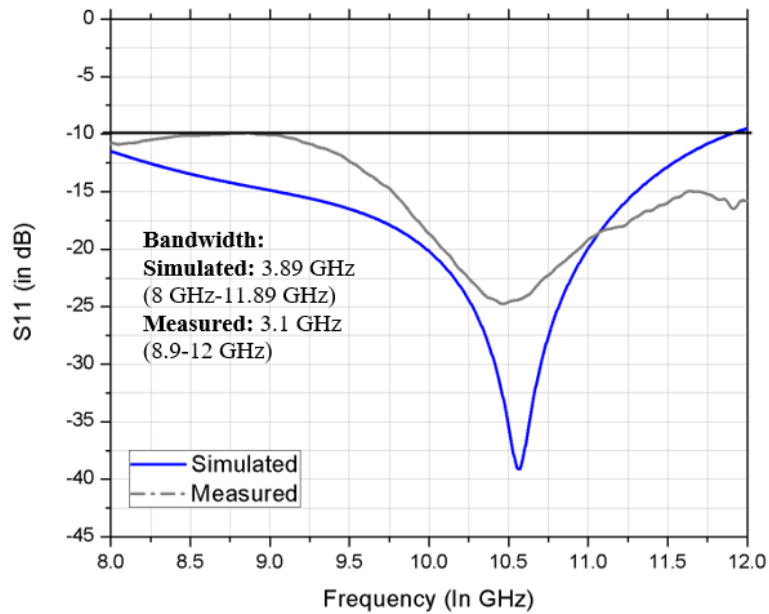
Figure 4.41: Simulated vs. measured values of return loss (S_{11})
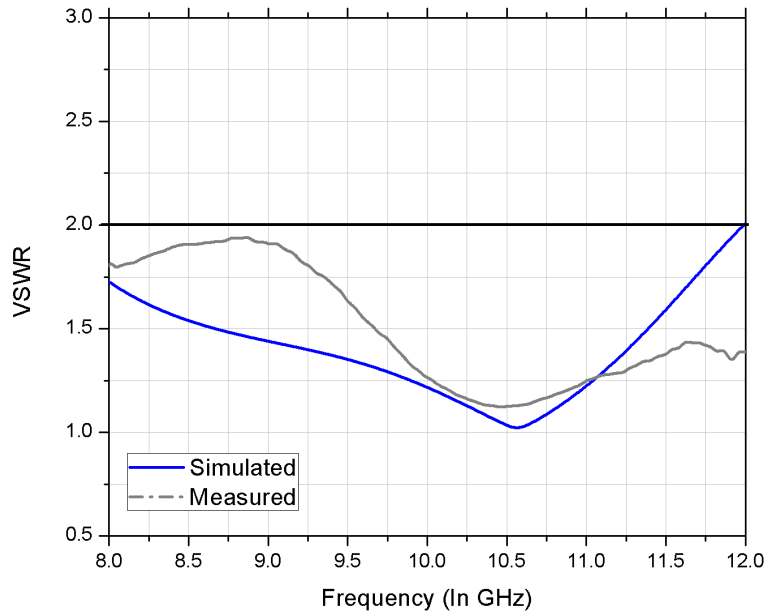
Figure 4.42: Simulated vs. measured values of Voltage Standing Wave Ratio (VSWR)
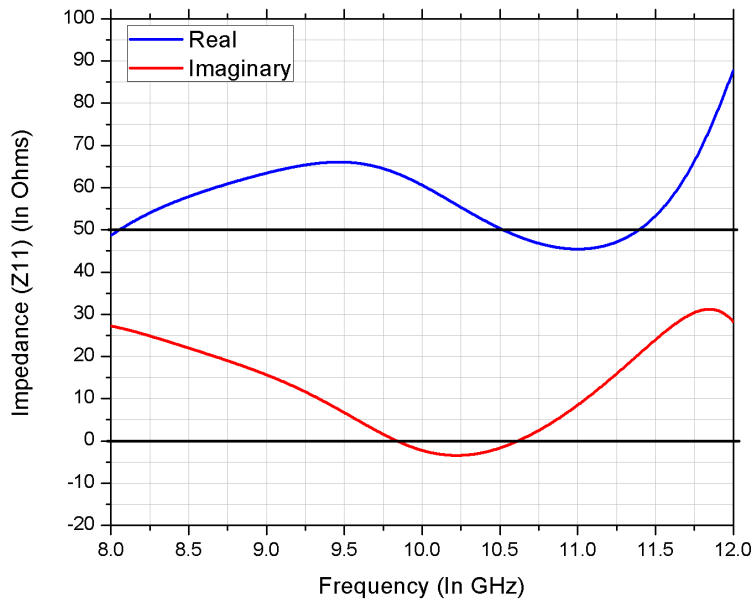
Figure 4.43: Simulated values of real and imaginary impedance (Z_{11})

Radiation Patterns (2D and 3D), E-Plane, H-Plane, Co and Cross Polarization:

Fig. 4.44 shows the simulated values of 3-Dimensional radiation patterns for gain and directivity at 10.5 GHz. The 2D plots of radiation patterns are shown in Fig. 4.45 for E-Plane and H-plane, respectively. A 2-D plot of co-polarization and cross-polarization at 10.5 GHz is shown in Fig. 4.46. Figs. 4.44 and 4.45 show the omnidirectional behavior of

the proposed antenna.
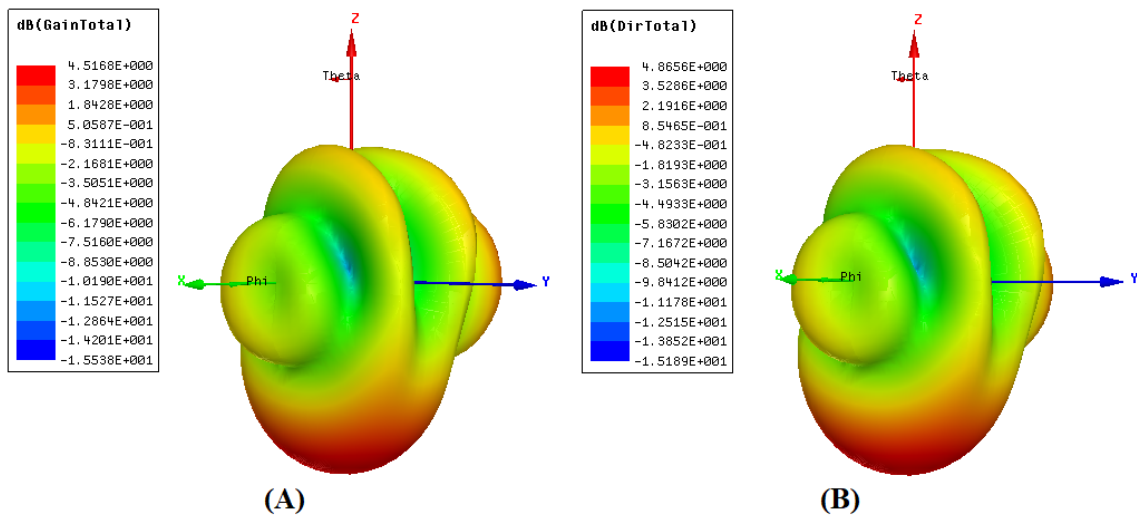
Figure 4.44: Simulated values of 3-Dimensional Radiation Patterns (A) Gain (B) Directivity
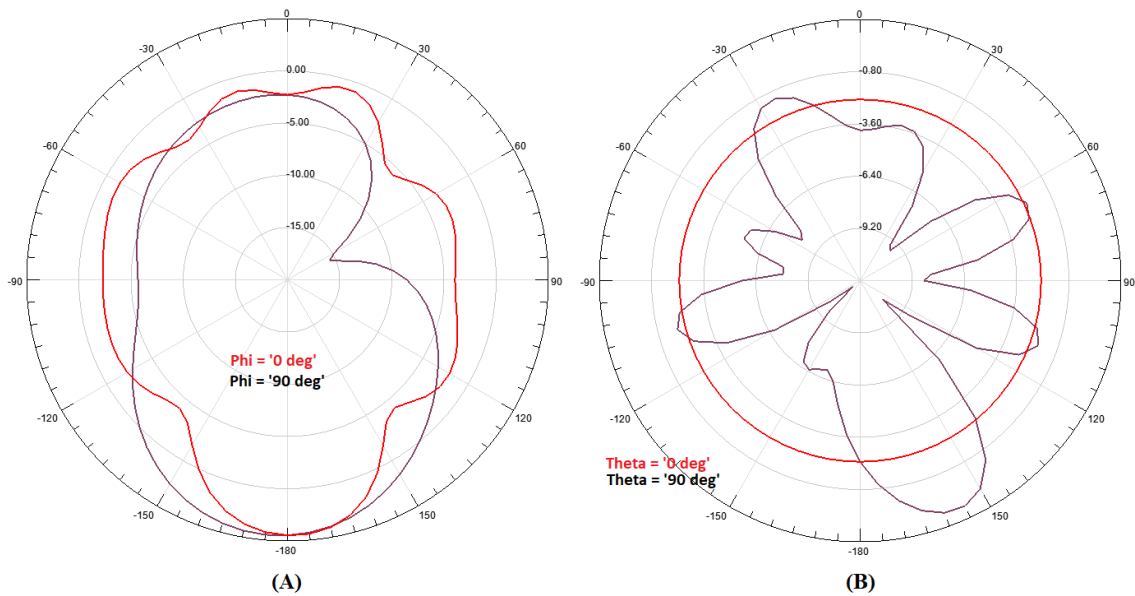
Figure 4.45: Simulated values of 2-Dimensional Radiation Patterns (A) Gain E-Plane (B) Gain H-Plane

Gain and Directivity:

A plot of gain and directivity over the impedance bandwidth of the proposed antenna is presented in the Fig. 4.47. At the resonant frequency of 10.5 GHz, the proposed antenna exhibits moderate simulated values of gain and directivity. The value of simulated gain is

113
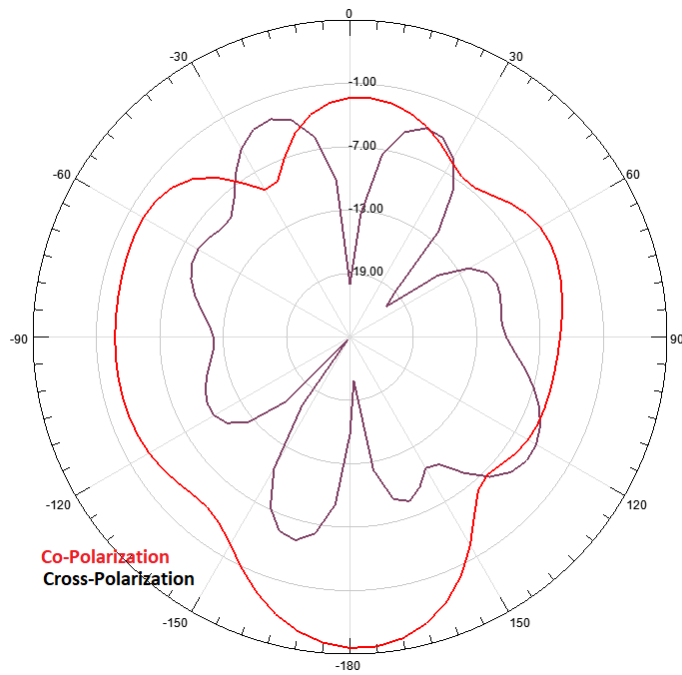
Figure 4.46: Simulated values of 2-Dimensional Radiation Patterns XZ-Plane (Co and Cross-Polarization)

2.82 dB, and directivity is 3.06 dB at 10.5 GHz.
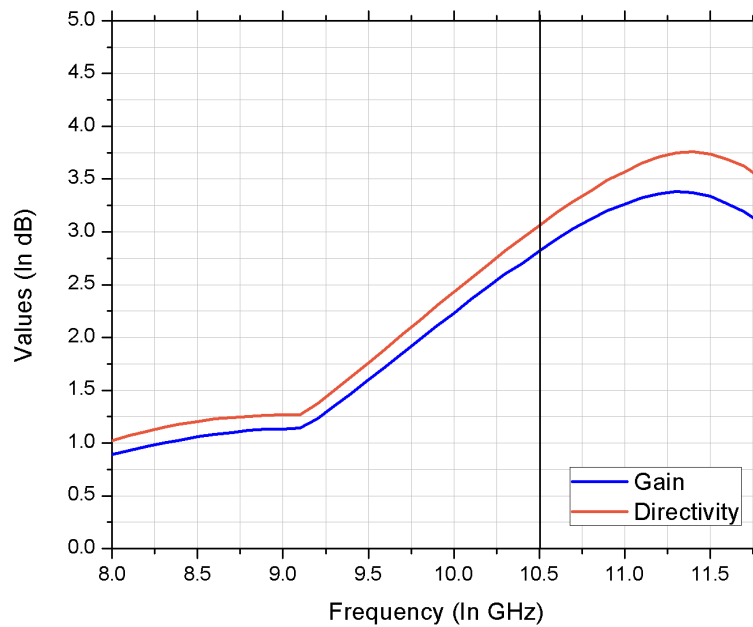
Figure 4.47: Simulated values of gain and directivity over the impedance bandwidth

4.3.3 Parametric Analysis of the Proposed Antenna

In the following subsection, an analysis is carried out to determine the effect of the microstrip patch antenna's design parameters on the resonating frequency and the impedance bandwidth. Fig. 4.48-4.54 demonstrates all the analyzed parameters. The participation of a specific parameter is analyzed at a time while preserving all other parameters to their suboptimal values (as per Table 4.9 – GWO converged antenna geometry). This parametric analysis shows the validity of the GWO converged antenna design.

4.3.3.1 Effect of length of the substrate (L_S)

The substrate's length is considered to be important as it impacts the overall size of the microstrip patch antenna. In this subsection, the effect of varying the length of the substrate (L_S), as illustrated in Fig. 4.48, is studied. It is observed that a significant change in the impedance bandwidth can be achieved by varying the L_S. Changes in the substrate's length can shift the resonating frequency slightly to the higher frequencies in the X-band, with changes in the impedance bandwidth as well. The optimized value of substrate's length is 18.73 mm, achieved return loss is -37.51 dB, and the bandwidth is 3.89 GHz.
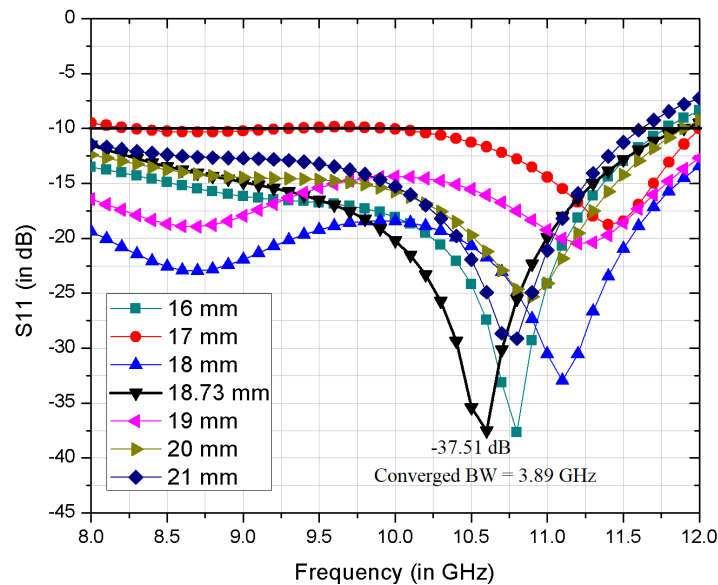
Figure 4.48: Effect of length of the substrate (L_S) (keeping all other parameters constant – as per Table 4.9)

4.3.3.2 Effect of the width of the substrate (W_S)

Like the length of the substrate, its width also impacts the overall size of the microstrip patch antenna and is thus considered an important factor in design. In this subsection, the effect of varying the width of the substrate (W_S), as illustrated in Fig. 4.49, is studied. It is observed that a slight change in the resonating frequency can be achieved by varying the W_S. Changes in the substrate's width can shift the resonating frequency to the higher frequencies in the X-band slightly. There are also not many changes in the impedance bandwidth of the designs. The optimized value of substrate's width is 41.72 mm, achieved return loss is -37.51 dB, and the bandwidth is 3.89 GHz.
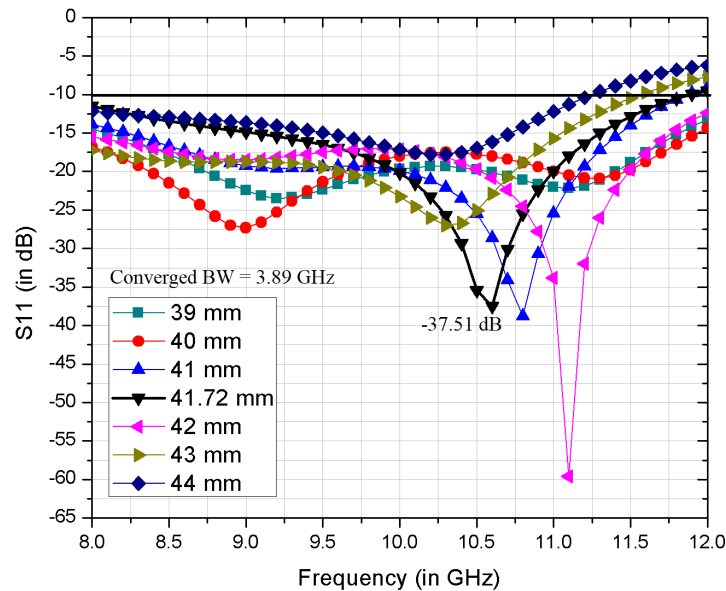
Figure 4.49: Effect of the width of the substrate (W_S) (keeping all other parameters constant – as per Table 4.9)

4.3.3.3 Effect of length of the patch (L_P)

The effect of varying the length of the patch (L_P), as illustrated in Fig. 4.50, is studied. It is observed that a significant change in the values of return loss (S_{11}) and the resonating frequency can be achieved by varying the L_P. Changes in the patch's length can shift the resonating frequency to the higher and lower frequencies in the X-band. While changing the L_P, impedance bandwidth is also changing in the designs. This parameter can be

considered as an important parameter for manual optimization. The optimized value of patch's length is 5 mm, achieved return loss is -37.51 dB, and the bandwidth is 3.89 GHz.
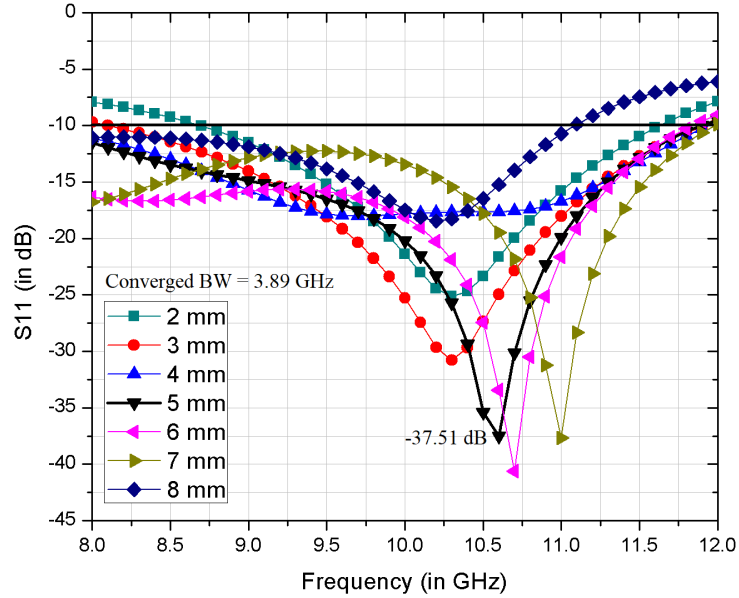
Figure 4.50: Effect of length of the patch (L_P) (keeping all other parameters constant – as per Table 4.9)

4.3.3.4 Effect of the width of the patch (W_P)

In this subsection, the effect of varying the width of the patch (W_P), as illustrated in Fig. 4.51, is studied. It is observed that a significant change in the resonating frequency, and impedance bandwidth, can be achieved by varying the (W_P). Changes in the width of the patch can slightly shift the resonating frequency to the higher and lower frequencies in the X-band. While changing the (W_P), impedance bandwidth is also changing in the designs. This parameter can also be considered as an important parameter for manual optimization. The optimized value of patch's width is 25.52 mm, achieved return loss is -37.51 dB, and the bandwidth is 3.89 GHz.

4.3.3.5 Effect of length of the feedline (L_{FL})

In this subsection, the effect of varying the length of the feedline (L_{FL}), as illustrated in Fig. 4.52, is studied. It is observed that, there is a significant shift in the resonating
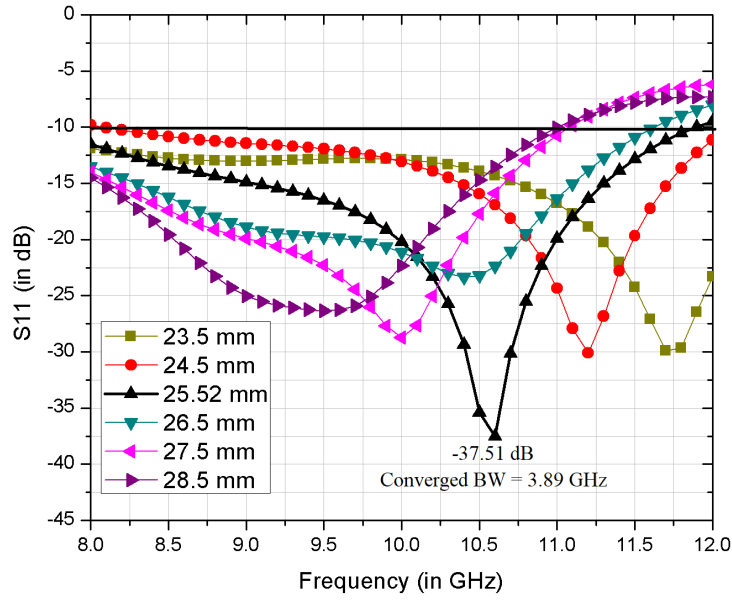
Figure 4.51: Effect of the width of the patch (W_P) (keeping all other parameters constant – as per Table 4.9)

frequency and impedance bandwidth with the change in length of feedline (L_{FL}). It is also observed that, there are significant changes in the value of return loss at the resonating frequency, and there is no significant improvement in the impedance bandwidth. The optimized value of feedline's length is 6.44 mm, achieved return loss is -37.51 dB, and the bandwidth is 3.89 GHz.
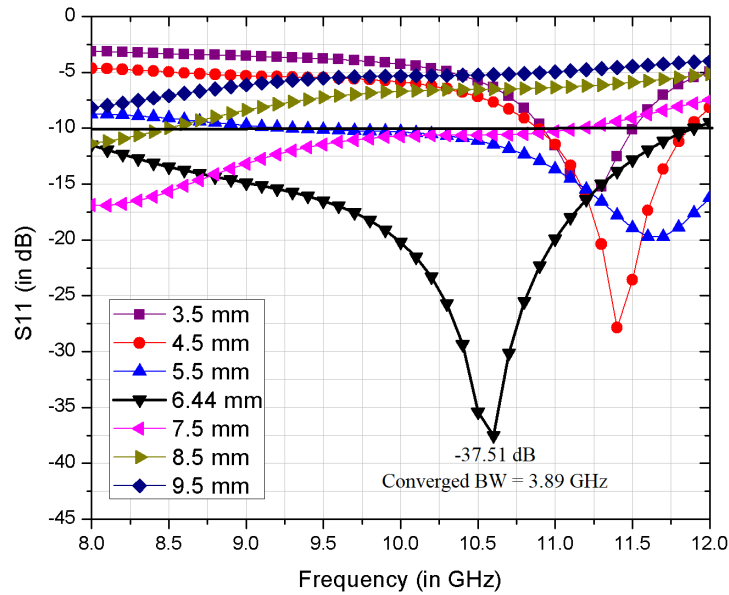
Figure 4.52: Effect of length of the feedline (L_{FL}) (keeping all other parameters constant – as per Table 4.9)

4.3.3.6 Effect of the width of the feedline (W_{FL})

In this subsection, the effect of varying the width of the feedline (W_{FL}), as illustrated in Fig. 4.53, is studied. It is observed that, there is a significant shift in the resonating frequency and impedance bandwidth with the change in the width of the feedline (W_{FL}). It is also observed that, tuning the resonating frequency is possible by changing the feedline (W_{FL}). It is also observed that, there is a significant improvement in the impedance bandwidth possible with the W_{FL} changes. The optimized value of feedline's width is 1.82 mm, achieved return loss is -37.51 dB, and the bandwidth is 3.89 GHz.
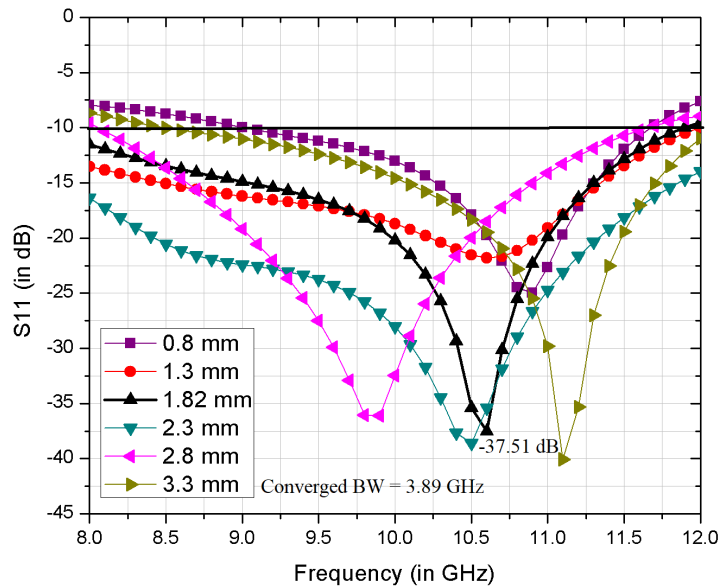
Figure 4.53: Effect of the width of the feedline (W_{FL}) (keeping all other parameters constant – as per Table 4.9)

4.3.3.7 Effect of length of the ground plane (L_G)

In this subsection, the effect of varying the length of the ground plane (L_G), as illustrated in Fig. 4.54, is studied. It is observed that, there is a significant impact on the resonating frequency and impedance bandwidth with the change in length of the feedline length of the ground plane (L_G). It is also observed that, there are significant changes in the value of return loss at the resonating frequency, and there is no significant improvement in the impedance bandwidth. The optimized value of ground plane's length is 5 mm,

achieved return loss is -37.51 dB, and the bandwidth is 3.89 GHz.
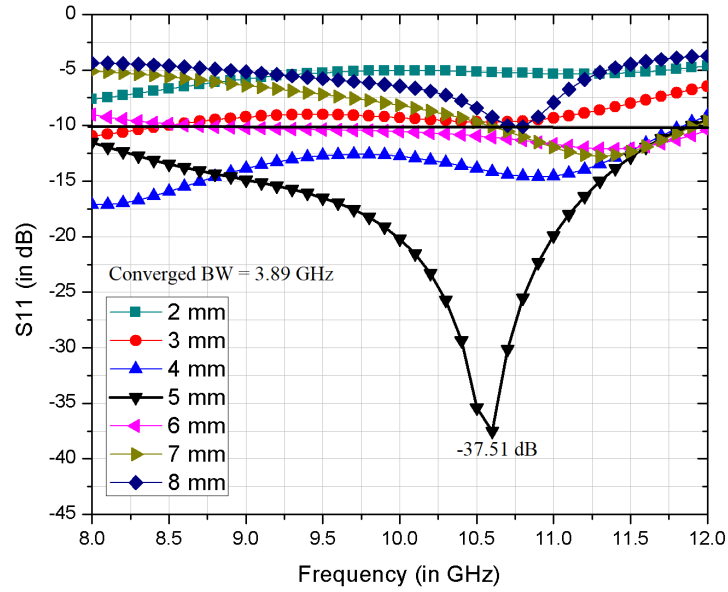
Figure 4.54: Effect of length of the ground plane (L_G) (keeping all other parameters constant – as per Table 4.9)

4.4   Comparison of Results

In this section, proposed designs are compared with the results of existing designs/ literature and is summarized in Table 4.10. It is observed that, all three designs exhibit decent values of return losses (S_{11}) at resonating frequency, sufficiently large bandwidth, high gain, and directivity. The first advantage with these designs is the cost of fabrication because of the inexpensive substrate material FR4. The second advantages of these designs are their low-profile dimensions. It can also be observed that the proposed design converged using Particle Swarm Optimization (PSO) technique is comparably better in terms of antenna dimensions, impedance bandwidth, gain and directivity. It is also observed that the design converged using Genetic Algorithm (GA) is slightly better in terms of gain and directivity at a cost of impedance bandwidth and antenna dimensions. Grey Wolf Optimization (GWO) is a novel technique used first time for the design and optimization of the microstrip patch antennas (to the best of our knowledge - as per literature review till 2018).

120

For further comparison, a summary of the five proposed antenna designs in this thesis is shown in Table 6.1.

Ref.	Operating frequency (f_o)	Impedance Bandwidth	Return Loss at f_o	Gain at f_o	Directivity at f_o	Dimensions (in mm^3)
[121]	10.5 GHz	3 GHz [M]	-20 dB [M]	5.35 dB [M]	Not available	30 x 21 x 1.5
[122]	10.5 GHz	1.7 GHz [M]	-14 dB [M]	4 dB [S]	Not available	30 x 30 x 1.58
[123]	10.04 GHz	2.95 GHz [S]	-42.57 [S]	1.06 dB [S]	1.21 dB [S]	30 x 35 x 1.58
Proposed Antenna GA	10.5 GHz	850 MHz [S]; 670 MHz [M]	-27.35 dB [S]; -21.51 [M]	4.26 dB [S]	7.36 dB [S]	41 x 45 x 1.58
Proposed Antenna PSO	10.5 GHz	1.9 GHz [S]; 1.6 GHz [M]	-28.40 dB [S]; -23.02 dB [M]	4.07 dB [S]	5.01 dB [S]	25.81 x 23.08 x 1.58
Proposed Antenna GWO	10.5 GHz	3.89 GHz [S]; 3.1 GHz [M]	-35.51 dB [S]; -24.59 dB [M]	2.82 dB [S]	3.06 dB [S]	18.73 x 41.72 x 1.58

Table 4.10: Comparison of the proposed antenna with existing literature. (Simulated [S] and Measured [M]).

4.5 Chapter Summary

This chapter presented the design, optimization, fabrication, and measurement of conventional rectangular shaped microstrip patch antennas with using three optimization techniques i.e. Genetic Algorithm, Particle Swarm Optimization, and Gray Wolf Optimization

resulting three different converged antennas. The objectives of these antenna designs were to achieve multi-objective optimized performance (this includes improvements in gain, impedance bandwidth, and reduction of return loss) and to compare the performance of different optimization techniques in terms rate of convergence and best antenna performance in terms of size, bandwidth and gain. The step-by-step procedure of the antenna optimization is discussed along with their convergence graphs, converged antenna designs, simulated, and measurement results. In all proposed designs, FR4 substrate with a height of 1.58 mm, dielectric constant of 4.3, and loss tangent of 0.02 is utilized for fabrication.

Genetic Algorithm (GA) is used in the process of design and optimization of the first proposed antenna. A step-by-step procedure of the antenna optimization using Genetic Algorithm (GA) is discussed along with the convergence graph, geometry of the converged antenna design, its simulated, and measurement results. The antenna proposed in this chapter radiates at a resonating frequency of 10.5 GHz and is useful for various wireless wideband applications in the X-Band. A number of potential applications in X-Band are discussed in chapter 1. The dimension of the converged antenna is 41 mm x 45 mm x 1.58 mm. The proposed antenna provides sufficiently large simulated bandwidth of 850 MHz (9.95-10.8 GHz) and measured bandwidth of 670 MHz (10.04-10.71 GHz). The values of return loss at the resonant frequency (of 10.5 GHz) is -27.35 dB (simulated) and -21.51 dB (measured). The simulated radiation patterns show the omnidirectional radiation characteristics. At the resonant frequency of 10.5 GHz, the proposed antenna exhibits higher simulated values of gain and directivity. The value of simulated gain is 4.26 dB, and directivity is 7.36 dB at 10.5 GHz. Parametric analysis is also presented in this chapter to further validate the converged design.

Particle Swarm Optimization (PSO) is used in the process of design and optimization of the second proposed antenna. A step-by-step procedure of the antenna optimization using Particle Swarm Optimization (PSO) is discussed along with the convergence graph, geometry of the converged antenna design, its simulated, and measurement results. The antenna proposed in this chapter radiates at a resonating frequency of 10.5 GHz and is useful for various wireless wideband applications in the X-Band. The dimension of the converged

antenna is 25.81 mm x 23.08 mm x 1.58 mm. The proposed antenna provides sufficiently large simulated bandwidth of 1.95 GHz (9.71-11.66 GHz) and measured bandwidth of 1.55 GHz (9.66-11.21 GHz). The values of return loss at the resonant frequency (of 10.5 GHz) is -28.40 dB (simulated) and -23.02 dB (measured). The simulated radiation patterns show the omnidirectional radiation characteristics. At the resonant frequency of 10.5 GHz, the proposed antenna exhibits higher simulated values of gain and directivity. The value of simulated gain is 4.07 dB, and directivity is 5.01 dB at 10.5 GHz. Parametric analysis is also presented in this chapter to further validate the converged design.

Gray Wolf Optimization (GWO) is used in the process of design and optimization of the third proposed antenna. A step-by-step procedure of the antenna optimization using Gray Wolf Optimization (GWO) is discussed along with the convergence graph, geometry of the converged antenna design, its simulated, and measurement results. The antenna proposed in this chapter radiates at a resonating frequency of 10.5 GHz and is useful for various wireless wideband applications in the X-Band. The dimension of the converged antenna is 18.73 mm x 41.72 mm x 1.58 mm. The proposed antenna provides sufficiently large simulated bandwidth of 3.89 GHz (8 GHz-11.89 GHz) and measured bandwidth of 3.1 GHz (8.9-12 GHz). The values of return loss at the resonant frequency (of 10.5 GHz) is -35.51 dB (simulated) and -24.59 dB (measured). The simulated radiation patterns show the omni-directional radiation characteristics. At the resonant frequency of 10.5 GHz, the proposed antenna exhibits simulated gain of 2.82 dB, and directivity of 3.06 dB. Parametric analysis is also presented in this chapter to further validate the converged design.

All three designs exhibit decent values of return losses (S_{11}) at resonating frequency, sufficiently large bandwidth, high gain, and directivity. The first advantage with these designs is the cost of fabrication because of the inexpensive substrate material FR4. The second advantages of these designs are their low-profile dimensions. For further comparison, a summary of the three converged designs are shown in Table 4.11. It can be observed that the proposed design converged using Particle Swarm Optimization (PSO) technique is comparably better in terms of antenna dimensions, impedance bandwidth, gain and directivity. It is also observed that the design converged using Genetic Algorithm (GA) is

slightly better in terms of gain and directivity at a cost of impedance bandwidth and antenna dimensions. Another key observation is the comparison between the convergence rate of

Parameters	Proposed GA Antenna	Proposed PSO Antenna	Proposed GWO Antenna
Optimization Technique	Genetic Algorithm (GA)	Particle Swarm Optimization (PSO)	Grey Wolf Optimization (GWO)
Operating Frequency (f_o) (X-Band)	10.5 GHz	10.5 GHz	10.5 GHz
Antenna dimensions (in mm^3)	41 x 45 x 1.58	25.81 x 23.08 x 1.58	18.73 x 41.72 x 1.58
Return Loss at f_o	-27.35 dB [S] -21.51 [M]	-28.40 dB [S] -23.02 dB [M]	-35.51 dB [S] -24.59 dB [M]
Impedance bandwidth	850 MHz [S] 670 MHz [M]	1.9 GHz [S] 1.6 GHz [M]	3.89 GHz [S] 3.1 GHz [M]
VSWR at f_o	1.096 [S] 1.183 [M]	1.079 [S] 1.152 [M]	1.034 [S] 1.125 [M]
Gain at f_o	4.26 dB [S]	4.07 dB [S]	2.82 dB [S]
Directivity at f_o	7.36 dB [S]	5.01 dB [S]	3.06 dB [S]

Table 4.11: Summary of three converged designs. (Simulated [S] and Measured [M]).

three optimization techniques i.e. Genetic Algorithm, Particle Swarm Optimization, and Gray Wolf Optimization. It can be observed (from Fig. 4.55) that the convergence time for Particle Swarm Optimization (PSO) is faster than the other two optimization techniques.

The limitation with these designs is the achieved gain and directivity. This is because of the limitation of the antenna structure [4]. In the next chapter, one CPW-fed slot dipole antenna design is proposed using the FR4 substrate material to improve the gain and directivity of the antenna. CPW fed antennas have limited surface waves and shows better results in terms of gain and directivity [1]-[4].
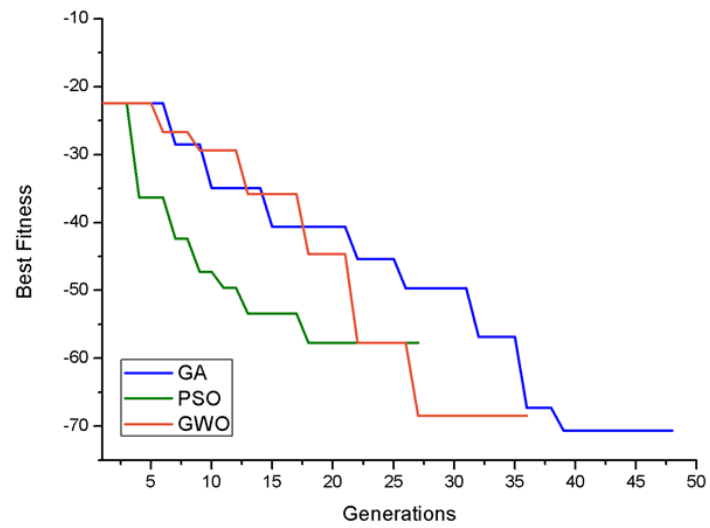
Figure 4.55: Comparison of the rate of convergence for GA, PSO, and GWO.

Chapter 5

DESIGN OF CPW-FED SLOT-DIPOLE ANTENNA

5.1 Design and Optimization using Genetic Algorithm (GA)

This chapter presents the design, optimization, fabrication, and measurement of a CPW-fed slot dipole antenna. Genetic Algorithm is used in the design and optimization of the antenna. This antenna is having a different structure in comparison with previous proposed designs, therefore it is discussed in a separate chapter. The step-by-step procedure of the antenna optimization is discussed along with the convergence graph, converged antenna design, simulated, and measurement results. The fabrication of antenna is done by using a computerized mechanical etching process. Vector Network Analyzer (VNA) is used for the validation of the simulated results.

5.1.1 Design objectives, cost-function and stepwise procedure of optimization

The objective was to design and simulate the microstrip antenna for its multi-objective optimized performance, i.e.:

- to radiate at a resonating frequency of 10.6 GHz;

- have minimum return loss at resonating frequency;

- have high impedance bandwidth (up to 1.5 GHz);

- achieve high gain.

The code for the GA algorithm is integrated with the HFSS environment using MAT-LAB. A block diagram of a GA based simple optimizer is shown in Fig. 1.14 [21].

Stepwise Genetic Algorithm procedure for antenna design is summarized as follows:

1. **Step 1 - Initializing a population**: A primary population is created by producing a random binary string. GA parameters such as a string of bits (chromosome), population size, and the total number of generations are used to optimize antenna geometry. These parameters are discussed in Table 5.1.

GA Parameters	Selected Values
Population Type	BitString
No. of decision variables (Chromosomes in Bit)	34
Total number of Generations and Population Size	200
Scaling Basis	Rank
Selection Criteria	Roulette
Reproduction Elite Count	2
Mutation	Uniform (0.01)
Crossover and its fraction	Single Point Crossover (0.8)
Penalty factor and Initial Penalty	100 and 10

Table 5.1: GA parameters used for the purpose of antenna design

2. **Step 2 - Process of pre-checking designs**: Some design checks (as shown in Fig. 5.1) are applied to validate the strings of bits (chromosomes). These design based checks helped in saving a lot of optimization time by discarding useless designs (chromosomes) from getting processed. In Fig. 5.1, the width of the substrate is shown as W_S, width of slot as W_{SLOT} (As the width of slot A and slot B are equal), length of the substrate as L_S, length of slot A and B as L_{SA} and L_{SB}. After completion of design checks, these conditions are solved in HFSS, the values of S_{11} parameter and gain at resonating frequency are calculated and returned to primary function automatically (in MATLAB). These returned values are used for further calculations by fitness function (in MATLAB).

3. **Step 3 - Evaluation of the fitness function**: Fitness function is defined in equation 5.1. If the stopping criterion is satisfied, then stop the GA procedure; otherwise,
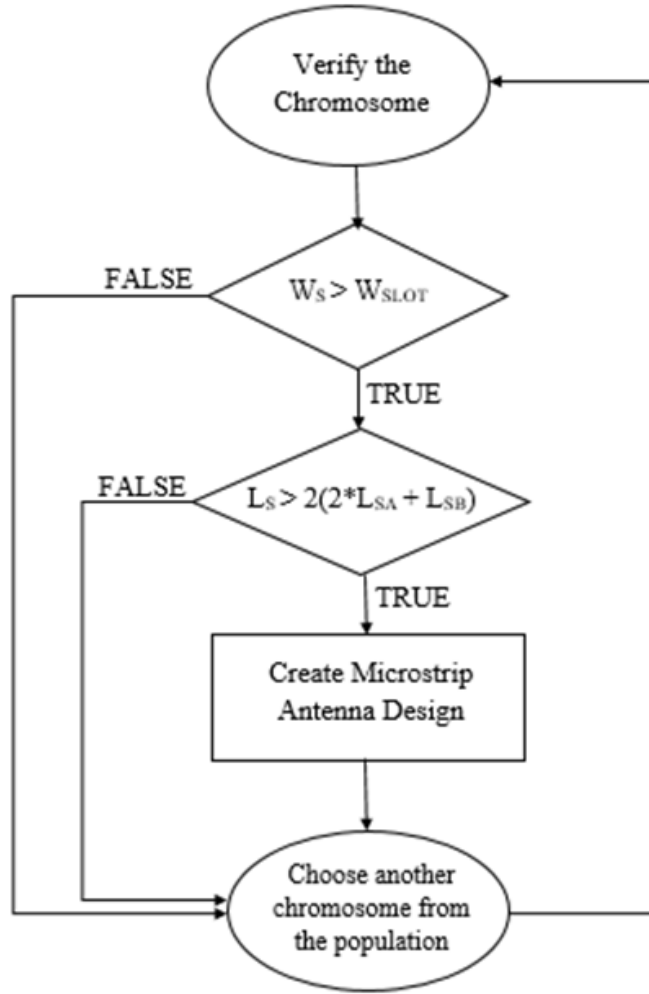
Figure 5.1: Flowchart of the design checks to validate the strings of bits (chromosomes)

go to Step 4. By default, the Genetic Algorithm minimizes the cost (fitness) function. The value of cost function will vary from 0 to the most optimal value of -90.

$$F = [-(3 * Gain) - (20 * BW) + S_{11(Res)}] \tag{5.1}$$

$$Gain = \begin{cases} 10 \text{ dB; for Gain}_{cal} \geq 10 \text{ dB;} \\ \text{Gain}_{cal}; \text{ for Gain}_{cal} < 10 \text{ dB;} \end{cases} \tag{5.2}$$

$$BW = \begin{cases} 1.5 \text{ GHz; for BW}_{cal} \geq 1.5 \text{ GHz;} \\ \text{BW}_{cal}; \text{ for BW}_{cal} < 1.5 \text{ GHz;} \end{cases} \tag{5.3}$$

$$BW_{cal} = f_H - f_L \tag{5.4}$$

$$S_{11(Res)} = \begin{cases} -30 \text{ dB; for S}_{11} \leq -30 \text{ dB;} \\ \text{S}_{11}; \text{ for S}_{11} > -30 \text{ dB;} \end{cases} \tag{5.5}$$

128

Where BW is the impedance bandwidth of the microstrip antenna calculated using equation 5.3. It is simply the difference between the upper operating frequency, f_H, and lower frequency, f_L. The value of BW_{cal}, as used in equation 5.3, is calculated using the formulae shown in equation 5.4 (implemented in MATLAB code) utilizing the simulated values of return loss received after simulating the design in HFSS. Similarly, the values of $S_{11}(f_1; \ldots; f_n)$ (used in equation 5.4) are the simulated values of return loss at different frequencies. $S_{11(Res)}$ is the value of return loss at resonating frequency calculated using equation 5.5.

4. **Step 4 - Creation of next-generation chromosomes**: Using the operators of the Genetic Algorithm such as scaling, selection, crossover, mutation, etc. (refer Table 5.1), next-generation is created.

5. **Step 5**: Repeat the process from Step#2 onwards unless the termination conditions are satisfied.

The initial geometry of the antenna is based on the values of bits (chromosomes), as discussed in Table 5.2. A random single-point crossover method and uniform mutation operation (with a factor of 0:01) are used. The convergence is obtained after the 39th iteration.

Slots (in mm)			**Substrate** (in mm)		**Feedline** (in mm)		**Air gap** (in mm)
Length of Slot A (L_{SA})	Width of Slot A and Slot B ($W_{SA} = W_{SB}$)	Length of Slot B (L_{SB})	Length (L_S)	Width (W_S)	Length (L_{FL})	Width (W_{FL})	Width (W_{AG})
1-20	10-80	1-20	50-110	50-110	$= W_S{-}1$	1-7	1-4
Resolution: 1 mm (for all parameters excl. width of feedline) Resolution: 0.5 mm (for width of feedline)							

Table 5.2: GA parameters (Chromosome selection) used for antenna design.

5.1.2   Optimization results, convergence graph, and converged antenna design

The objective of the antenna design was to achieve multi-objective optimized performance (this includes improvements in gain, impedance bandwidth, and reduction of return

loss). The antenna proposed is in X-band of super-high frequency to radiate at a resonating frequency of 10.6 GHz. The antenna design is having a CPW-fed slot dipole structure having three slots. The configuration of the antenna optimized using the Genetic Algorithm (GA) is represented in Fig. 5.2. Fig. 5.3 displays the fabricated antenna converged using GA. In this design, an FR4 substrate is utilized as it is inexpensive and eases in fabrication. The height of the FR4 substrate is 1.58 mm, having a dielectric constant of 4.3 and a loss tangent of 0.02. The converged antenna geometry is summarized in Table 5.3. The fabrication of antenna is done by a computerized photolithography process. The Return loss (S_{11}) of the fabricated antenna are measured using a Vector Network Analyzer (VNA). Fig. 5.4 shows the rate of convergence for GA optimization.
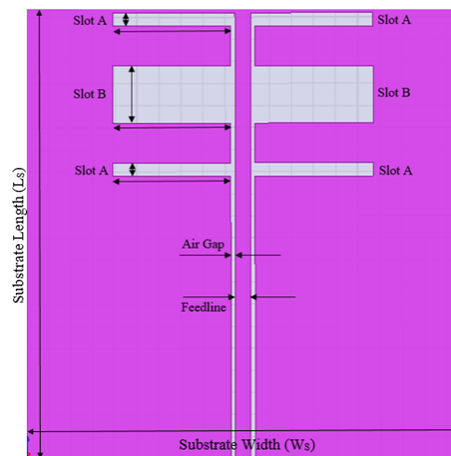
Figure 5.2: Proposed CPW-fed slot dipole antenna configuration
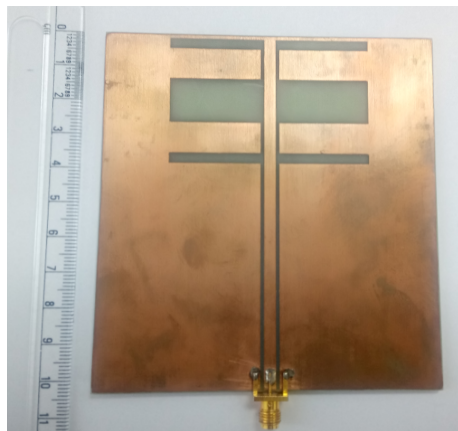
Figure 5.3: Fabricated CPW-fed slot dipole antenna
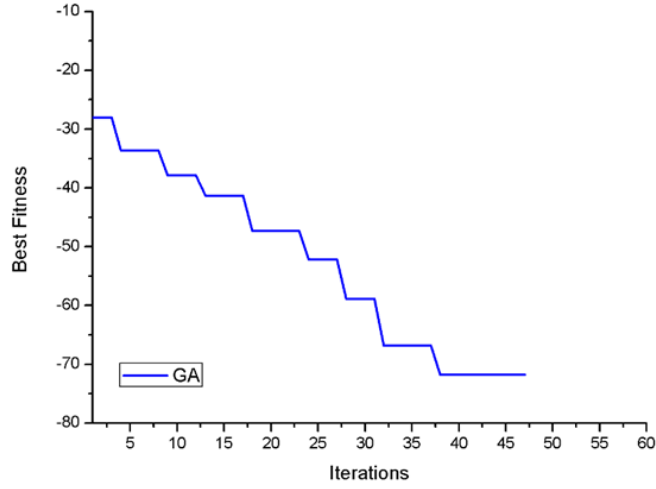
Figure 5.4: Rate of convergence for GA optimization

Parameters	Values (in mm)
Substrate Length (L_S)	102
Substrate Width (W_S)	98
Length of Slot A (L_{SA})	3
Width of Slot A (W_{SA})	59
Length of Slot B (L_{SB})	13
Width of Slot B (W_{SB})	59
Air Gap	1
Feedline Width (W_{FL})	3.5
Feedline Length (L_{FL})	101

Table 5.3: GA converged antenna geometry.

5.1.2.1 Simulated and Measured Results

Return loss (S_{11}), Voltage Standing Wave Ratio (VSWR), Real and Imaginary Impedance (Z_{11}):

Fig. 5.5 shows the simulated and measured values of return loss (S_{11}) at 10.6 GHz in the X-Band. The proposed antenna shows -25.83 dB (simulated values) and -23.08 (measured values) of S_{11} at the resonant frequency of 10.6 GHz. The proposed antenna shows 1.4 GHz (simulated values) from 10.1 GHz to 11.5 GHz and 1.3 GHz (measured values) from 9.85 GHz to 11.15 GHz of impedance bandwidth. Fig. 5.6 shows the simulated values of Voltage Standing Wave Ratio (VSWR), the value of VSWR at 10.6 GHz is 1.108. Fig. 5.7 shows the simulated values of real and imaginary impedance (Z_{11}). The values of real impedance at 10.6 GHz are 50.02 Ω, and imaginary impedance at 10.6 GHz is 5.09 Ω.

131
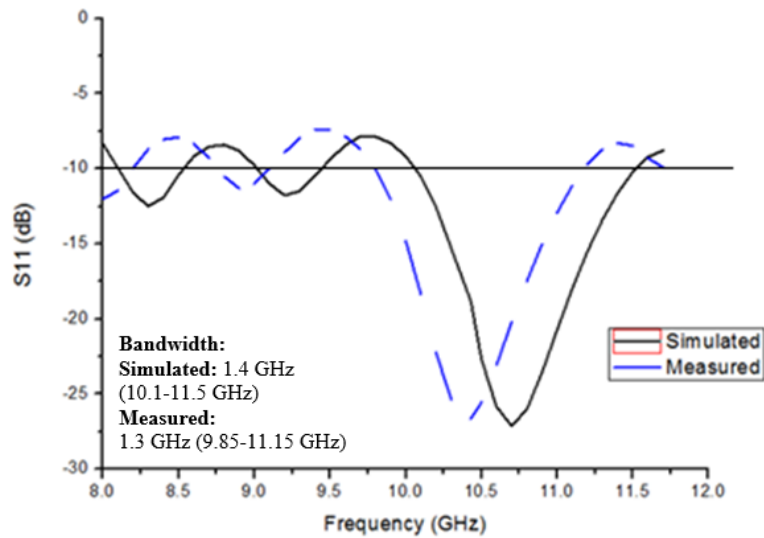
Figure 5.5: Simulated vs. measured values of return loss (S_{11})
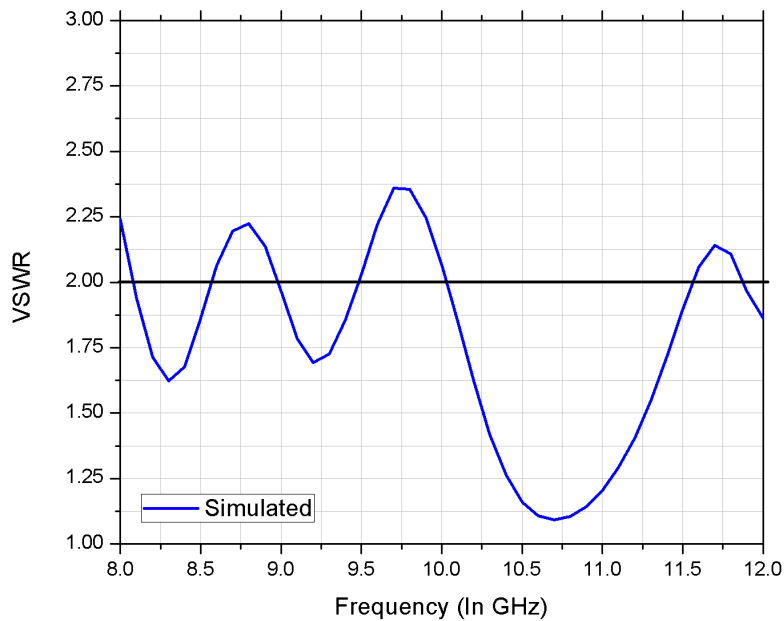
Figure 5.6: Simulated values of Voltage Standing Wave Ratio (VSWR)

Radiation Patterns (2D and 3D), E-Plane, H-Plane, Co and Cross Polarization:

Fig. 5.8 shows the simulated values of 3-Dimensional radiation patterns for gain and directivity at 10.6 GHz. The 2D plots of radiation patterns are shown in Fig. 5.9 for E-Plane and H-plane, respectively. A 2-D plot of co-polarization and cross-polarization at 10.6 GHz is shown in Fig. 5.10. Figs. 5.8 and 5.9 show the directive behavior of the proposed antenna.

132
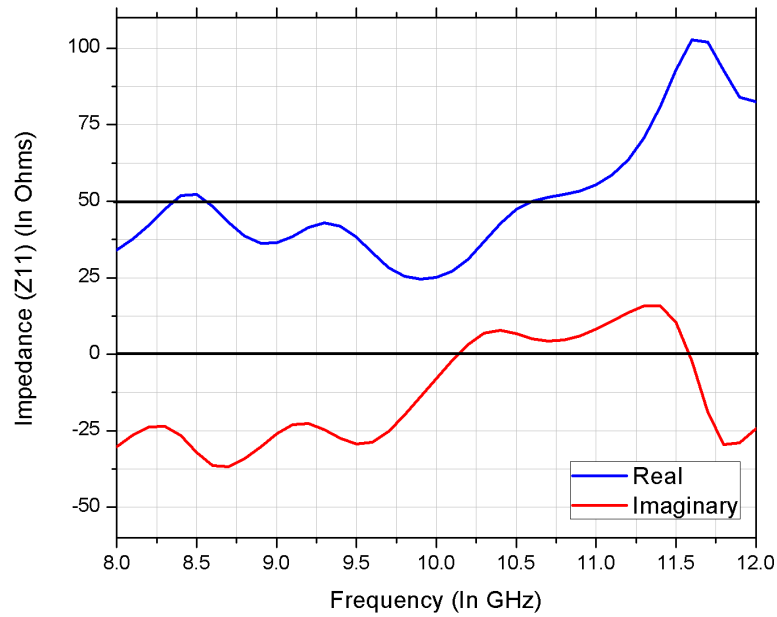
Figure 5.7: Simulated values of real and imaginary impedance (Z_{11})

(A)   **(B)**
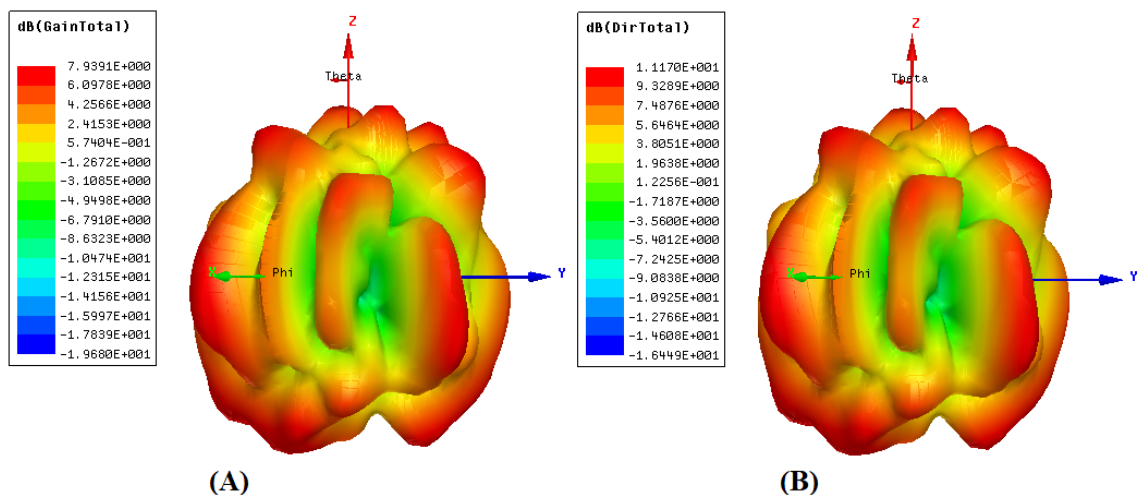
Figure 5.8: Simulated values of 3-Dimensional Radiation Patterns (A) Gain (B) Directivity

Gain and Directivity:

A plot of gain and directivity over the antenna's impedance bandwidth is presented in Fig. 5.11. At the resonant frequency of 10.6 GHz, the proposed antenna exhibits higher simulated values of gain and directivity (6 dB and 12.62 dB, respectively).
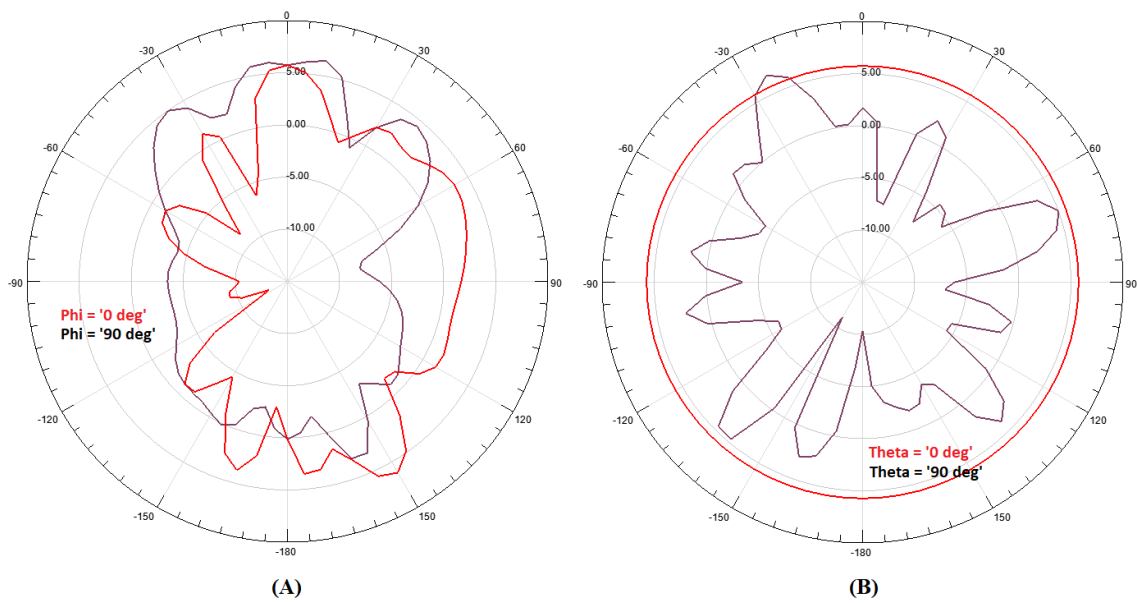
Figure 5.9: Simulated values of 2-Dimensional Radiation Patterns (A) Gain E-Plane (B) Gain H-Plane
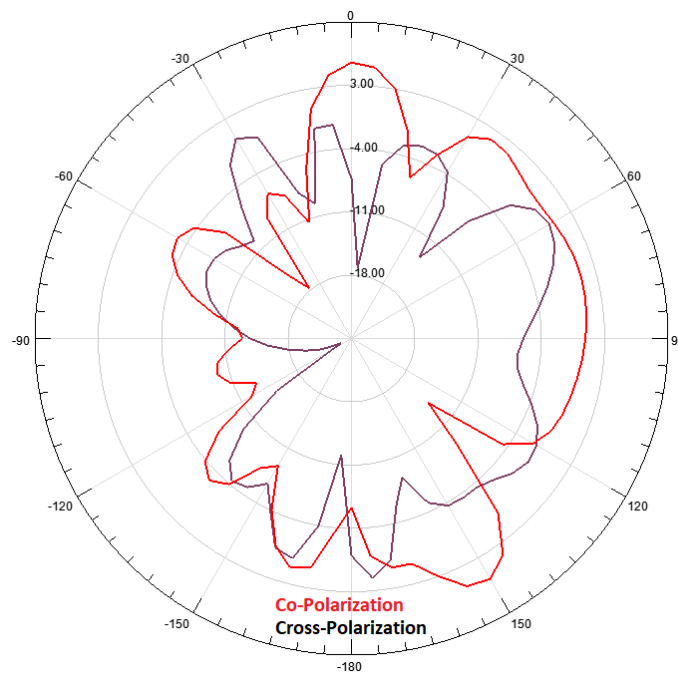
Figure 5.10: Simulated values of 2-Dimensional Radiation Patterns XZ-Plane (Co and Cross-Polarization)

5.1.3 Parametric Analysis of the Proposed Antenna

In the following subsection, an analysis is carried out to determine the effect of the microstrip patch antenna's design parameters on the resonating frequency and the impedance
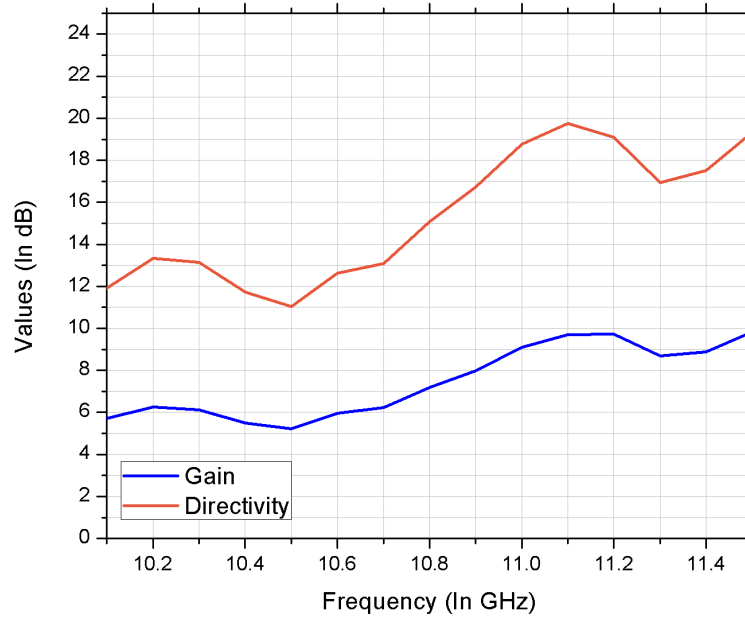
Figure 5.11: Simulated values of gain and directivity over the impedance bandwidth

bandwidth. Fig. 5.12-5.18 demonstrates all the analyzed parameters. The participation of a specific parameter is analyzed at a time while preserving all other parameters to their suboptimal values (as per Table 5.3 – GA converged antenna geometry). This parametric analysis shows the validity of the GA converged antenna design.

5.1.3.1 Effect of length of the substrate (L_S)

The length of the substrate is considered to be important as it impacts the overall size of the microstrip patch antenna. In this subsection, the effect of varying the length of the substrate (L_S), as illustrated in Fig. 5.12, is studied. It is observed that a significant change in the resonating frequency, as well as impedance bandwidth, can be achieved by varying the L_S from 99 mm to the optimal value of 102 mm. It is also observed that a decrement in the length of the substrate can shift the resonating frequency to the lower frequencies in the X-band. While incrementing the L_S, impedance bandwidth is improved. It is also found that the antenna is kept on radiating ($S_{11} <$ -15 dB) throughout the studied range of L_S. This parameter can be considered as an important parameter for manual optimization. The optimized value of substrate's length is 102 mm, achieved return loss is -27.18 dB, and the bandwidth is 1.4 GHz.
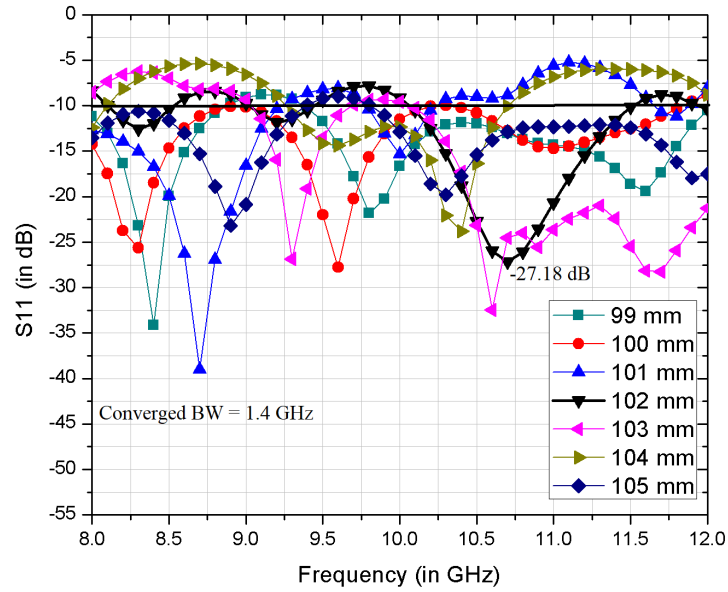
Figure 5.12: Effect of changes in the length of the substrate (keeping all other parameters constant – as per Table 5.3)

5.1.3.2 Effect of the width of the substrate (W_S)

Similar to the length of the substrate, its width is also impacting the overall size of the microstrip patch antenna and thus considered to be an important factor in design. In this subsection, the effect of varying the width of the substrate (W_S), as illustrated in Fig. 5.13, is studied. It is observed that a significant change in the resonating frequency, as well as impedance bandwidth, can be achieved by varying the W_S from 95 mm to the optimal value of 98 mm. It is also observed that a decrement in the width of the substrate can shift the resonating frequency to the lower frequencies in the X-band, and also shows multi-band behaviors. While incrementing the W_S, impedance bandwidth is improved in the designs. The optimized value of substrate's width is 98 mm, achieved return loss is -27.18 dB, and the bandwidth is 1.4 GHz.

5.1.3.3 Effect of the width of the air gap (W_{AG})

From the Fig. 5.2, it can be observed that the ground plane and the feedline is separated by a thin air gap (W_{AG}). In this subsection, the effect of varying the width of the air gap (W_{AG}), as illustrated in Fig. 5.14, is studied. It is observed that a significant change
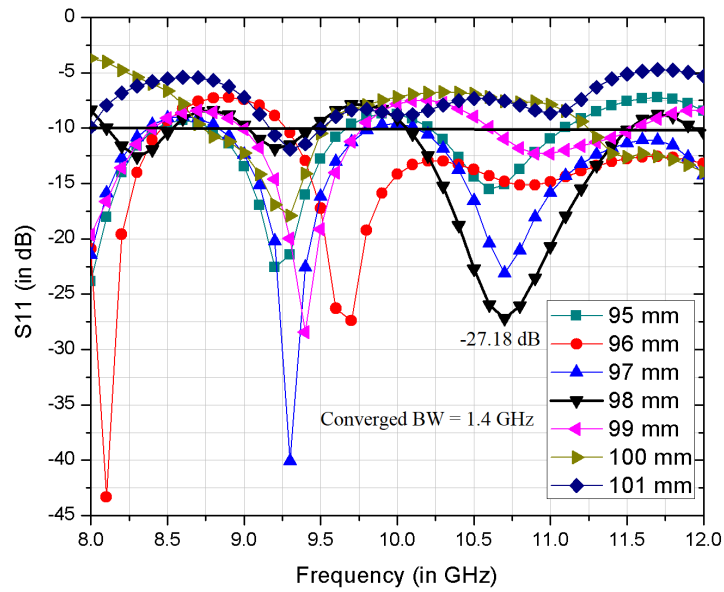
Figure 5.13: Effect of changes in the width of the substrate (keeping all other parameters constant – as per Table 5.3)

in the resonating frequency, as well as return loss (S_{11}), can be achieved by varying the W_{AG}. Increment in the width of the air gap can increase the value of return loss (S_{11}) at the resonating frequency. It is also observed that there is no significant change in the impedance bandwidth and the optimized value of the width of air gap is 1 mm.
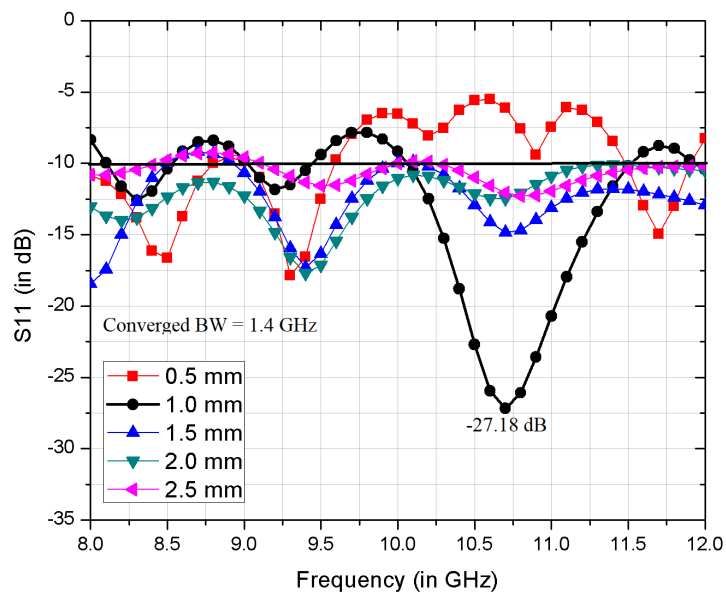
Figure 5.14: Effect of changes in the width of the air gap (keeping all other parameters constant – as per Table 5.3)

5.1.3.4 Effect of the width of the feedline (W_{FL})

In this subsection, the effect of varying the width of the feedline (W_{FL}), as illustrated in Fig. 5.15, is studied. It is observed that a significant change in the resonating frequency, as well as impedance bandwidth, can be achieved by varying the W_{FL}. It is also observed that a decrement in the width of the feedline can shift the resonating frequency to the lower frequencies in the X-band, and also shows multi-band behaviors. While incrementing the W_{FL}, impedance bandwidth is improved in the designs. The optimized value of feedline's width is 3.5 mm, achieved return loss is -27.18 dB, and the bandwidth is 1.4 GHz.
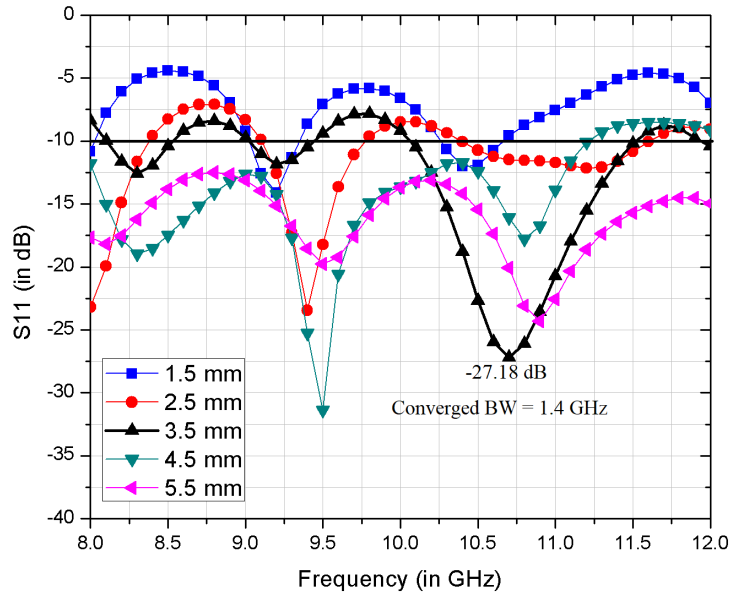
Figure 5.15: Effect of changes in the width of the feedline (keeping all other parameters constant – as per Table 5.3)

5.1.3.5 Effect of length of the slot A (L_{SA})

In this subsection, the effect of varying the length of slot A (L_{SA}), as illustrated in Fig. 5.16, is studied. It is observed that a significant change in the resonating frequency, as well as impedance bandwidth, can be achieved by varying the L_{SA}. It is also observed that the antenna is kept on radiating ($S_{11} < $ -15 dB) throughout the studied range of L_{SA}. This parameter can be considered as an important parameter for manual Optimization of the impedance bandwidth and resonating frequency. The optimized value of the length of

slot A is 3 mm, achieved return loss is -27.18 dB, and the bandwidth is 1.4 GHz.
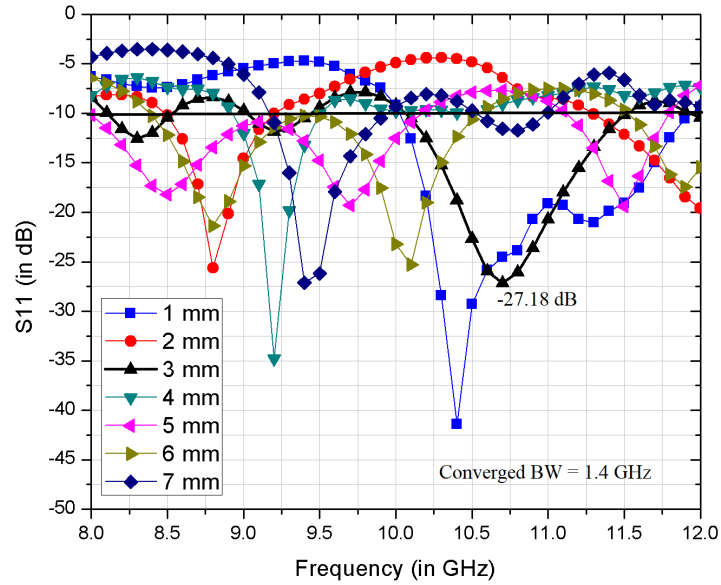
Figure 5.16: Effect of changes in the length of the slot A (keeping all other parameters constant – as per Table 5.3)

5.1.3.6 Effect of length of the slot B (L_{SB})

In this subsection, the effect of varying the length of slot B (L_{SB}), as illustrated in Fig. 5.17, is studied. It is observed that a significant change in the resonating frequency, as well as impedance bandwidth, can be achieved by varying the L_{SB}. It is also observed that a decrement in the length of the slot B can shift the resonating frequency to the lower frequencies in the X-band, and also shows multi-band behaviors. This parameter can be considered as an important parameter for manual Optimization of the impedance bandwidth and resonating frequency. The optimized value of the length of slot B is 13 mm, achieved return loss is -27.18 dB, and the bandwidth is 1.4 GHz.

5.1.3.7 Effect of the width of the slot A and B (W_{SA} and W_{SB})

In this subsection, the effect of varying the width of slot A and B (W_{SA} and W_{SB}) together, as illustrated in Fig. 5.18, is studied. It is observed that a significant change in the resonating frequency, as well as impedance bandwidth, can be achieved by varying the

139
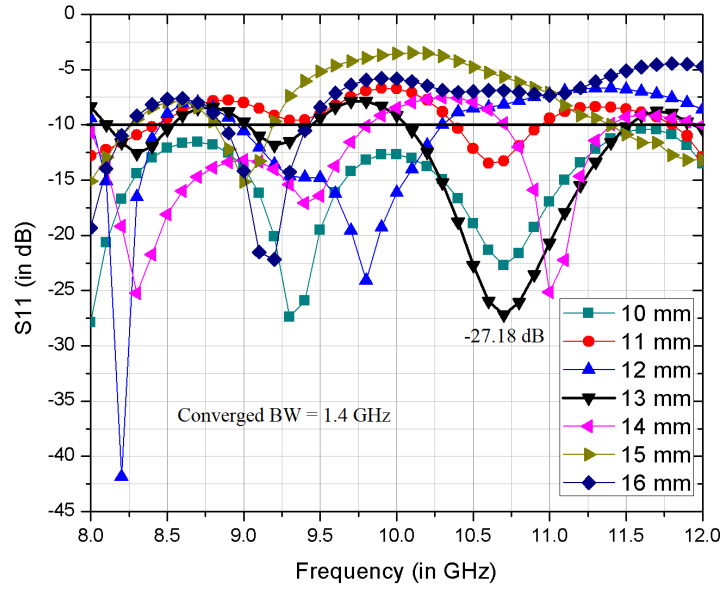
Figure 5.17: Effect of changes in the length of the slot B (keeping all other parameters constant – as per Table 5.3)

W_{SA} and W_{SB} together. It is also observed that decrementing the width of slot A and B together can shift the resonating frequency to the lower frequencies in the X-band, and also shows multi-band behaviors. It is also found that the antenna is kept on radiating ($S_{11} <$ -15 dB) throughout the studied range of W_{SA} and W_{SB}. The optimized value of the width of slot A and B is 59 mm, achieved return loss is -27.18 dB, and the bandwidth is 1.4 GHz.
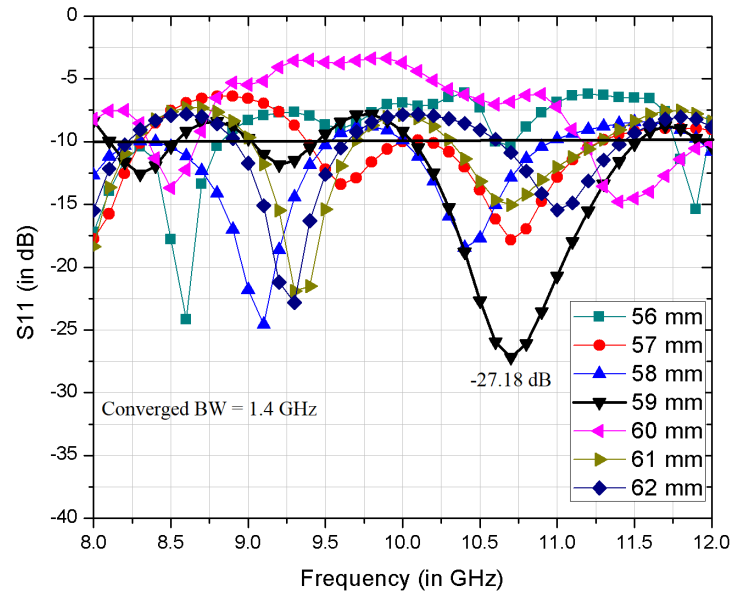
Figure 5.18: Effect of changes in the width of the slot A and B (keeping all other parameters constant – as per Table 5.3)

5.2 Comparison of Results

In this section, proposed design result is compared with the results of existing designs/literature and is summarized in Table 5.4. It can be observed that the proposed design is better in terms of its achieved gain and directivity.

Ref.	Operating frequency (f_o)	Impedance Bandwidth	Return Loss at f_o	Gain at f_o	Directivity at f_o	Dimensions (in mm^3)
[121]	10.5 GHz	3 GHz [M]	-20 dB [M]	5.35 dB [M]	Not available	30 x 21 x 1.5
[122]	10.5 GHz	1.7 GHz [M]	-14 dB [M]	4 dB [S]	Not available	30 x 30 x 1.58
[123]	10.04 GHz	2.95 GHz [S]	-42.57 [S]	1.06 dB [S]	1.21 dB [S]	30 x 35 x 1.58
Proposed CPW-fed Antenna	10.6 GHz	1.4 GHz [S]; 1.3 GHz [M]	-25.83 dB [S]; -23.08 dB [M]	6 dB [S]	12.62 dB [S]	102 x 98 x 1.58

Table 5.4: Comparison of the proposed antenna with existing literature. (Simulated [S] and Measured [M]).

5.3 Chapter Summary

This chapter presented the design, optimization, fabrication, and measurement of a CPW-fed slot dipole antenna. The Genetic Algorithm is used in the process of design and optimization of a CPW-fed slot dipole antenna with three slots. The objective of the antenna design was to achieve multi-objective optimized performance (this includes improvements in gain, impedance bandwidth, and reduction of return loss). A step-by-step procedure of the antenna optimization using Genetic Algorithm (GA) is discussed along with the convergence graph, geometry of the converged antenna design, its simulated, and measurement results. The antenna proposed in this chapter radiates at a resonating frequency of 10.6 GHz and is useful for various wireless wideband applications in the X-Band. A number of potential applications in X-Band are discussed in chapter 1. In this design, FR4 substrate with a height of 1.58 mm, dielectric constant of 4.3, and loss tangent of 0.02 is utilized for fabrication. The dimension of the converged antenna is 102 mm x 98 mm x 1.58 mm. The proposed antenna shows sufficiently large simulated bandwidth of 1.4 GHz (10.1-11.5 GHz) and measured bandwidth of 1.3 GHz (9.85-11.15 GHz). The values of return loss at the resonant frequency (of 10.6 GHz) is -25.83 dB (simulated) and -23.08 (measured). The simulated radiation patterns show the omnidirectional radiation characteristics. The only limitation with this design was the antenna's size because of the use of FR4 substrate material. But, the gain and directivity of the proposed antenna design is higher than the previous proposed designs fabricated using FR4 substrate material. The proposed antenna design shows high values of simulated gain (6 dB), and directivity (12.62 dB) at the resonating frequency of 10.6 GHz. Parametric analysis is also presented in this chapter to further validate the converged design. The comparison of results with existing designs/literature is also presented. It can be observed that the proposed design is better in terms of its sufficiently large impedance bandwidth, achieved gain and directivity. However the antenna dimensions are more than the previous proposed designs.

Chapter 6

CONCLUSION AND FUTURE SCOPE

6.1   Conclusion

The methodology of antenna design, simulated and experimental investigations are described in the previous chapters. In this chapter, the conclusions drawn from those extensive results are summarized. Few suggestions on carrying out future scope related to the work are also discussed at the end of this chapter.

In this thesis work, a total of five antenna designs are proposed. These proposed antenna designs belong to three different types of structures. The objective of the antenna design was to achieve multi-objective optimized performance (this includes improvements in gain, impedance bandwidth, and reduction of return loss). All five antennas proposed in this thesis radiates at a resonating frequency between 10.5-10.9 GHz and are useful in various wireless wideband applications in the X-Band. A number of potential applications in X-Band are discussed in chapter 1.

Conventional square-shaped microstrip patch antenna with complete ground plane

The converged antenna radiates at a resonating frequency of 10.9 GHz and is useful in various wireless wideband applications in the X-Band. A number of potential applications in X-Band are discussed in chapter 1. RT/duroid with a height of 1.574 mm and a dielectric constant of 2.2 is used as a substrate material of the proposed antenna. The transmission line is connected with a stub for perfect impedance matching. The dimension of the converged antenna is 38.4 mm x 38.4 mm x 1.574 mm. The proposed antenna shows the simulated bandwidth of 550 MHz (10.66-11.21 GHz) and measured bandwidth of 450 MHz (10.7-11.15 GHz). The values of return loss at the resonant frequency (of 10.9 GHz) is -32 dB (simulated) and -27 dB (measured). The simulated radiation patterns show the directional radiation characteristics. The simulated value of Voltage Standing Wave Ratio (VSWR) at 10.9 GHz is 1.288. The values of real impedance (Z_{11}) at 10.9 GHz are 56.23 , and imaginary impedance (Z_{11}) at 10.9 GHz is 11.96 . The only limitation with this design is the cost of fabrication because of the cost of substrate material RT/duroid. The proposed antenna design shows high values of simulated gain (8.35 dB), and directivity (8.35 dB) at the resonating frequency of 10.9 GHz. Parametric analysis is also presented in this chapter to further validate the converged design. The comparison of results with existing designs/literature is done (in Table 3.4) and it is observed that the proposed design is better in terms of its achieved gain and directivity.

Conventional rectangular-shaped microstrip patch antenna with partial ground plane

The rectangular shaped microstrip patch antenna is designed by using three optimization techniques i.e. Genetic Algorithm, Particle Swarm Optimization, and Gray Wolf Optimization resulting three different converged antennas.

The converged antenna, based on Genetic Algorithm, radiates at a resonating frequency of 10.5 GHz and is useful for various wireless wideband applications in the X-Band. A

number of potential applications in X-Band are discussed in chapter 1. The dimension of the converged antenna is 41 mm x 45 mm x 1.58 mm. The proposed antenna provides sufficiently large simulated bandwidth of 850 MHz (9.95-10.8 GHz) and measured bandwidth of 670 MHz (10.04-10.71 GHz). The values of return loss at the resonant frequency (of 10.5 GHz) is -27.35 dB (simulated) and -21.51 dB (measured). The value of Voltage Standing Wave Ratio (VSWR) at 10.5 GHz is 1.096 (simulated) and 1.183 (measured). The values of real impedance at 10.5 GHz are 49.25 , and imaginary impedance at 10.5 GHz is 4.29 . The simulated radiation patterns show the omnidirectional radiation characteristics. At the resonant frequency of 10.5 GHz, the proposed antenna exhibits higher simulated values of gain and directivity. The value of simulated gain is 4.26 dB, and directivity is 7.36 dB at 10.5 GHz. Parametric analysis is also presented in this chapter to further validate the converged design.

The converged antenna, based on PSO, radiates at a resonating frequency of 10.5 GHz and is useful for various wireless wideband applications in the X-Band. The dimension of the converged antenna is 25.81 mm x 23.08 mm x 1.58 mm. The proposed antenna provides sufficiently large simulated bandwidth of 1.95 GHz (9.71-11.66 GHz) and measured bandwidth of 1.55 GHz (9.66-11.21 GHz). The values of return loss at the resonant frequency (of 10.5 GHz) is -28.40 dB (simulated) and -23.02 dB (measured). The values of Voltage Standing Wave Ratio (VSWR) at 10.5 GHz is 1.079 (simulated) and 1.152 (measured). The values of real impedance (Z_{11}) at 10.5 GHz are 48.39 , and imaginary impedance (Z_{11}) at 10.5 GHz is 3.38 . The simulated radiation patterns show the omnidirectional radiation characteristics. At the resonant frequency of 10.5 GHz, the proposed antenna exhibits higher simulated values of gain and directivity. The value of simulated gain is 4.07 dB, and directivity is 5.01 dB at 10.5 GHz. Parametric analysis is also presented in this chapter to further validate the converged design.

The converged antenna, based on Gray Wolf Optimization (GWO), radiates at a resonating frequency of 10.5 GHz and is useful for various wireless wideband applications in the X-Band. The dimension of the converged antenna is 18.73 mm x 41.72 mm x 1.58 mm. The proposed antenna provides sufficiently large simulated bandwidth of 3.89 GHz

(8 GHz-11.89 GHz) and measured bandwidth of 3.1 GHz (8.9-12 GHz). The values of return loss at the resonant frequency (of 10.5 GHz) is -35.51 dB (simulated) and -24.59 dB (measured). The values of Voltage Standing Wave Ratio (VSWR) at 10.5 GHz is 1.034 (simulated) and 1.125 (measured). The values of real impedance (Z_{11}) at 10.5 GHz are 50.33 , and imaginary impedance (Z_{11}) at 10.5 GHz is 1.64 . The simulated radiation patterns show the omnidirectional radiation characteristics. At the resonant frequency of 10.5 GHz, the proposed antenna exhibits simulated gain of 2.82 dB, and directivity of 3.06 dB. Parametric analysis is also presented in this chapter to further validate the converged design.

All three proposed designs are compared with the results of existing designs/literature and is summarized in Table 4.10. It can be observed that, all three designs exhibit decent values of return losses (S_{11}) at resonating frequency, sufficiently large bandwidth, high gain, and directivity. The advantage with these designs is the cost of fabrication because of the inexpensive substrate material FR4. For further comparison, a summary of the three converged designs are also shown in Table 4.11. It can be observed that the proposed design converged using Particle Swarm Optimization (PSO) technique is comparably better in terms of antenna dimensions, impedance bandwidth, gain and directivity. It is also observed that the design converged using Genetic Algorithm (GA) is slightly better in terms of gain and directivity at a cost of impedance bandwidth and antenna dimensions.

Another key observation is the comparison between the convergence rate of three optimization techniques i.e. Genetic Algorithm, Particle Swarm Optimization, and Gray Wolf Optimization. It can be observed (from Fig. 4.55) that the convergence time for Particle Swarm Optimization (PSO) is faster than the other two optimization techniques.

146

CPW-fed slot dipole microstrip patch antenna

The converged antenna, based on Genetic Algorithm (GA), radiates at a resonating frequency of 10.6 GHz and is useful in various wireless wideband applications in the X-Band. In this design, FR4 substrate with a height of 1.58 mm, dielectric constant of 4.3, and loss tangent of 0.02 is utilized for fabrication. The dimension of the converged antenna is 102 mm x 98 mm x 1.58 mm. The proposed antenna shows sufficiently large simulated bandwidth of 1.4 GHz (10.1-11.5 GHz) and measured bandwidth of 1.3 GHz (9.85-11.15 GHz). The values of return loss at the resonant frequency (of 10.6 GHz) is -25.83 dB (simulated) and -23.08 (measured). The simulated values of Voltage Standing Wave Ratio (VSWR) at 10.6 GHz is 1.108. The simulated values of real impedance (Z_{11}) at 10.6 GHz are 50.02 , and imaginary impedance (Z_{11}) at 10.6 GHz is 5.09 . The simulated radiation patterns show the omnidirectional radiation characteristics. The only limitation with this design was the antenna's size because of the use of FR4 substrate material. But, the gain and directivity of the proposed antenna design is higher than the previous proposed designs fabricated using FR4 substrate material. The proposed antenna design shows high values of simulated gain (6 dB), and directivity (12.62 dB) at the resonating frequency of 10.6 GHz. Parametric analysis is also presented in this chapter to further validate the converged design. The comparison of results with existing designs/literature is done (in Table 5.4) and it is observed that the proposed design is better in terms of its achieved gain and directivity.

For further comparison, a summary of the five proposed antenna designs are shown in Table 6.1.

Parameters	Proposed Antenna # 1	Proposed Antenna # 2	Proposed Antenna # 3	Proposed Antenna # 4	Proposed Antenna # 5
Type of Antenna	Microstrip Patch Antenna (RT/Duroid)	Microstrip Patch Antenna (FR4)	Microstrip Patch Antenna (FR4)	Microstrip Patch Antenna (FR4)	CPW-fed Slot Dipole Antenna (FR4)
Optimization Technique	Genetic Algorithm (GA)	Genetic Algorithm (GA)	Particle Swarm Optimization (PSO)	Grey Wolf Optimization (GWO)	Genetic Algorithm (GA)
Operating Frequency (f_o) (X-Band)	10.9 GHz	10.5 GHz	10.5 GHz	10.5 GHz	10.6 GHz
Antenna dimensions (in mm^3)	38.4 x 38.4 x 1.574	41 x 45 x 1.58	25.81 x 23.08 x 1.58	18.73 x 41.72 x 1.58	102 x 98 x 1.58
Return Loss at f_o	-32 dB [S] -27 dB [M]	-27.35 dB [S] -21.51 dB [M]	-28.40 dB [S] -23.02 dB [M]	-35.51 dB [S] -24.59 dB [M]	-25.83 dB [S] -23.08 dB [M]
Impedance bandwidth	550 MHz [S] 450 MHz [M]	850 MHz [S] 670 MHz [M]	1.9 GHz [S] 1.6 GHz [M]	3.89 GHz [S] 3.1 GHz [M]	1.4 GHz [S] 1.3 GHz [M]
VSWR at f_o	1.288 [S]	1.096 [S] 1.183 [M]	1.079 [S] 1.152 [M]	1.034 [S] 1.125 [M]	1.108 [S]
Gain at f_o [S]	8.35 dB	4.26 dB	4.07 dB	2.82 dB	6 dB
Directivity at f_o [S]	8.35 dB	7.36 dB	5.01 dB	3.06 dB	12.62 dB

Table 6.1: Summary of five proposed Antenna designs. (Simulated [S] and Measured [M]).

6.2 Suggestions for Future Scope of Work

The study reported here has opened for the following interesting points for further investigations:

1. More refined optimization can be experimented by combining GA with other methods like PSO, GSA, etc. (Hybrid approach).

2. Miniaturization of the antenna can be an optimization goal.

3. High Gain UWB antennas can be designed using optimization techniques.

4. Multi-channel Antennas can be designed using optimization techniques.

5. Antennas for higher bands (e.g., for 5G applications) can be designed using optimization techniques.

Bibliography

[1] Constantine A. Balanis, (2016), *Antenna Theory: Analysis and Design*, Book 4th Edition, ISBN: 978-1-118-64206-1.

[2] Kraus, J. D., Marhefka, R. J., (2002), *Antennas for all applications*, Book McGraw-Hill.

[3] Marco Zennaro, Carlo Fonda, (2004), *Radio Laboratory Handbook of the ICTP "School of Digital Radio Communications for Research and Training in Developing Countries*, Book Volume 1 - Cables and Antennas, ISBN: 92-95003-24-1.

[4] R. B. Waterhouse, (2003), *Microstrip Patch Antennas—A Designer's Guide*, Boston, MA: Kluwer Academic Publishers, 10.1007/978-1-4757-3791-2.

[5] Ranjan Mishra, (2016), *An overview of microstrip antenna*, HCTL Open International Journal of Technology Innovations and Research, Vol. 21, Issue 2, Page 1-17.

[6] Vardhini, K.K., Sitamahalakshmi, T. (2016), A Review on Nature-based Swarm Intelligence Optimization Techniques and its Current Research Directions. Indian journal of science and technology, 9.

[7] Wang, Shengwei Ma, Zhenjun (2008), Supervisory and Optimal Control of Building HVAC Systems: A Review. HVACR Research. 14. 3-32. 10.1080/10789669.2008.10390991.

[8] J. H. Holland (1975), *Adaptation in Natural and Artificial Systems*, MIT Press.

[9] K. A. de Jong, (1975), *An analysis of the behavior of a class of genetic adaptive systems* [Ph.D. thesis], University of Michigan Press, Ann Arbor, Mich, USA.

[10] Haupt, R. L. and S. E. Haupt, (2004), *Practical Genetic Algorithms*, John Wiley.

[11] D. E. Goldberg, (1989), *Genetic Algorithms in Search, Optimization and Machine Learning*, Addison-Wesley, Reading, Mass, USA.

[12] R. L. Haupt, (1995) *An introduction to genetic algorithms for electromagnetics*, IEEE Antennas and Propagation Magazine, vol. 37, no. 2, pp. 7–15.

[13] J. M. Johnson and Y. Rahmat-Samii, (1997), *Genetic algorithms in engineering electromagnetics*, IEEE Antennas and Propagation Magazine, vol. 39, no. 4, pp. 7–21.

[14] J. M. Johnson and Y. Rahmat-samii, (1994), *Genetic algorithm optimization and its application to antenna design*, in Proceedings of the IEEE Antennas and Propagation International Symposium, pp. 326–329.

[15] B. Orchard, (2002), *Optimising algorithms for antenna design* [M.S. dissertation], University of the Witwatersrand.

[16] R. L. Haupt and D. H. Werner, (2007), *Genetic Algorithms in Electromagnetics*, John Wiley Sons, Upper Saddle River, NJ, USA.

[17] Vijini Mallawaarachchi, (2017), *Introduction to Genetic Algorithms — Including Example Code*. https://towardsdatascience.com/introduction-to-genetic-algorithms-including-example-code-e396e98d8bf3

[18] Anke Meyer-Baese, Volker Schmid, (2014) *Chapter 5 - Genetic Algorithms, Pattern Recognition and Signal Analysis in Medical Imaging* (Second Edition), Academic Press, Pages 135-149, ISBN 9780124095458, https://doi.org/10.1016/B978-0-12-409545-8.00005-4

[19] Stylianos C. Panagiotou, Stelios C. A. Thomopoulos, Christos N. Capsalis, (2014) *Genetic Algorithms in Antennas and Smart Antennas Design Overview: Two Novel Antenna Systems for Triband GNSS Applications and a Circular Switched Parasitic Array for WiMax Applications Developments with the Use of Genetic Algorithms*, International Journal of Antennas and Propagation, Volume 2014, Article ID 729208, https://doi.org/10.1155/2014/729208

[20] *Genetic Algorithms: The Reality*, https://www.doc.ic.ac.uk/project/examples/2005 /163/g0516312/Algorithms/Reality.html

[21] M. Lamsalli, A. El Hamichi, M. Boussouis, N. Amar Touhami, and T. El-hamadi, (2016) *Genetic Algorithm Optimization for Microstrip Patch Antenna Miniaturization*, Progress In Electromagnetics Research Letters, Vol. 60, 113-120. doi:10.2528/PIERL16041907

[22] Daniel S. Weile, Eric Michielssen, (1997), *Genetic Algorithm Optimization Applied to Electromagnetics: A Review*, IEEE Transactions on Antennas and Propagation, vol. 45, no. 3.

[23] H. Choo and H. Ling, (2002) *Design of multiband microstrip antennas using a genetic algorithm*, in IEEE Microwave and Wireless Components Letters, vol. 12, no. 9, pp. 345-347. doi: 10.1109/LMWC.2002.803144

[24] Neela Chattoraj, Jibendu Sekhar Roy, (2006), *Application of Genetic Algorithm to the Optimization of Microstrip Antennas with and without Superstrate*, Microwave Review, Volume 12, No. 2.

[25] R. K. Shaw and D. H. Werner, (2006), *Design of Optimal Broadband Microstrip Antenna Elements in the Array Environment using Genetic Algorithms*, 2006 IEEE Antennas and Propagation Society International Symposium, Albuquerque, NM, pp. 3727-3730. doi: 10.1109/APS.2006.1711432

[26] M. John and M. J. Ammann, (2006), *Design Of A Wide-Band Printed Antenna Using A Genetic Algorithm On An Array Of Overlapping Sub-Patches*, IEEE International Workshop on Antenna Technology Small Antennas and Novel Metamaterials, 2006., Crowne Plaza Hotel, White Plains, New York, USA, pp. 92-95, doi: 10.1109/IWAT.2006.1608983.

[27] John, M. and M. J. Ammann, (2007), *Wideband printed monopole design using genetic algorithm*, IEEE Antennas Wireless Propagation Letters., Vol. 6, 447-449. doi:10.1109/LAWP.2007.891962

[28] P. Mythili, S. Mridula, B. Paul and S. Sreeja, (2008), *Design of a compact genetic microstrip antenna with improved performance*, 2008 IEEE Antennas and Propagation Society International Symposium, San Diego, CA, pp. 1-4, doi: 10.1109/APS.2008.4618940.

[29] S. Y. Sun, Ying-Hua Lu and Dong-Sheng La, (2009), *Application of genetic algorithm in broadband microstrip antenna design*, Environmental Electromagnetics, CEEM 2009. 5th Asia-Pacific Conference on, Xian, 2009, pp. 192-195. doi: 10.1109/CEEM.2009.5305755

[30] Si-Yang Sun, Ying-Hua Lu, (2009), *Design of Broadband Microstrip Antenna Utilizing Genetic Algorithm*, Proceedings of the 2009 International Symposium on EMC, Kyoto, The Institute of Electronics, Information and Communication Engineers.

[31] Sun, S., Lu, Y., Zhang, J., Fangming Ruan, (2010), *Genetic algorithm optimization of broadband microstrip antenna*, Frontiers of Electrical and Electronic Engineering in China, Volume 5, Issue 2, pp 185–187. doi: 10.1007/s11460-010-0015-0

[32] S. Sun, Y. LV and J. Zhang, (2010), *The application of genetic algorithm optimization in broadband microstrip antenna design*, 2010 IEEE Antennas and Propagation Society International Symposium, Toronto, ON, pp. 1-4, doi: 10.1109/APS.2010.5561992.

[33] S. Sun, Y. Lv, J. Zhang, Z. Zhao and F. Ruan, (2010), *Optimization based on genetic algorithm and HFSS and its application to the semiautomatic design of antenna*, 2010 International Conference on Microwave and Millimeter Wave Technology, Chengdu, pp. 892-894, doi: 10.1109/ICMMT.2010.5525163.

[34] Naveen K. Saxena, Mohd A. Khan, Nitendar Kumar, Pradeep K. S. Pourush, (2011), *Application of Genetic Algorithm for Optimization of Important Parameters of Magnetically Biased Microstrip Circular Patch Antenna*, Journal of Software Engineering and Applications, 2011, 4, 129-136. doi: 10.4236/jsea.2011.42014

[35] J. M. J. W. Jayasinghe, D.N. Uduwawala, (2011), *Design of a Dual Band Antenna for Bluetooth and HIPERLAN2 Applications using Genetic Algorithm Optimization*,

2011 IEEE 6th International Conference on Industrial and Information Systems, ICIIS 2011, Aug. 16-19, 2011, Sri Lanka.

[36] S. K. Josan, J. S. Sohal and B. S. Dhaliwal, (2012), *Design of elliptical microstrip patch antenna using Genetic Algorithms*, Communication Systems (ICCS), 2012 IEEE International Conference on, Singapore, 2012, pp. 140-143. doi: 10.1109/ICCS.2012.6406125

[37] Jeevani Jayasinghe, Jaume Anguera, Disala Uduwawala, (2013), *Genetic Algorithm Optimization of a High-Directivity Microstrip Patch Antenna Having a Rectangular Profile*, The Radioengineering Journal, VOL. 22, No. 3, Sept. 2013.

[38] M. H. Miry, G. A. Al-Suhail, F. Abdussalam, M. B. Child and R. A. Abd-Alhameed, (2015), *Design of a small ultra wideband antenna using a genetic algorithm approach*, 2015 Internet Technologies and Applications (ITA), Wrexham, pp. 461-465, doi: 10.1109/ITechA.2015.7317448.

[39] Bruno Seixas Gomes de Almeida, Victor Coppo Leite, (2019), *Particle Swarm Optimization: A Powerful Technique for Solving Engineering Problems*, Swarm Intelligence - Recent Advances, New Perspectives and Applications. DOI: 10.5772/intechopen.89633.

[40] Meng, X., Pian, Z. (2016), *Theoretical Basis for Intelligent Coordinated Control*, Intelligent Coordinated Control of Complex Uncertain Systems for Power Distribution Network Reliability, 15–50. doi:10.1016/b978-0-12-849896-5.00002-7

[41] Kennedy J, Eberhart RC., (1995), *A new optimizer using particles swarm theory*, In: Proceedings of Sixth International Symphosium on Micro Machine and Human Science IEEE, pp. 39-43. DOI: 10.1109/MHS.1995.494215

[42] Kennedy J, Eberhart RC., (1995,)*Particle swarm optimization*, In: Proceedings of the International Conference on Neural Networks; Institute of Electrical and Electronics Engineers, Vol. 4, pp. 1942-1948. DOI: 10.1109/ICNN.1995.488968

[43] G. Chen, J. Jia, Qi. Han, (2006), *Study on decreasing inertia weight strategy of particle swarm optimization*, Acad. J. Xi'an Jiao Tong Univ. 40 (1) 53–61.

[44] A. El-Gallad, M. El-Hawary, A. Sallam, A. Kalas, (2002), *Enhancing particle swarm optimizer via proper parameters selection*, IEEE CCECE02 Proceedings, Piscataway, NJ. 2.

[45] J. Kennedy, (1997), *The particle swarm: social adaptation of knowledge*, Proceedings of 1997 IEEE International Conference on Evolutionary Computation (ICEC '97), Indianapolis, IN, USA, pp. 303-308, doi: 10.1109/ICEC.1997.592326.

[46] Abdmouleh, Zeineb Gastli, Adel Ben-Brahim, L. Haouari, Mohamed Al-Emadi, Nasser. (2017), *Review of optimization techniques applied for the integration of distributed generation from renewable energy sources*, Renewable Energy. 113. 10.1016/j.renene.2017.05.087.

[47] Nanbo Jin and Y. Rahmat-Samii, (2005), *Design of E-shaped dual-band and wideband patch antennas using parallel PSO/FDTD algorithm*, 2005 IEEE Antennas and Propagation Society International Symposium, Washington, DC, pp. 37-40 vol. 2A. doi: 10.1109/APS.2005.1551729

[48] R. N. Biswas and A. Kar, (2008), *A novel PSO-IE3D based design and optimization of a low profile Dual Slot Microstrip Patch Antenna*, TENCON 2008 - IEEE Region 10 Conference, Hyderabad, pp. 1-4. doi: 10.1109/TENCON.2008.4766781

[49] V. S. Chintakindi, S. S. Pattnaik, O. P. Bajpai, S. Devi, P. K. Patra and K. M. Bakwad, (2008), *Resonant frequency of equilateral triangular microstrip patch antenna using particle swarm optimization technique*, 2008 International Conference on Recent Advances in Microwave Theory and Applications, Jaipur, pp. 20-22. doi: 10.1109/AMTA.2008.4763004

[50] M. T. Islam, N. Misran, T. C. Take and M. Moniruzzaman, (2009), *Optimization of microstrip patch antenna using Particle swarm optimization with curve fitting*, 2009 International Conference on Electrical Engineering and Informatics, Selangor, pp. 711-714. doi: 10.1109/ICEEI.2009.5254724

[51] F. A. Ali and K. T. Selvan, (2009), *A study of PSO and its variants in respect of microstrip antenna feed point optimization*, 2009 Asia Pacific Microwave Conference, Singapore, pp. 1817-1820. doi: 10.1109/APMC.2009.5384147

[52] Y. Choukiker, S. K. Behera, D. Mishra and R. K. Mishra, (2009), *Optimization of dual band microstrip antenna using PSO*, 2009 Applied Electromagnetics Conference (AEMC), Kolkata, pp. 1-4. doi: 10.1109/AEMC.2009.5430685

[53] M. Gangopadhyaya, P. Mukherjee and B. Gupta, (2009), *The resonant frequency optimization of aperture-coupled microstrip antenna using particle swarm optimization algorithm*, 2009 Applied Electromagnetics Conference (AEMC), Kolkata, pp. 1-4. doi: 10.1109/AEMC.2009.5430724

[54] Y. K. Choukiker, S. K. Behera, B. K. Pandey and R. Jyoti, (2010), *Optimization of plannar antenna for ISM band using PSO*, 2010 Second International conference on Computing, Communication and Networking Technologies, Karur, pp. 1-4. doi: 10.1109/ICCCNT.2010.5591601

[55] M. Gangopadhyaya, P. Mukherjee and B. Gupta, (2010), *Resonant frequency optimization of coaxially fed rectangular microstrip antenna using Particle Swarm Optimization algorithm*, 2010 Annual IEEE India Conference (INDICON), Kolkata, pp. 1-3. doi: 10.1109/INDCON.2010.5712677

[56] M. Capek and P. Hazdra, (2010), *Design of IFS patch antenna using particle swarm optimization*, Proceedings of the Fourth European Conference on Antennas and Propagation, Barcelona, pp. 1-5.

[57] S. Chamaani, M. S. Abrishamian and S. A. Mirtaheri, (2010), *Time-Domain Design of UWB Vivaldi Antenna Array Using Multiobjective Particle Swarm Optimization*, in IEEE Antennas and Wireless Propagation Letters, vol. 9, pp. 666-669. doi: 10.1109/LAWP.2010.2053691

[58] S. K. Jain, A. Patnaik and S. N. Sinha, (2011), *Neural network based particle swarm optimizer for design of dual resonance X/Ku band stacked patch antenna*, 2011 IEEE International Symposium on Antennas and Propagation (APSURSI), Spokane, WA, 2011, pp. 2932-2935. doi: 10.1109/APS.2011.5997142

[59] S. Kumar, R. Kumar and B. K. Kanaujia, (2011), *Optimization of Resonant Frequency of Circular Patch Microstrip Antenna Using Particle Swarm Optimization*,

2011 International Conference on Computational Intelligence and Communication Networks, Gwalior, pp. 578-581. doi: 10.1109/CICN.2011.124

[60] J. Kovitz and Y. Rahmat-Samii, (2011), *Micro-actuated pixel patch antenna design using particle swarm optimization*, 2011 IEEE International Symposium on Antennas and Propagation (APSURSI), Spokane, WA, pp. 2415-2418. doi: 10.1109/APS.2011.5997009

[61] I. Vilović, N. Burum and M. Brailo, (2013), *Microstrip antenna design using neural networks optimized by PSO*, ICECom 2013, Dubrovnik, pp. 1-4. doi: 10.1109/ICECom.2013.6684759

[62] R. Nagpal, D. S. Dhaliwal and B. P. Garg, (2013), *Rectangular microstrip patch antenna parameters calculations using parallel Particle Swarm Optimization technique*, 2013 2nd International Conference on Information Management in the Knowledge Economy, Chandigarh, pp. 75-79.

[63] A. A. Minasian and T. S. Bird, (2013), *Particle Swarm Optimization of Microstrip Antennas for Wireless Communication Systems*, in IEEE Transactions on Antennas and Propagation, vol. 61, no. 12, pp. 6214-6217. doi: 10.1109/TAP.2013.2281517

[64] B. R. Behera, H. Pradhan and B. B. Mangaraj, (2014), *A new approach of performance comparison between microstrip rectangular and circular patch antenna using PSO*, 2014 International Conference on Circuits, Power and Computing Technologies, Nagercoil, pp. 1175-1179. doi: 10.1109/ICCPCT.2014.7055019

[65] I. Vilovic and N. Burum, (2014), *Optimization of feed position of circular microstrip antenna using PSO*, The 8th European Conference on Antennas and Propagation (EuCAP 2014), The Hague, pp. 2170-2172. doi: 10.1109/EuCAP.2014.6902239

[66] E. R. Schlosser, S. M. Tolfo and M. V. T. Heckler, (2015), *Particle Swarm Optimization for antenna arrays synthesis*, 2015 SBMO/IEEE MTT-S International Microwave and Optoelectronics Conference (IMOC), Porto de Galinhas, pp. 1-6. doi: 10.1109/IMOC.2015.7369120

[67] S. Dey, A. Sinha, B. Gill, M. Gangopadhyaya and S. Ray, , (2016) *Resonant frequency optimization of rectangular gap coupled Microstrip Antenna using Particle Swarm Optimization algorithm*, 2016 IEEE 7th Annual Information Technology, Electronics and Mobile Communication Conference (IEMCON), Vancouver, BC, pp. 1-4. doi: 10.1109/IEMCON.2016.7746360

[68] Ç. Korkuç and E. Afacan, (2016), *Optimization of circular antenna arrays using particle swarm optimization*, 2016 24th Signal Processing and Communication Application Conference (SIU), Zonguldak, pp. 449-452. doi: 10.1109/SIU.2016.7495774

[69] A. Bhattacharya, B. Roy, M. Islam, S. K. Chowdhury and A. K. Bhattacharjee, (2016), *An UWB Monopole antenna with hexagonal patch structure designed using particle swarm optimization algorithm for wireless applications*, 2016 International Conference on Microelectronics, Computing and Communications (MicroCom), Durgapur, pp. 1-5. doi: 10.1109/MicroCom.2016.7522413

[70] A. V. Miranda, P. Ashwin, P. Sharan, V. S. Gangwar, A. K. Singh and S. P. Singh, (2017), *An efficient synthesis of unequally spaced antenna array with electronic scan capability utilizing particle swarm optimization*, 2017 IEEE MTT-S International Microwave and RF Conference (IMaRC), Ahmedabad, pp. 255-258. doi: 10.1109/IMaRC.2017.8611005

[71] A. Lalbakhsh, M. U. Afzal and K. P. Esselle, (2017), *Multiobjective Particle Swarm Optimization to Design a Time-Delay Equalizer Metasurface for an Electromagnetic Band-Gap Resonator Antenna*, in IEEE Antennas and Wireless Propagation Letters, vol. 16, pp. 912-915. doi: 10.1109/LAWP.2016.2614498

[72] L. Pappula and D. Ghosh, (2017), *Unequally spaced linear antenna array synthesis using multi-objective cauchy mutated cat swarm optimization*, 2017 IEEE International Symposium on Antennas and Propagation USNC/URSI National Radio Science Meeting, San Diego, CA, pp. 313-314. doi: 10.1109/APUS-NCURSINRSM.2017.8072199

[73] S. Narayanan, A. K. Manoj and S. Natarajamani, (2018), *A Circularly-polarized Patch Antenna using Pin-loaded Technique with PSO*, 2018 International Conference on Advances in Computing, Communications and Informatics (ICACCI), Bangalore, pp. 1627-1630. doi: 10.1109/ICACCI.2018.8554943

[74] Nanbo Jin and Yahya Rahmat-Samii, (2008), *Particle Swarm Optimization for Antenna Designs in Engineering Electromagnetics*, Journal of Artificial Evolution and Applications, Volume 2008, Article ID 728929, doi:10.1155/2008/728929

[75] Abunaser, Amal Doush, Iyad Mansour, Nahed Alshattnawi, Sawsan. (2014). *Underwater Image Enhancement Using Particle Swarm Optimization*, Journal of Intelligent Systems. 10.1515/jisys-2014-0012.

[76] Mirjalili, S., Mirjalili, S. M., Lewis, A. (2014), *Grey Wolf Optimizer. Advances in Engineering Software*, 69, 46–61, Jan 2014. doi:10.1016/j.advengsoft.2013.12.007

[77] Panda, M., Das, B. (2019), *Grey Wolf Optimizer and Its Applications: A Survey*, Proceedings of the Third International Conference on Microelectronics, Computing and Communication Systems, 179–194, May 2019. doi:10.1007/978-981-13-7091-5_17

[78] Li, X., Luk, K. M. (2019), *The Grey Wolf Optimizer and its Applications in Electromagnetics*, IEEE Transactions on Antennas and Propagation, 1–1. doi:10.1109/tap.2019.2938703

[79] N. Jayakumar, (2015) *PhD Thesis - Economic Dispatch of Combined Heat and Power Generating Systems in the Feasible Domain by Grey Wolf Optimization Algorithm*, Annamalai University.

[80] Muro C, Escobedo R, Spector L, Coppinger RP, (2011), *Wolf-pack (Canis lupus) hunting strategies emerge from simple rules in computational simulations*, Behav Proc 88(3):192–197.

[81] Wolpert DH, Macready WG., (1997), *No free lunch theorems for optimization*. Evolut. Comput., IEEE Trans; 1:67–82.

[82] Vijay Ramasami, *ANSYS HFSS MATLAB API*, RSL, Univ. of Kansas, Lawrence, KS, 66046. https://github.com/yuip/hfss-api

[83] Robinson, J. and Rahmat-Samii, Y., (2004), *Particle Swarm Optimization in Electromagnetics*, IEEE Transactions on Antennas and Propagation 52. 2, 397-407.

[84] L. Lizzi, F. Viani, R. Azaro and A. Massa, (2007), *Optimization of a Spline-Shaped UWB Antenna by PSO*, IEEE Antennas and Wireless Propagation Letters, vol. 6, pp. 182-185. doi: 10.1109/LAWP.2007.894157.

[85] Anguera J., C. Puente, C. Borja, and J. Soler, (2007), *Dual frequency broadband stacked microstrip antenna using a reactive loading and a fractal-shaped radiating edge*, IEEE Antennas and Wireless Propagation Letters 6: 309-312.

[86] Matthias John; Max J. Ammann, (2009), *Antenna Optimization With a Computationally Efficient Multi-objective Evolutionary Algorithm*, IEEE Transactions on Antennas and Propagation, Vol. 57, No. 1.

[87] Jahromi A.G., F. Mohajeri and N. Feiz, (2013), *Miniaturization of a Rectangular Microstrip Patch Antenna Loaded with Metamaterial*, World Academy of Science, Engineering and Technolog, 7: 668-671.

[88] Jayasinghe J.M.J.W. and D.N. Uduwawala, (2013), *Optimization of the performance of patch antennas using genetic algorithms*, Journal of National Science Foundation 41. 2: 115-122.

[89] Ahsan, M.R., M.T. Islam, M. Habib Ullah, W. N. L. Mahadi, and T. A. Latef, (2014), *Compact Double-P Slotted Inset-Fed Microstrip Patch Antenna on High Dielectric Substrate*, The Scientific World Journal, 2014, Article ID 909854, 6 pages.

[90] Islam M.T., and M. Samsuzzaman, (2014), *Miniaturized Dual Band Multislotted Patch Antenna on Polytetrafluoroethylene Glass Microfiber Reinforced for C/X Band Applications*, The Scientific World Journal 2014, Article ID 673846, 14 pages.

[91] A. Deb, J. S. Roy and B. Gupta, (2014), *Performance Comparison of Differential Evolution, Particle Swarm Optimization and Genetic Algorithm in the Design*

of Circularly Polarized Microstrip Antennas, IEEE Transactions on Antennas and Propagation, vol. 62, no. 8, pp. 3920-3928. doi: 10.1109/TAP.2014.2322880

[92] Ali Y.E.M., and A.J.A. Qader, (2014), *Design of Dual Band Circular Polarization Stacked Microstrip Antenna for GPS Applications*, Al-Rafidain Engineering Journal, 22.3:225-232, (2014).

[93] Rahimi, M., F.B. Zarrabi, R. Ahmadian, Z. Mansouri, and A. Keshtkar, (2014), *Miniaturization of Antenna for Wireless Application with Difference Metamaterial Structures*, Progress In Electromagnetics Research, 145:19-29.

[94] Q. Pi and H. Ye, (2015), *Survey of particle swarm optimization algorithm and its applications in antenna circuit*, 2015 IEEE International Conference on Communication Problem-Solving (ICCP), Guilin, pp. 492-495. doi: 10.1109/IC-CPS.2015.7454212.

[95] Jayasinghe J.M.J.W. and D.N. Uduwawala, (2015), *A Novel Multiband Miniature Planar Inverted F Antenna Design for Bluetooth and WLAN Applications*, International Journal of Antennas and Propagation, Article ID 970152, 6 pages.

[96] E. J. B. Rodrigues, H. W. C. Lins and A. G. D'Assunçao, (2016), *Fast and accurate synthesis of electronically reconfigurable annular ring monopole antennas using particle swarm optimisation and artificial bee colony algorithms*, IET Microwaves, Antennas Propagation, vol. 10, no. 4, pp. 362-369. doi: 10.1049/iet-map.2015.0106.

[97] J. Li, (2007), *Optimizing Design of Antenna Using Differential Evolution*, 2007 Asia-Pacific Microwave Conference, Bangkok, pp. 1-4. doi: 10.1109/APMC.2007.4554614

[98] A. Chatterjee, G. K. Mahanti and P. R. S. Mahapatra, (2010), *Optimum ring spacing and interelement distance for sidelobe reduction of a uniform concentric ring array antenna using differential evolution algorithm*, 2010 IEEE International Conference on Communication Systems, Singapore, pp. 254-258. doi: 10.1109/ICCS.2010.5686077

[99] A. M. Montaser, K. R. Mahmoud and H. A. Elmikati, (2011), *Compact Ultra-Wideband monopole antenna design for wireless communication using differential evolution optimization algorithm*, 2011 28th National Radio Science Conference (NRSC), Cairo, pp. 1-7. doi: 10.1109/NRSC.2011.5873583

[100] A. Deb, J. S. Roy and B. Gupta, (2011), *Application of differential evolution algorithm to the design of a dual frequency microstrip antenna*, 2011 4th IEEE International Symposium on Microwave, Antenna, Propagation and EMC Technologies for Wireless Communications, Beijing, pp. 42-45. doi: 10.1109/MAPE.2011.6156151

[101] A. Chatterjee, G. K. Mahanti and Priya Ranjan Sinha Mahapatra, (2011), *Design of phase-differentiated dual-beam concentric ring array antenna using differential evolution algorithm*, 2011 International Conference on Communications and Signal Processing, Calicut, pp. 280-283. doi: 10.1109/ICCSP.2011.5739319

[102] S. K. Goudos, K. Siakavara, T. Samaras, E. E. Vafiadis and J. N. Sahalos, (2011), *Self-Adaptive Differential Evolution Applied to Real-Valued Antenna and Microwave Design Problems*, in IEEE Transactions on Antennas and Propagation, vol. 59, no. 4, pp. 1286-1298. doi: 10.1109/TAP.2011.2109678

[103] A. Deb, J. S. Roy and B. Gupta, (2011), *Design of a probe-fed microstrip antenna using differential evolution algorithm*, 2011 4th IEEE International Symposium on Microwave, Antenna, Propagation and EMC Technologies for Wireless Communications, Beijing, pp. 46-49. doi: 10.1109/MAPE.2011.6156156

[104] A. K. Behera, A. Ahmad, S. K. Mandal, G. K. Mahanti and R. Ghatak, (2013), *Synthesis of cosecant squared pattern in linear antenna arrays using differential evolution*, 2013 IEEE Conference on Information Communication Technologies, Thuckalay, Tamil Nadu, India, pp. 1025-1028. doi: 10.1109/CICT.2013.6558248

[105] S. Das, D. Mandal, R. Kar and S. P. Ghoshal, (2014), Interference suppression of linear antenna arrays with combined Backtracking Search Algorithm and Differential Evolution, 2014 International Conference on Communication and Signal Processing, Melmaruvathur, pp. 162-166. doi: 10.1109/ICCSP.2014.6949820

[106] M. Gangopadhyaya, P. Mukherjee, U. Sharma, B. Gupta and S. Manna, (2015), Design optimization of microstrip fed rectangular microstrip antenna using differential evolution algorithm, 2015 IEEE 2nd International Conference on Recent Trends in Information Systems (ReTIS), Kolkata, pp. 49-52. doi: 10.1109/ReTIS.2015.7232851

[107] A. Mukhopadhyay, S. Manna, S. Lahiri, U. Sharma, M. Gangopadhyaya, P. Mukherjee, B. Gill, (2016), *Bandwidth enhancement of microstrip patch antenna using Curve fitting based Differential Evolution and Cuckoo Search optimization - a comparative study*, 2016 IEEE 7th Annual Information Technology, Electronics and Mobile Communication Conference (IEMCON), Vancouver, BC, pp. 1-5. doi: 10.1109/IEMCON.2016.7746346

[108] A. Mukherjee, S. K. Mandal and R. Ghatak, (2016), *Synthesis of non-uniformly spaced planar array geometry using Differential Evolution algorithm*, 2016 IEEE Indian Antenna Week (IAW 2016), Madurai, pp. 63-66. doi: 10.1109/IndianAW.2016.7883599

[109] H. Liu, H. Zhao, W. Li and B. Liu, (2016), *Synthesis of Sparse Planar Arrays Using Matrix Mapping and Differential Evolution*, in IEEE Antennas and Wireless Propagation Letters, vol. 15, pp. 1905-1908. doi: 10.1109/LAWP.2016.2542882

[110] A. Deb, J. S. Roy and B. Gupta, (2018), *A Differential Evolution Performance Comparison: Comparing How Various Differential Evolution Algorithms Perform in Designing Microstrip Antennas and Arrays*, in IEEE Antennas and Propagation Magazine, vol. 60, no. 1, pp. 51-61. doi: 10.1109/MAP.2017.2774146

[111] K. Tenglong, Z. Xiaoying, W. Jian and D. Yihan, (2011), *A modified ACO algorithm for the optimization of antenna layout*, 2011 International Conference on Electrical and Control Engineering, Yichang, pp. 4269-4272. doi: 10.1109/ICECENG.2011.6057613

[112] R.E. Zich, M. Mussetta, F. Grimaccia, R. Albi, A. Carbonara, P. D'Antuono, T. Guffanti, E. Zucchelli, (2012), *Comparison of different optimization techniques in*

antenna design - Part I, Proceedings of the 2012 IEEE International Symposium on Antennas and Propagation, Chicago, IL, pp. 1-2.doi: 10.1109/APS.2012.6348757

[113] R.E. Zich, M. Mussetta, F. Grimaccia, J. Banchetti, T. Guggiari, A. Oregio Cate-lan, F. Lo Presti, O. Testoni, T. Zanelli, (2012), *Comparison of different optimization techniques in antenna design - Part II*, Proceedings of the 2012 IEEE International Symposium on Antennas and Propagation, Chicago, IL, 2012, pp. 1-2. doi: 10.1109/APS.2012.6348756

[114] Y. Yang, S. Yan, J. Liu and J. Liang, (2014), *Genetic-Ant Colony Optimization algorithm and its application to design of antenna*, 2014 10th International Conference on Natural Computation (ICNC), Xiamen, pp. 611-616. doi: 10.1109/ICNC.2014.6975905

[115] M. Akila, P. Anusha, M. Sindhu and K. T. Selvan, (2017), *Examination of PSO, GA-PSO and ACO algorithms for the design optimization of printed antennas*, 2017 IEEE Applied Electromagnetics Conference (AEMC), Aurangabad, pp. 1-2. doi: 10.1109/AEMC.2017.8325661

[116] A. REINEIX and C. GUIFFAUT, (2018), *Equivalent dipole model optimized by Ant Colony Optimization Algorithm for modeling antennas in their context*, 2018 13th Annual Conference on System of Systems Engineering (SoSE), Paris, pp. 259-264. doi: 10.1109/SYSOSE.2018.8428763

[117] R. Holtzman, R. Kastner, E. Heyman and R. W. Ziolkowski, (2001), *Ultra-wideband antenna design using the Green's function method (GFM) ABC with genetic algorithm*, IEEE Antennas and Propagation Society International Symposium. 2001 Digest. Held in conjunction with: USNC/URSI National Radio Science Meeting (Cat. No.01CH37229), Boston, MA, USA, pp. 238-241 vol.4. doi: 10.1109/APS.2001.959441

[118] J. Yang, W. Li, X. Shi, L. Xin and J. Yu, (2013), *A Hybrid ABC-DE Algorithm and Its Application for Time-Modulated Arrays Pattern Synthesis*, in IEEE Transactions on Antennas and Propagation, vol. 61, no. 11, pp. 5485-5495. doi: 10.1109/TAP.2013.2279093

[119] X. Zhang, X. Zhang and L. Wang, (2018), *Antenna Design by an Adaptive Variable Differential Artificial Bee Colony Algorithm*, in IEEE Transactions on Magnetics, vol. 54, no. 3, pp. 1-4. doi: 10.1109/TMAG.2017.2747095

[120] P. Swain, S. K. Mohanty and B. B. Mangaraj, (2016), *Linear Dipole Antenna Array design and optimization using Gravitational Search Algorithm*, 2016 2nd International Conference on Advances in Electrical, Electronics, Information, Communication and Bio-Informatics (AEEICB), Chennai, pp. 514-518. doi: 10.1109/AEEICB.2016.7538343

[121] Mourad Meloui, Mohammad Essaaidi, (2014), *A Dual Ultra Wide Band Slotted Antenna for C and X Bands Application*, Progress In Electromagnetics Research Letters, Vol. 47, 91–96.

[122] Vivek Singh, Brijesh Mishra, Rajeev Singh, (2015), *A Compact and Wide Band Microstrip Patch Antenna for X-Band Applications*, IEEE Second International Conference on Advances in Computing and Communication Engineering.

[123] Indra Bhooshan Sharma, Fateh Lal Lohar, Ravi Kumar Maddila, Abhinav Deshpande, and M.M. Sharma, (2018), *Tri-Band Microstrip Patch Antenna for C, X, and Ku Band Applications*, Optical and Wireless Technologies, Lecture Notes in Electrical Engineering, Vol. 472.

[124] *Cubesat Antenna: X-Band Single Element Patch Antenna*, Endurosat User Manual.

List of Publications

1. Raj Gaurav Mishra, Ranjan Mishra, N. Prasanthi Kumari, Sushabhan Choudhury, Piyush Kuchhal (2019), **Design and Optimization of Genetic Algorithm (GA) based High Gain and Directive CPW-Fed Slot Dipole Antenna for Wideband Applications**, *International Journal of Engineering and Advanced Technology* (ISSN: 2249-8958), Volume-9 Issue-2, December 2019. DOI: 10.35940/ijeat.B3931.129219. [**Scopus Indexed**]

2. Raj Gaurav Mishra, Ranjan Mishra, Piyush Kuchhal and N. Prasanthi Kumari (2018), **Analysis of the Microstrip Patch Antenna designed using Genetic Algorithm based Optimization for Wide-Band Applications**, *International Journal of Pure and Applied Mathematics* (ISSN: 1314-3395), Volume 118, No. 11: Special Issue on Engineering and Applied Mathematics. March 2018. [**Scopus Indexed**]

3. Raj Gaurav Mishra, Ranjan Mishra, Piyush Kuchhal and N. Prasanthi Kumari (2018), **Optimization and Analysis of High Gain Wideband Microstrip Patch Antenna using Genetic Algorithm**, *International Journal of Engineering Technology* (ISSN: 2227-524X), Volume 7, Issue 1.5, January 2018. [**Scopus Indexed**]

4. Raj Gaurav Mishra, Ranjan Mishra, Piyush Kuchhal and N. Prasanthi Kumari (2017), **Design and Analysis of CPW-Fed Microstrip Patch Antennas for Wide Band Applications**, *Proceedings of the 2nd IEEE International Conference on Inventive Computing and Informatics* (ICICI 2017), Coimbatore, ISBN: 978-1-5386-4031-9, 23-24 November 2017. [**Scopus Indexed**]

5. Raj Gaurav Mishra, Ranjan Mishra, Piyush Kuchhal and N. Prasanthi Kumari (2017), **Analysis of Bandwidth and Directivity of Rectangular Microstrip Antenna by Inserting Slots, Notches and Slits**, *Proceedings of the 2nd IEEE International Conference on Communication and Electronics Systems* (ICCES 2017), Coimbatore, ISBN: 978-1-5090-5013-0, 19-20 October 2017. [**Scopus Indexed**]

Raj Gaurav Mishra

raj.g.mishra@gmail.com   +91 97608 57220

Synopsis

⇨ Currently working as an **Assistant Professor (Sel. Grade)** at the **Department of Electrical and Electronics, School of Engineering (SOE), University of Petroleum and Energy Studies, Dehradun**, UK, India since **August 2015.**

⇨ **Total experience of about 14+ years** in academics, research and industry.

⇨ **Master of Science (MS) in Space Engineering** from Umeå University, Department of Space Sciences-Kiruna, **Sweden**. (September 2005 – March 2007).

⇨ Worked with **Info VII - Robotics and Telematics**, Julius Maximilans University of Wuerzburg **Germany**, on Master Thesis Project Development of the JMUW Ground Station.

⇨ **B.E. (Electronics & Instrumentation)** from Institute of Technology & Management - Gwalior (Affiliated to RGPV-Bhopal) in 2004.

⇨ Successfully handled a number of projects in Software, Electronics and Robotics.

⇨ Excellent communication, interpersonal & analytical skills with the ability to grasp new concepts & utilise the same in a productive manner.

Academic/Research/Industrial Experience

⇨ August 2015 – till date - working as an **Assistant Professor (SG)** at the at the **Department of Electrical and Electronics, School of Engineering (SOE), University of Petroleum and Energy Studies, Dehradun**, UK, India.

⇨ From August 2013 – July 2015 – worked as **faculty member (Asst. Prof.)** at the **Department of Electronics & Communication Engineering, Faculty of Science & Technology, The ICFAI University, Dehradun**, UK, India.

⇨ From December 2010 to June 2013 – worked as a **full-time Researcher** at **Division of Microelectronics, Indian Institute of Information Technology – Allahabad**, UP, India.

⇨ April 2009 to December 2010 – worked as a **full-time faculty member (Asst. Prof.)** at the **Faculty of Science & Technology, The ICFAI University, Dehradun**, UK, India.

⇨ August 2008 - March 2009 - worked as a **full-time faculty member (Lecturer)** at **NRI-Institute of Technology & Management, Gwalior**, India.

⇨ July 2007 – July 2008 - worked as a **Software Engineer** at **Patni Computer Systems Ltd. Mumbai,** MH, India.

⇨ August 2004 – August 2005 - worked as a **Software Engineer Trainee** at **Satyam Computer Services Ltd. Hyderabad,** AP, India.

Awards / Fellowships

⇨ Received **Indo-Swiss Joint Research Program (ISJRP) Fellowship** to visit EPFL-Lausanne, Switzerland, as a **Guest Researcher** from November 2011 to February 2012.

Research Projects Completed/Ongoing

Project Title: **Multi-objective Performance Optimization of Microstrip Patch Antenna for Wide-Band Applications**
Duration: 4 Years (Submitted)
Scope: Doctoral Research Project
Employer: **Department of Electrical and Electronics, University of Petroleum and Energy Studies, Dehradun. Uttarakhand, India.**

Project Title: **Identification and Localization of Events using Extended Sensors**
Duration: 3 Years (Completed)
Scope: Sponsored Research Project
Employer: **Division of Microelectronics, Indian Institute of Information Technology – Allahabad, UP, India.**

Project Title: **Development of a JMUW Satellite Ground Station**
Duration: 6 months(Completed)
Scope: Master Thesis Project.
Employer: **Info VII - Robotics and Telematics, Julius Maximilans University of Wuerzburg-Germany.**

Project Title: **ADIA – Altitude Determination by Image Analysis**
Duration: 4 months(Completed)
Scope: Master Student's Project.
Employer: **Department of Space Sciences – Kiruna and Swedish Space Corporation – Kiruna.**

Project Title: **SSETI ESEO - European Student Earth Orbiter**
Duration: 4 months(Completed)
Scope: Master Student's Project.
Employer: **Department of Space Sciences – Kiruna and European Space Agency - Netherlands.**

Areas of Interest

- Image processing
- Robotics and Mechatronics
- Internet of Things (IoT)
- Microprocessors and Microcontrollers
- Digital System Design

- Space Engineering
- Embedded System Design & Development
- FPGA based real-time system development
- Digital Signal Processing
- Microstrip Antenna Design

Personal Details

Father's Name   :   Mr. Pushp Raj Mishra
Permanent Address: C-102, Janki Apartments, Kolar Road, Bhopal - 462042, MP India
Current Address   :   Priyalok Colony, Phase 1, Sewla Kalan, Dehradun - 468001 (U.K.), India.
Marital Status   :   Married
Date of Birth   :   08th April, 1983

Raj Gaurav Mishra

14th September 2020

UPES

UNIVERSITY WITH A PURPOSE

PLAGIARISM CERTIFICATE

1. We, **Dr. Piyush Kuchhal** (Supervisor), **Dr. N. Prasanthi Kumari** (Co-Supervisor); certify that the Thesis titled **MULTI-OBJECTIVE PERFORMANCE OPTIMIZATION OF MICROSTRIP PATCH ANTENNA FOR WIDE-BAND APPLICATIONS** submitted by Scholar **Mr. Raj Gaurav Mishra** having SAP ID 500049145, has been run through a Plagiarism Check Software and the Plagiarism Percentage is reported to be 8%.

2. Plagiarism Report generated by the Plagiarism software is attached.

14/09/2020

Dr. Piyush Kuchhal

(Supervisor)

N. Prasanthi Kumari, Ph.D

(Co-Supervisor)

Raj Gaurav Mishra

(Research Scholar)

RGM_PhD_Thesis_Sept_2020

ORIGINALITY REPORT

8%	**2**%	**7**%	%
SIMILARITY INDEX	INTERNET SOURCES	PUBLICATIONS	STUDENT PAPERS

PRIMARY SOURCES

1	"Handbook of Antenna Technologies", Springer Science and Business Media LLC, 2016 Publication	**2**%
2	ijtir.hctl.org Internet Source	**1**%
3	Deepati, Anil Kumar, Arun Kumar Kadian, and Pankaj Biswas. "Numerical and experimental study on influence of tool plunging force and shoulder size on thermal history of friction stir welding", International Journal of Manufacturing Research, 2015. Publication	**1**%
4	"Proceedings of 2nd International Conference on Micro-Electronics, Electromagnetics and Telecommunications", Springer Science and Business Media LLC, 2018 Publication	**1**%
5	"Optical And Microwave Technologies", Springer Science and Business Media LLC, 2018 Publication	**1**%

Raj Gaurav Mishra
(Research Scholar)

Dr. Piyush Kuchhal 14/09/2020
(Supervisor)

Dr. N. Prasanthi Kumari
(Co-Supervisor)